Document made available under the Patent Cooperation Treaty (PCT)

International application number: PCT/US04/041863

International filing date: 13 December 2004 (13.12.2004)

Document type: Certified copy of priority document

Document details: Country/Office: US
Number: 60/481,771
Filing date: 11 December 2003 (11.12.2003)

Date of receipt at the International Bureau: 31 March 2005 (31.03.2005)

Remark: Priority document submitted or transmitted to the International Bureau in compliance with Rule 17.1(a) or (b)

World Intellectual Property Organization (WIPO) - Geneva, Switzerland
Organisation Mondiale de la Propriété Intellectuelle (OMPI) - Genève, Suisse

1299654

THE UNITED STATES OF AMERICA

TO ALL TO WHOM THESE PRESENTS SHALL COME:

UNITED STATES DEPARTMENT OF COMMERCE

United States Patent and Trademark Office

March 22, 2005

THIS IS TO CERTIFY THAT ANNEXED HERETO IS A TRUE COPY FROM THE RECORDS OF THE UNITED STATES PATENT AND TRADEMARK OFFICE OF THOSE PAPERS OF THE BELOW IDENTIFIED PATENT APPLICATION THAT MET THE REQUIREMENTS TO BE GRANTED A FILING DATE.

APPLICATION NUMBER: *60/481,771*
FILING DATE: *December 11, 2003*
RELATED PCT APPLICATION NUMBER: *PCT/US04/41863*

Certified by

Jon W. Dudas

Under Secretary of Commerce
for Intellectual Property
and Director of the United States
Patent and Trademark Office

TRANSMITTAL

Electronic Version v1.1

Stylesheet Version v1.1.0

Title of Invention	METHOD AND APPARATUS FOR EFFICIENT DATA ACQUISITION AND INTERPOLATION

Application Number :

Date :

First Named Applicant: Dr. Gregory Beylkin

Confirmation Number:

Attorney Docket Number: 2703-03-13

I hereby certify that the use of this system is for OFFICIAL correspondence between patent applicants or their representatives and the USPTO. Fraudulent or other use besides the filing of official correspondence by authorized parties is strictly prohibited, and subject to a fine and/or imprisonment under applicable law.

I , the undersigned, certify that I have viewed a display of document(s) being electronically submitted to the United States Patent and Trademark Office, using either the USPTO provided style sheet or software, and that this is the document(s) I intend for initiation or further prosecution of a patent application noted in the submission. This document(s) will become part of the official electronic record at the USPTO.

Submitted By:	Elec. Sign.	Sign. Capacity
Mr. Michael Roddy Nichols Registered Number: 46,959	Michael Roddy Nichols	Attorney

Documents being submitted:	Files
us-fee-sheet	2703-03-13-EFS-usfees.xml
	us-fee-sheet.xsl
	us-fee-sheet.dtd
us-request	2703-03-13-EFS-usrequ.xml
	us-request.dtd
	us-request.xsl
application-body	pr2.xml
	application-body.dtd
	wipo.ent
	mathml2.dtd
	mathml2-qname-1.mod
	isoamsa.ent
	isoamsb.ent
	isoamsc.ent
	isoamsn.ent
	isoamso.ent
	isoamsr.ent
	isogrk3.ent
	isomfrk.ent
	isomopf.ent
	isomscr.ent
	isotech.ent
	isobox.ent
	isocyr1.ent
	isocyr2.ent
	isodia.ent
	isolat1.ent
	isolat2.ent
	isonum.ent
	isopub.ent
	mmlextra.ent
	mmlalias.ent
	soextblx.dtd
	us-application-body.xsl
	beylaa.tif
	beylab.tif
	beylac.tif
	beylad.tif
	beylae.tif
	beylaf.tif
	beylag.tif
	beylah.tif
	beylai.tif
	beylaj.tif
	beylak.tif
	beylal.tif
	beylam.tif
	beylan.tif
	beylao.tif

beylap.tif
beylaq.tif
beylar.tif
beylas.tif
beylat.tif
beylau.tif
beylav.tif
beylaw.tif
beylax.tif
beylay.tif
beylaz.tif
beylba.tif
beylbb.tif
beylbc.tif
beylbd.tif
beylbe.tif
beylbf.tif
beylbg.tif
beylbh.tif
beylbi.tif
beylbj.tif
beylbk.tif
beylbl.tif
beylbm.tif
beylbn.tif
beylbo.tif
beylbp.tif
beylbq.tif
beylbr.tif
beylbs.tif
beylbt.tif
beylbu.tif
beylbv.tif
beylbw.tif
beylbx.tif
beylby.tif
beylbz.tif
beylca.tif
beylcb.tif
beylcc.tif
beylcd.tif
beylce.tif
beylcf.tif
xiao-aa.tif
xiao-ab.tif
xiao-ac.tif
xiao-ad.tif
xiao-ae.tif
xiao-af.tif
xiao-ag.tif
xiao-ah.tif

	xiao-ai.tif xiao-aj.tif xiao-ak.tif xiao-al.tif xiao-am.tif xiao-an.tif xiao-ao.tif xiao-ap.tif xiao-aq.tif xiao-ar.tif xiao-as.tif xiao-at.tif xiao-au.tif xiao-av.tif xiao-aw.tif xiao-ax.tif xiao-ay.tif xiao-az.tif xiao-ba.tif xiao-bb.tif xiao-bc.tif xiao-bd.tif xiao-be.tif xiao-bf.tif xiao-bg.tif xiao-bh.tif img0001.tif img0002.tif
Comments	

APPLICATION DATA SHEET

Electronic Version v14

Stylesheet Version v14.0

Title of Invention	METHOD AND APPARATUS FOR EFFICIENT DATA ACQUISITION AND INTERPOLATION

Application Type :	provisional, utility
Attorney Docket Number :	2703-03-13

Correspondence address:

Customer Number: 30960

Inventor Information:

Inventor 1:

Applicant Authority Type:	Inventor
Citizenship:	US
Name prefix:	Dr.
Given Name:	Gregory
Family Name:	Beylkin
Residence:	
City of Residence:	Boulder
State of Residence:	CO
Country of Residence:	US
Address-1 of Mailing Address:	3897 Promontory Ct.
Address-2 of Mailing Address:	
City of Mailing Address:	Boulder
State of Mailing Address:	CO
Postal Code of Mailing Address:	80304
Country of Mailing Address:	US
Phone:	
Fax:	
E-mail:	

Attorney Information:

practitioner(s) at Customer Number:

30960

as my attorney(s) or agent(s) to prosecute the application identified above, and to transact all business in the United States Patent and Trademark Office connected therewith.

Electronic Version
Stylesheet Version v1.1.1

Claims

[c1] A method for acquisition of data where the data are collected at the nodes, which are arranged as the nodes of the generalized Gaussian quadratures for exponentials.

[c2] A method for acquisition of data where the data are collected at the nodes, which are arranged as the nodes of the generalized Gaussian quadratures for exponentials on intervals in dimension one, and/or rectangles and/or disks in dimension two, parallepipeds, and/or balls.

[c3] The method of claim 1 where the generalized Gaussian quadratures for exponentials are used as a basis for bandlimited non-periodic data sequences

[c4] The method of claim 1, where the accuracy of the nodes of the generalized Gaussian quadratures is selected and the nodes corresponding to this accuracy are computed.

[c5] The method of claim 3, where for a given bandlimit of the bandlimited data and a given accuracy the number of nodes is selected to be less than the number of data points.

[c6] The method of claim 3 where prolate spheroidal wave

functions are used as the approximating basis instead of generalized Gaussian quadratures.

[c7] The method of method of claim 5, where for a specified approximation accuracy the nodes are computed.

[c8] The method of claim 6, where the number of nodes is controlled to be less than the number of the data points.

[c9] The method of claim 7, where the number of nodes for the Prolate Spheroidal Wave Functions is automatically computed.

[c10] The method of claim 8, where the coefficients for generalized Gaussian quadratures for exponentials used as approximating basis are computed from the coefficients of the Prolate Spheroidal Wave Functions.

[c11] The method of claim 9, where the generalized Gaussian quadratures are used as interpolating basis for bandlimited data.

[c12] The method of claim 7 where it is applied to non-periodic data.

[c13] The method of claim 1, where it is applied to seismic data with arbitrary linear moveout.

[c14] The method of claim 4 where it is applied to seismic data

with arbitrary linear moveout

[c15] The method of claim 9 where the seismic data are computed at times different than the discrete time samples of the given seismic data set.

[c16] The method of claim 1 applied to spatially aliased seismic data by applying a linear moveout correction parallel to the dominant dip of the seismic data in a local data window moving around the seismic data volume.

[c17] The method of claim 4 applied to spatially aliased seismic data by applying a linear moveout correction parallel to the dominant dip of the seismic data in local data window moving around the seismic data volume

[c18] The method of claim 7 applied to spatially aliased seismic data, wherein selecting the accuracy and the number of the nodes corresponding to this accuracy, applying a linear moveout correction parallel to the dominant dip of the seismic data in local data window moving around the seismic data volume, effectively flattening the seismic data, computing the coefficients of the Prolate Spheroidal Wave Functions, estimating the seismic data for this approximating basis and undoing the linear moveout applied to the local data window.

Electronic Version

Stylesheet Version v1.1.1

METHOD AND APPARATUS FOR EFFICIENT DATA ACQUISITION AND INTERPOLATION

Abstract

An acquisition system that has a minimal number of nodes for a fixed bandwidth of the measured data and a given accuracy of measurements is disclosed.

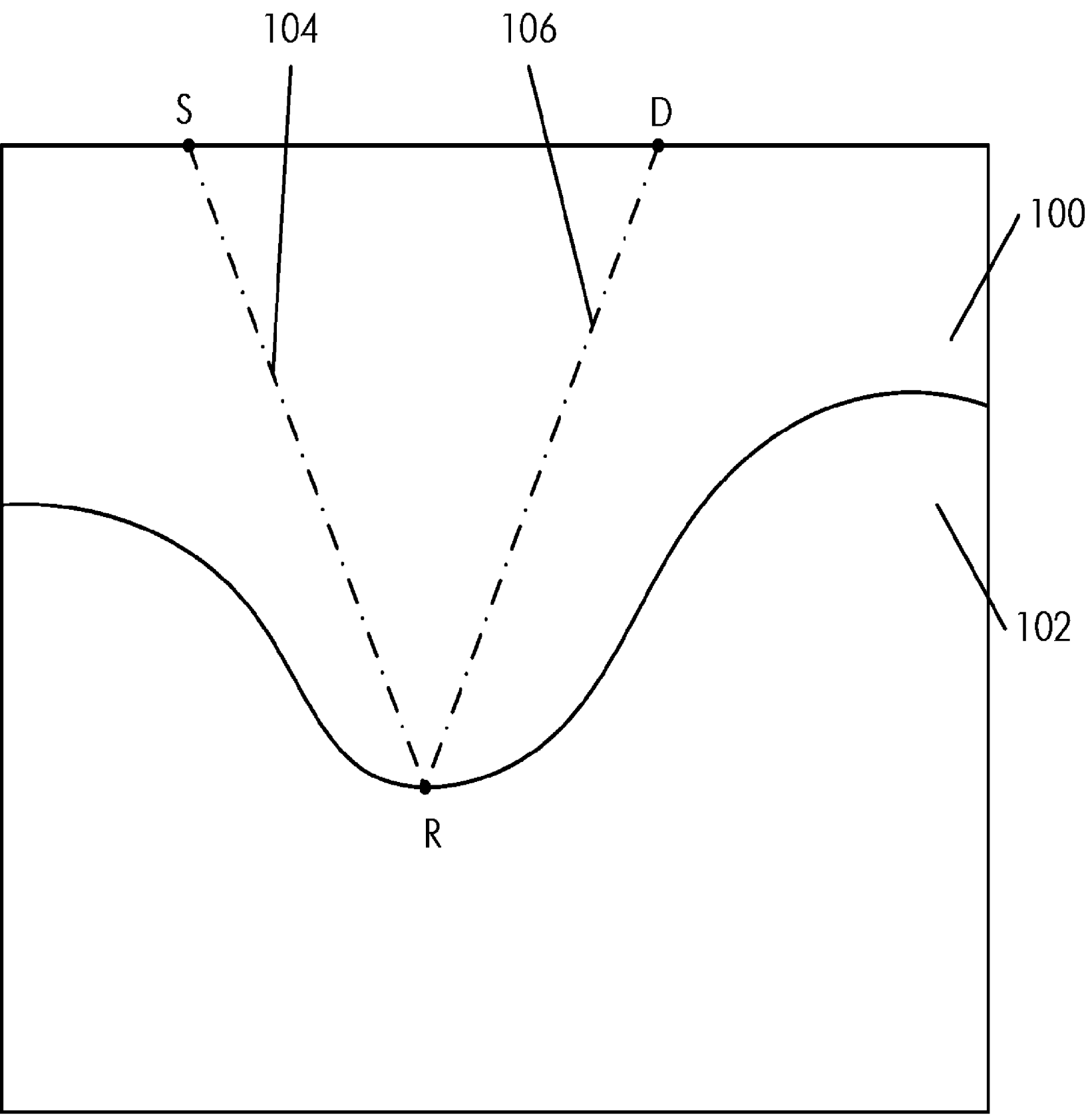

FIGURE 1

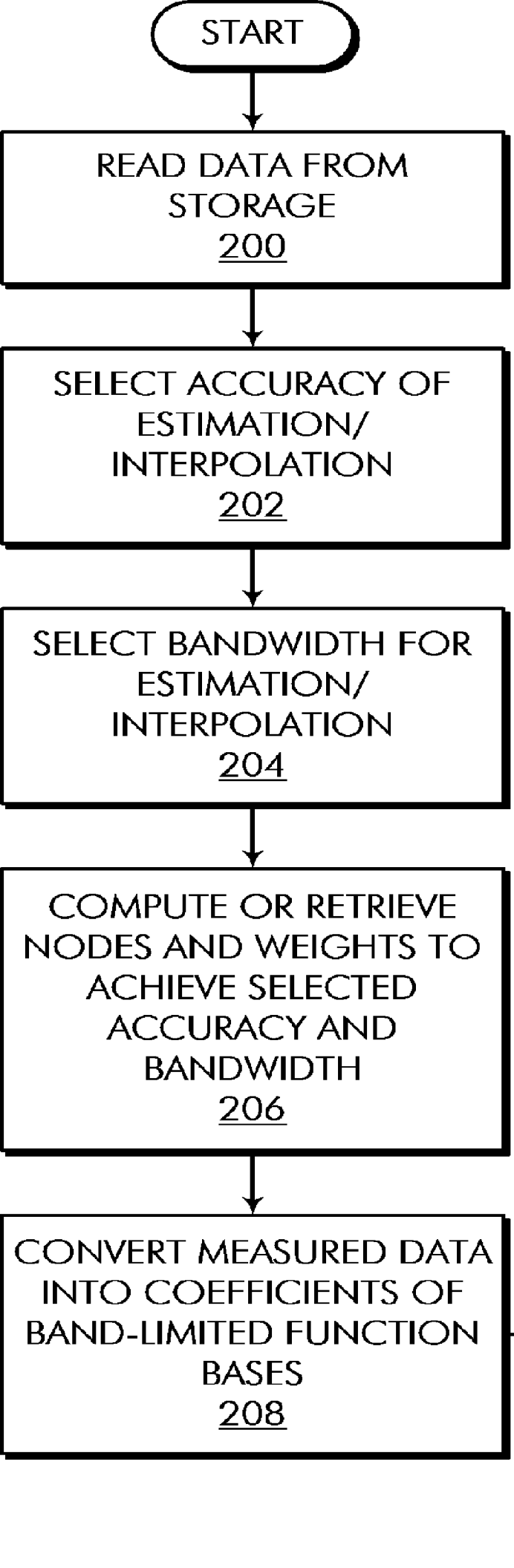
START
READ DATA FROM STORAGE
200
SELECT ACCURACY OF ESTIMATION/ INTERPOLATION
202
SELECT BANDWIDTH FOR ESTIMATION/ INTERPOLATION
204
COMPUTE OR RETRIEVE NODES AND WEIGHTS TO ACHIEVE SELECTED ACCURACY AND BANDWIDTH
206
CONVERT MEASURED DATA INTO COEFFICIENTS OF BAND-LIMITED FUNCTION BASES
208
EVALUATE INTERPOLATED MEASURED DATA FOR FURTHER PROCESSING
210
END

FIGURE 2

Electronic Version
Stylesheet Version v1.1.1

Description

METHOD AND APPARATUS FOR EFFICIENT DATA ACQUISITION AND INTERPOLATION

CONTEXTUAL SUMMARY OF THE INVENTION

[0001] In a spectrum of very diverse industries, data sequences are recorded and users of these data wish to approximate the underlying functions at points other than the data recording points. Some examples of data acquired/recorded include but are not limited to seismic data, gravity data, magnetic data, digital and scanned pictures, moving pictures, etc.

[0002] Typically the data sequences are sampled at equally spaced nodes like in the case of digital pictures and the typical methods used currently for approximating/interpolating these data sequences are based on Fourier methods and/or on polynomials. There are two problems with using Fourier and/or polynomials for approximating non-periodic data. First, the approximation at the edges of the

data is of poorer quality than that in the middle. Second, the number of nodes necessary for a quality approximation is higher than minimally possible.

[0003] A preferred embodiment of the present invention deals with both problems, by providing a high quality approximation at the edges and at the same time using the minimal number of nodes for the approximation. The teachings of the present invention may be applied in many different industries and to many different types of data, since they enable a computationally efficient data approximation /interpolation for general types of non-periodic non-equally spaced band-limited data with no additional assumptions.

[0004] A preferred embodiment of the present invention applies the general teachings of the present invention to the area of seismic data acquisition and data processing.

[0005] Almost all geophysical exploration, and in particular hydrocarbon exploration, includes the use of seismic methods. Seismic exploration generally begins with a seismic data acquisition in an area that has been identified as promising for hydrocarbon exploration. Seismic data acquisition surveys use acoustic sources (generally referred to as “shots”) as a source of seismic waves. Those seismic

waves propagate radially through the ground in accordance with the acoustic impedance (analogous to electrical impedance in electric circuit theory) of the geologic layer(s) through which the waves travel. For example, in Figure 1, point S represents the location of such an acoustic source with respect to a vertical cross-section of ground showing two geologic layers or "strata" 100 and 102. Line 104 represents the direction of travel for a point on the radiating seismic wavefront generated by the source at S. Point R lies on the interface between two geologic layers having different acoustic impedances. According to basic principles of physics, when a wavefront comes into contact with the interface between two media of different impedances (*i.e.*, an impedance "mismatch"), at least a portion of the wave energy is reflected back from the interface in the general direction of the source. Generally speaking, a portion of the wave energy will also be transmitted across the interface, although the direction of the transmitted wavefront may change. This change in direction is known as diffraction. Well-understood physical laws, such as Snell's law, govern the velocity and direction of these reflected and refracted waves. Thus, because the velocity and direction of incident and reflected or re-

fracted waves can be determined mathematically, it is possible to identify the locations of acoustic impedance mismatches by measuring the amount of time it takes for a reflected/refracted wave to reach an observation point on the surface.

[0006] For example, in Figure 1, an incident wavefront travelling in the direction of line 104 will reach the interface between layer 100 and layer 102 at point R, at which point the impedance mismatch between layer 100 and layer 102 causes a reflection of the wave to travel in the direction of line 106 to point D (the detection point) where the arrival time of the reflected wave can be measured. Since the velocity and direction of travel of the incident and reflected wave can be determined mathematically, the depth of point R, as measured from the surface can be determined from the arrival time of the reflected wave. This process is known as reflection seismography, and it provides information about the locations, shapes, and material compositions of various geologic features. Knowledge of these features may be used for locating hydrocarbons or other mineral resources, as well as for other uses, such as determining the geologic structure of a particular site for civil engineering purposes, for example. Another applica-

tion for this general type of technology is in the medical field, where ultrasonic acoustic waves are used in a similar fashion to perform medical imaging (*e.g.*, sonograms).

[0007] Returning now to the problem of geophysical exploration, however, it is customary to employ multiple seismic detectors at different points will be used in conjunction with a single acoustic source, to allow seismic data to be obtained over a broad area. Different types of acoustic sources are used in different arrangements, depending on the environment in question. Typically in onshore areas, "Vibroseis" acoustic sources are used to transmit seismic waves on the subsurface, which are transmitted and reflected off several subterranean layers, and eventually a portion of the originally transmitted energy is reflected back towards the earth's surface and received at detectors (receivers), which are spaced at predetermined spatial positions as to minimize the acquisition cost and increase the seismic data acquisition survey resolution. (Vibroseis was formerly a registered trademark of Conoco, Inc., but is now recognized as a generic term in the art). For offshore areas, the seismic vessel performing the seismic data acquisition uses airguns or waterguns which generate a significant pressure wave that propagates in the

subsurface. The reflected seismic energy travelling back from the subsurface towards the ocean bottom is either received at receiver streamer cables towed by the seismic vessel or by ocean-bottom receivers placed by oil and gas companies.

[0008] Seismic survey data can also be categorized by the dimensionality of the data. "Two-dimensional" seismic data is obtained by placing the detectors in a single line. The information obtained in a two-dimensional survey provides the same type of visual perspective as Figure 1, where the two dimensions are linear position along the line of detectors (horizontal) and depth (vertical, plotted downward). One of ordinary skill in the art will recognize that the depth coordinate is interchangeable with time, since the arrival time of a reflected wave determines the depth of the reflector. Mathematically speaking, two-dimensional seismic data is represented as two dimensional scalar field, where the scalar value represents a magnitude of the seismic signal received at a particular surface position at a particular time.

[0009] "Three-dimensional" seismic data is obtained by arranging the detectors over a two-dimensional area on the surface. Usually, the detectors are arranged in some form of

grid. A set of three-dimensional seismic data is a three-dimensional scalar field that represents a magnitude of the seismic signal received at a particular surface position at a particular time. During seismic data acquisition, the data are typically recorded in digital media, and their sheer volume, particularly in the case of a three-dimensional survey, can easily exceed several terabytes (1×10^{12} bytes).

[0010] After the raw seismic data is obtained, it is then processed to extract useful information, typically in a graphic format. A variety of seismic data processing algorithms have been developed over the years. These algorithms take into account the seismic source and receiver positions, estimate the acoustic/elastic constants of the subsurface, and finally "migrate" the data, meaning that they identify the proper locations of the subsurface reflectors (*i.e.,* the geologic features that cause the reflection of seismic waves).

[0011] An objective of the present invention is to provide an acquisition system that has a minimal number of nodes for a fixed bandwidth of the measured data and a given accuracy of measurements. If the measured data were periodic, then the optimal distribution of nodes is that of equally spaced nodes, where the minimal number of

nodes is given by the Nyquist criterion. Specifically, it is sufficient to have two nodes per highest wavelength (or wave number) that we want to measure.

[0012] Since data periodicity rarely occurs in the real world, data periodicity is often enforced by applying smooth windows on the edges of the data, thus reducing the useable portion of the data. Alternatively, one can use polynomial-based interpolation, which requires sampling at rates higher (by at least a factor of two in practical applications) than the Nyquist criterion. The present invention provides a method and apparatus for optimal data acquisition using the generalized Gaussian nodes for band-limited exponentials. These generalized Gaussian nodes and corresponding weights are constructed for a given bandwidth and for a given accuracy of measurements. It can be shown that for a large number of nodes, the sampling rate of this method for non-periodic data approaches the Nyquist sampling rate for the periodic data (2 nodes per wavelength), and is optimal for a given bandwidth and a given accuracy of measurements.

[0013] The generalized Gaussian nodes can be computed via the algorithm described in the herein-incorporated reference BEYLKIN, Gregory. On generalized Gaussian quadratures

for exponentials and their applications. *Applied and Computational Harmonic Analysis,* 2002 vol. 12, no. 3, p. 332-373. Alternatively, the generalized Gaussian nodes can be computed via the algorithm described in the herein-incorporated reference XIAO, H.Prolate spheroidal wavefunctions, quadrature and interpolation. *Inverse Problems,* 2001 vol. 17, p. 805-838.

[0014] Additional weighting can be incorporated into the nodes and weights using the algorithm in the aforementioned BEYLKIN, et al. reference.

[0015] It should be noted that the nodes of the generalized Gaussian quadratures do not accumulate excessively near the end points. It should further be noted that the rate of accumulation reported in the aforementioned XIAO, et al. reference is in error.

[0016] In case of malfunctioning hardware or problems with positioning of sensors, some of the desired data points may be absent. A preferred embodiment of the present invention allows one to fill in the missing information, perhaps using a lower band limit, provided that the number of missing points is not excessive.

[0017] A preferred embodiment of the present invention comprises the following steps (presented in flowchart form in

Figure 2):

- reading from a magnetic disk or tape or RAM or any other storage device, or directly from the sensors a set of data, which may be one, two or three-dimensional, or may be multidimensional (block 200);
- selecting an accuracy with which the data is to be estimated and/or interpolated; typically, this accuracy will correspond to the accuracy of the measurements (block 202);
- selecting a bandwidth within which the data is to be estimated and/or interpolated; typically this is guided by the practical requirements of the acquisition system (block 204);
- computing the nodes and the weights that are minimally required to achieve the selected accuracy and bandwidth or retrieving pre-computed nodes and weights to achieve the selected accuracy and bandwidth (block 206);
- converting the measured data into the coefficients of band-limited exponentials and/or the Prolate Wave Spheroidal Functions and/or any other bases for band-limited functions. The estimation is done using either exact or approximate prolate spheroidal wave

functions or interpolating basis of band-limited functions in order to control the condition numbers of matrices involved (block 208);

•using the coefficients computed at step 5, evaluate the interpolated measured data at any point for any and/or all tasks that maybe required for said data, including but not limited to further processing, and/or graphical rendering, and/or transmission, and/or storage (block 210).

On Generalized Gaussian Quadratures for Exponentials and their Applications

G. Beylkin [1] and *L. Monzón* [2]

Department of Applied Mathematics
University of Colorado at Boulder
526 UCB, Boulder, CO 80309-0526

Abstract

We introduce new families of Gaussian-type quadratures for weighted integrals of exponential functions and consider their applications to integration and interpolation of bandlimited functions.

We use a generalization of a representation theorem due to Carathéodory to derive these quadratures. For each positive measure, the quadratures are parameterized by eigenvalues of the Toeplitz matrix constructed from the trigonometric moments of the measure. For a given accuracy ϵ, selecting an eigenvalue close to ϵ yields an approximate quadrature with that accuracy. To compute its weights and nodes, we present a new fast algorithm.

These new quadratures can be used to approximate and integrate other essentially bandlimited functions, such as Bessel functions and prolate spheroidal wave functions. We also develop, for a given precision, an interpolating basis for bandlimited functions on an interval.

[1] Research supported in part by DARPA grants F49620-98-1-0491 and F30602-98-1-0154 and University of Virginia subcontract MDA972-00-1-0016.

[2] Research supported in part by DARPA grant F30602-98-1-0154.

On Generalized Gaussian Quadratures for Exponentials and their Applications

G. Beylkin [1] and *L. Monzón* [2]

Department of Applied Mathematics
University of Colorado at Boulder
526 UCB, Boulder, CO 80309-0526

I Introduction

In this paper we relate the Carathéodory representation of finite sequences in terms of exponential sums with the computation of generalized Gaussian quadratures for exponentials. Generalized Gaussian quadratures were investigated by Markov [16, 17], Krein [12], Karlin [11] and, more recently, by Yarvin and Rokhlin [29]. In [29] the authors introduce practical algorithms for computing the nodes and weights of generalized Gaussian quadratures. The resulting approximations have a number of important applications in a variety of fast algorithms [30], [3].

The Carathéodory representation theorem asserts existence and uniqueness of the representation of a finite sequence of complex numbers $\boldsymbol{c} = (c_1, c_2, \ldots, c_N)$, $\boldsymbol{c} \neq 0$, in the form

$$c_k = \sum_{j=1}^{M} \rho_j e^{i\pi\theta_j k}, \tag{1.1}$$

for $k = 1, 2, \ldots, N$ and $M \leq N$, where $-1 < \theta_j \leq 1$ and $\rho_j > 0$. Carathéodory representation (1.1) has been the foundation for a number of algorithms for spectral estimation, in particular [19] is known in electrical engineering literature as the Pisarenko method. In this paper we develop a fast algorithm for finding M, the phases $\boldsymbol{\theta} = (\theta_1, \cdots, \theta_M)$ with $|\theta_j| \leq 1$, and the weights $\boldsymbol{\rho} = (\rho_1, \cdots, \rho_M)$. Our algorithm differs from that described in [19], although the basic approach is similar. We achieve finite but arbitrary accuracy and our algorithm requires $O(N(\log N)^2)$ operations ($O(N^2)$ in a simpler version).

One can view finding M, the phases $\boldsymbol{\theta}$, and the weights $\boldsymbol{\rho}$ as a nonlinear inverse problem for the unequally spaced discrete Fourier transform [4], [1]. It is interesting to note that the associated linear problem, namely the problem where M and $|\theta_j| \leq 1$ in (1.1) are given, can be arbitrarily ill conditioned. In other words, the condition number

[1]Research supported in part by DARPA grants F49620-98-1-0491 and F30602-98-1-0154 and University of Virginia subcontract MDA972-00-1-0016.

[2]Research supported in part by DARPA grant F30602-98-1-0154.

of the Vandermonde matrix $\{e^{i\pi\theta_j k}\}_{k,j=1,\ldots,M}$ can be arbitrarily large. On the other hand, the nonlinear problem is well posed and we will show the l^2-norm estimate

$$\|\boldsymbol{\rho}\|_2 \leq \sqrt{2}\,\|\mathbf{c}\|_2. \tag{1.2}$$

The main goal of this paper is to extend Carathéodory representation and use it to compute quadratures for integrals involving exponentials, as well as the Bessel and the prolate spheroidal wave functions (PSWF). These bandlimited or essentially bandlimited functions play a central role in many problems of signal processing and numerical analysis. We also consider the associated interpolation problem involving these functions. Specifically, we develop methodology to represent bandlimited functions on an interval using exponentials $\{e^{ic x t_l}\}_{l=1}^{M}$, where the bandlimit c is a positive real constant and t_l, $|t_l| \leq 1$, are phases computed for a given c and accuracy ϵ. With this approach, we are no longer limited to representing periodic functions as is the case with Fourier series.

In order to consider bandlimited functions on an interval, the PSWF were introduced in [23] and [14]. Recently, a method for computing generalized Gaussian quadratures for PSWF and, as a consequence, for bandlimited exponentials, was introduced in [28]. In [28] the authors first construct quadratures for the PSWF using the fact that the first n of these functions form a Chebyshev system, for any n. The approach for computing generalized Gaussian quadratures in [29] relies on a variant of Newton's method in conjunction with a continuation procedure. As a method it is quite general but is computationally intensive, although in many applications speed is not a limitation.

Our approach differs from that in [28]. We first develop a method for constructing optimal nodes and weights for integrals involving exponentials and then show that the same nodes and weights also provide quadratures for other essentially bandlimited functions, e. g. the PSWF.

The reader familiar with Gaussian quadratures should be warned that our methodology for generating quadratures is substantially different from the existing methods. The resulting quadrature formulas do not coincide with any other existing quadrature but, numerically, they are close to those in [28].

As a method for constructing generalized Gaussian quadratures, our results are limited to integrals (with a fairly arbitrary measure) involving exponentials. Our algorithm involves finding eigenvalues and eigenvectors of a Toeplitz matrix constructed from trigonometric moments of the measure and then computing the roots on the unit circle for appropriate eigenpolynomials. In particular, each eigenpolynomial with distinct roots gives rise to an identity which, for small eigenvalues, provides us with a Gaussian-type quadrature and also with a representation of positive definite Hermitian Toeplitz matrices. In these identities the size of the eigenvalue determines the accuracy of the quadrature formula.

It turns out that in the case of the weight leading to PSWF, the nodes of the corresponding Gaussian quadratures are zeros (appropriately scaled to the interval $[-1, 1]$)

of discrete PSWF corresponding to small eigenvalues.

As an application, we use the new quadratures to obtain efficient approximations of nonperiodic bandlimited functions in terms of linear combinations of exponentials. In fact, we consider integrals of the form

$$u(x) = \int_{-1}^{1} \mathrm{e}^{\mathrm{i}\,c\,t\,x}\, d\mu(t), \tag{1.3}$$

where $d\mu(t)$ is a measure, typically $d\mu(t) = w(t)dt$, with w a weight function (w is a real, non-negative, integrable function with $\int_{-1}^{1} w(\tau)d\tau > 0$). For a given bandlimit $c > 0$ and accuracy $\epsilon > 0$, our goal is to approximate $u(x)$ on the interval $[-1, 1]$ using the sum

$$\tilde{u}(x) = \sum_{k=1}^{M} w_k \mathrm{e}^{\mathrm{i}\,c\,\theta_k\,x}, \tag{1.4}$$

where $w_k > 0$ and $M = M(c, \epsilon)$, so that

$$|u(x) - \tilde{u}(x)| \leq \epsilon \quad \text{for} \quad x \in [-1, 1]\,. \tag{1.5}$$

Since it is appropriate to view (1.4) as a quadrature, we will refer to θ_k as nodes and w_k as weights.

In order to find $\tilde{u}$ as in (1.4)–(1.5), we sample the function u in (1.3) at equally spaced points so that we satisfy or exceed the sampling rate dictated by the Nyquist criterion. The equally spaced samples of u can be viewed as the trigonometric moments of the (rescaled) measure in (1.3). We extend Carathéodory representation to find M, the nodes $\{\theta_k\}_{k=1}^{M}$, and the weights $\{w_k\}_{k=1}^{M}$. We then use the same M, nodes, and weights to define $\tilde{u}$ in (1.4) for all $x \in (-1, 1)$ and show that (1.5) holds if u in (1.3) was sufficiently oversampled.

For the interpolation problem for bandlimited functions, we consider the linear space of functions $\mathcal{E}_c = \left\{ f \in L_\infty[-1, 1] : f(x) = \sum_{k\in\mathbb{Z}} a_k \mathrm{e}^{\mathrm{i}b_k\,x} : \{a_k\} \in l^1\,,\ |b_k| \leq c,\ \forall k. \right\}$. These functions are not necessarily periodic in $[-1, 1]$. The interpolation problem amounts to representing, with accuracy ϵ, the functions in $\mathcal{E}_c$ by a fixed set of exponentials $\left\{\mathrm{e}^{\mathrm{i}c\,t_k\,x}\right\}_{k=1}^{M}$, where M is as small as possible. We show that by finding quadrature nodes $\{t_k\}_{k=1}^{M}$ for exponentials with bandlimit $2c$ and accuracy ϵ^2, we in fact obtain, with accuracy ϵ, a basis for bandlimited functions with bandlimit c. The connection between the generalized Gaussian quadratures for exponentials and the interpolation problem was first described in [28]. We use similar results to construct interpolatory bases for arbitrary accuracy ϵ.

The paper is organized as follows. We present a brief description of the Pisarenko method to obtain the classical Carathéodory representation and we derive the estimate (1.2) in Section II. In Section III we discuss generalized Gaussian quadratures for weighted integrals and prove some of their properties for weights supported

inside $[-\frac{1}{2}, \frac{1}{2}]$. In Section IV we introduce new families of Gaussian-type quadratures. We develop a fast algorithm in Section V to compute the nodes and weights of these quadratures. We solve the approximation problem (1.3)–(1.5) in Section VI and use it in the next two sections to obtain quadratures and interpolating bases for bandlimited functions. We also discuss various examples to illustrate these results. Finally, conclusions are presented in Section IX and auxiliary material in the Appendix.

II Caratheodory representation

Carathéodory representation solves the trigonometric moments problem and can be stated as follows (see [7, Chapter 4]),

Theorem II.1 *Given N complex numbers $\boldsymbol{c} = (c_1, c_2, \ldots, c_N)$, not all zero, there exist unique $M \leq N$, positive numbers $\boldsymbol{\rho} = (\rho_1, \rho_2, \ldots, \rho_M)$ and distinct real numbers $\theta_1, \theta_2, \ldots, \theta_M$, $-1 < \theta_j \leq 1$, such that*

$$c_k = \sum_{j=1}^{M} \rho_j e^{i\pi\theta_j k} \quad \textit{for} \quad k = 1, 2, \ldots, N. \tag{2.1}$$

Although the theorem applies to all finite sequences $\boldsymbol{c}$ of complex numbers, it is useful in practical applications if there is a reason to seek representations of the form (2.1) with positive weights ρ_j. For example, if the sequence $\boldsymbol{c}$ are the values of a covariance function, then this theorem provides the foundation for several spectral estimation algorithms in signal processing, e.g. the so-called Pisarenko method (see [19] for more details). In this paper, we are interested in the case where the sequence $\boldsymbol{c}$ contains the trigonometric moments of a positive weight.

Given $\boldsymbol{c}$, finding M, the phases $\boldsymbol{\theta} = (\theta_1, \cdots, \theta_M)$, $|\theta_j| \leq 1$ and the positive weights $\boldsymbol{\rho}$ can be viewed as a nonlinear inverse problem for the unequally spaced discrete Fourier transform [4], [1].

As discussed in the introduction, the problem of finding $\boldsymbol{\rho}$ where $\boldsymbol{c}$, M, and $|\theta_j| \leq 1$ are given, can be arbitrarily ill conditioned. In contrast, the phases θ_j in Carathéodory representation are related to the vector $\boldsymbol{c}$ and we have a stability estimate:

Theorem II.2 *Vectors $\boldsymbol{c}$ and $\boldsymbol{\rho}$ as in Theorem II.1 satisfy*

$$\|\boldsymbol{\rho}\|_2 \leq \sqrt{2}\, \|\boldsymbol{c}\|_2.$$

For the proof see Appendix A.

Grenander and Szegö's proof of Carathéodory representation [7] provides a method to obtain M, the phases $\boldsymbol{\theta}$, and the weights $\boldsymbol{\rho}$. It is also the foundation for Pisarenko's method for spectral estimation [19]. We now outline its main points.

II.1 Algorithm I: Method to obtain M, $\boldsymbol{\theta}$, and $\boldsymbol{\rho}$.

1) Given $\boldsymbol{c} = (c_1, c_2, \ldots, c_N)$, we extend the definition of c_k to negative k as $c_{-k} = \overline{c_k}$ and we define c_0 so that the $(N+1) \times (N+1)$ Toeplitz matrix $\boldsymbol{T}_N$ of elements $(\boldsymbol{T}_N)_{kj} = c_{j-k}$, has nonnegative eigenvalues and at least one eigenvalue is equal to zero.

2) Define M as the rank of $\boldsymbol{T}_N$. By construction, we have $M \leq N$. We also say that M is the *rank* of the representation (2.1).

3) Let $\boldsymbol{T}_M$ be the top left principal submatrix of order $M+1$ of $\boldsymbol{T}_N$. That is, the matrix $\boldsymbol{T}_M$ has elements $(c_{j-k})_{0\leq k,j\leq M}$. Find the eigenvector $\boldsymbol{q}$ corresponding to the zero eigenvalue of $\boldsymbol{T}_M$.

4) Construct the polynomial (eigenpolynomial) whose coefficients are the entries of the eigenvector $\boldsymbol{q}$. As shown in [7, p. 58], the M roots of this eigenpolynomial are distinct and have absolute value one. The phases of these roots are the numbers θ_j.

5) Find the weights $\boldsymbol{\rho}$ by solving the Vandermonde system (2.1) for $k = 1, \cdots, M$. They will, in addition, satisfy $\sum_k \rho_k = c_0$.

Remark II.1 With the extension of the sequence c_k, (2.1) is valid for $|k| \leq N$. If $\boldsymbol{q} = (q_0, \cdots, q_M)$ is the eigenvector obtained in Part 3) of Algorithm II.1, then

$$\sum_{k=0}^{M} c_{k+s} q_k = 0, \tag{2.2}$$

for all $s, -N \leq s \leq 0$. In other words, we have found an order M recurrence relation for the original sequence $\{c_k\}_{k=1}^{N}$.

Remark II.2 In practice, we are interested in using Carathéodory representation if M is small compared with N, or more generally, if most weights are smaller than the accuracy sought. However, in such cases, $\boldsymbol{T}_N$ has a large (numerical) null subspace that causes severe numerical problems in determining c_0, the rank M, and the eigenvector $\boldsymbol{q}$.

Nevertheless, if the sequence $\boldsymbol{c}$ are the trigonometric moments of an appropriate weight, we will be able to modify the previous method in order to obtain the phases θ_j in an efficient manner. In this setting, the phases and weights in Carathéodory representation can be thought of as the nodes and weights of a Gaussian-type quadrature for weighted integrals. Once the phases are obtained, Theorem II.2 assures that the computation of the weights is a well-posed problem. In Section V.2 we present a fast algorithm to obtain the weights by evaluating certain polynomials at the nodes $\mathrm{e}^{\mathrm{i}\pi\theta_j}$.

Remark II.3 Given any Hermitian Toeplitz matrix $\boldsymbol{T}$, let us consider its smallest eigenvalue $\lambda^{(N)}$. It is easy to see that Carathéodory representation implies the following representation of $\boldsymbol{T}$ as a sum of rank one Hermitian Toeplitz matrices,

$$(\boldsymbol{T} - \lambda^{(N)}\boldsymbol{I})_{kl} = \sum_{j=1}^{M} \rho_j \mathrm{e}^{\mathrm{i}\pi\theta_j(l-k)}, \tag{2.3}$$

where ρ_j are positive and $\mathrm{e}^{\mathrm{i}\theta_j}$ are the zeros of the eigenpolynomial corresponding to the eigenvalue $\lambda^{(N)}$.

III Generalized Gaussian Quadratures for Exponentials

III.1 Preliminaries: Chebyshev Systems

In this section we collect some definitions and results related to Chebyshev systems. We follow mostly Karlin and Studden [11] (see also [12]). Readers familiar with this topic may skip this section.

A family of $n+1$ real-valued functions $u_0, \ldots, u_n$ defined on an interval $I = [a, b]$ is a *Chebyshev system* (T-system) if any nontrivial linear combination

$$u(t) = \sum_{j=0}^{n} \alpha_j u_j(t), \tag{3.1}$$

has at most n zeros on the interval I. This property of a T-system can be viewed as a generalization of the same property for polynomials. Indeed, the family $\{1, t, t^2, \ldots, t^n\}$ provides the simplest example of a Chebyshev system.

Alternatively, a T-system over $[a, b]$ may be defined by the condition that the $n+1$ order determinant is non-vanishing,

$$\det \begin{bmatrix} u_0(t_0) & u_0(t_1) & \cdots & u_0(t_n) \\ u_1(t_0) & u_1(t_1) & \cdots & u_1(t_n) \\ \cdots & \cdots & \cdots & \cdots \\ u_n(t_0) & u_n(t_1) & \cdots & u_n(t_n) \end{bmatrix} \neq 0, \tag{3.2}$$

whenever $a \leq t_0 < t_1 < \cdots < t_n \leq b$. Without loss of generality, the determinant can be assumed positive.

Let $u_0, \ldots, u_n$ be a T-system on the interval I. The moment space $\mathcal{M}_{n+1}$ with respect to $u_0, \ldots, u_n$ is defined as the set

$$\mathcal{M}_{n+1} = \{\boldsymbol{c} = (c_0, \ldots, c_n) \in \mathbb{R}^{n+1} \,|\, c_j = \int_I u_j(t)\, d\mu(t),\ j = 0, \ldots, n\}, \tag{3.3}$$

where the measure $\mu(t)$ ranges over the family of nondecreasing right-continuous functions of bounded variation on the interval I. It can be shown that the moment space is a closed convex cone. We will denote the *interior* of the moment space $\mathrm{Int}(\mathcal{M}_{n+1})$.

Let us consider a representation of a point $\boldsymbol{c} = (c_0, \ldots, c_n) \in \mathcal{M}_{n+1}$

$$c_j = \sum_{k=1}^{m} \rho_k u_j(t_k), \quad j = 0, \ldots, n\,, \tag{3.4}$$

where $\rho_k > 0$, $a \leq t_k \leq b$, $k = 1, \ldots, m$. The *index* $\mathcal{I}(\boldsymbol{c})$ of a point $\boldsymbol{c} \in \mathcal{M}_{n+1}$ is defined as the minimum number of points t_k that are used in the representation (3.4), where the

boundary points $t_k = a$ and $t_k = b$ are counted as $1/2$ and the points in the interior of the interval $a < t_k < b$ are counted as 1.

The representation (3.4) induces a generalized Gaussian quadrature for the integral with the measure that defines the point $\boldsymbol{c}$ in the moment space while the index describes the number of nodes necessary for the quadrature. The following theorems (see [11] and [12]) generalize to any T-system the usual Gaussian quadratures for the polynomials $\{1, t, \cdots, t^n\}$.

Theorem III.1 *A point $\boldsymbol{c} \in \mathcal{M}_{n+1}$, $\boldsymbol{c} \neq 0$, is a* boundary *point of $\mathcal{M}_{n+1}$ if and only if $\mathcal{I}(\boldsymbol{c}) < (n+1)/2$.*

Theorem III.2 *Let $u_0, \ldots, u_{2m}$ be a T-system on $[a, b]$ and $\boldsymbol{c}$ be a boundary point of $\mathcal{M}_{2m+1}$. Then there exist a unique representations with the index less than $m+1$ which involves no more than $m+1$ nodes.*

Theorem III.3 *Let $u_0, \ldots, u_{2m}$ be a T-system on $[a, b]$ and $\boldsymbol{c}$ be an interior point of $\mathcal{M}_{2m+1}$. Then there exist at least two representations with the index $m+1/2$ (with $m+1$ terms). Both of them have $m+1$ nodes one of which is the end point of the interval.*

If the functions $u_0, \ldots, u_n$ are periodic on the interval I and satisfy (3.2), then they define a periodic T-system. A periodic T-system always involves an odd number of functions. Indeed, since the system is defined on a circle, the equally spaced values $(t_0, \cdots, t_n)$ can be continuously rotated into $(t_n, \cdots, t_0)$. If the number of functions were even, such rotation would change the sign of the determinant in (3.2) and, due to the continuous dependence on $(t_0, \cdots, t_n)$, would force the determinant to vanish at some intermediate point.

For periodic systems holds ([11], [12]):

Theorem III.4 *Let $u_0, \ldots, u_{2m}$ be a periodic T-system on $[-1, 1]$ and $\boldsymbol{c}$ be an interior point of $\mathcal{M}_{2m+1}$. Then for each point t_0, $-1 \leq t_0 \leq 1$, there exist a unique representation with the index $\mathcal{I}(\boldsymbol{c}) = m+1$ (with $m+1$ terms) involving t_0 as a node.*

III.2 Generalized Gaussian Quadratures for Exponentials

Let us consider a family of real periodic functions

$$1, \cos(\pi t), \sin(\pi t), \ldots, \cos(\pi m t), \sin(\pi m t) \tag{3.5}$$

on the interval $[-1, 1]$. We treat the boundary points -1 and 1 as identical so that (3.5) is defined on the circle. The system of functions in (3.5) is a periodic Chebyshev system (T-system) in $[-1, 1]$ (see [11], [12] and Section III.1 for a brief summary).

We also consider this family on a proper subinterval of $[-1, 1]$. On any subinterval $[a, b] \subset [-1, 1]$ the family in (3.5) is a T-system.

Let us consider the moments of the measure $\omega(\tau)d\tau$, where $\omega(\tau)$ is a weight function,

$$\alpha_k = \int_{-1}^{1} \omega(\tau)\cos(\pi k\tau)d\tau,\ k = 0, 1, \ldots, m, \tag{3.6}$$

and

$$\beta_k = \int_{-1}^{1} \omega(\tau)\sin(\pi k\tau)d\tau,\ k = 1, \ldots, m. \tag{3.7}$$

We also consider complex-valued moments,

$$\gamma_k = \alpha_k + \mathrm{i}\beta_k = \int_{-1}^{1} \omega(\tau)\mathrm{e}^{\mathrm{i}\pi k\tau}d\tau,\ k = 1, \ldots, m. \tag{3.8}$$

Let $\mathcal{M}_{2m+1}$ be the moment space and $\mathrm{Int}(\mathcal{M}_{2m+1})$ its interior, as defined in Section III.1. We have

Theorem III.5 ([11], VI, Sec.4) *For the periodic T-system* (3.5) *a point* $\mathbf{c} = \{\alpha_0, \alpha_1, \beta_1, \ldots, \alpha_m, \beta_m\}$ *is a point of the moment space* $\mathcal{M}_{2m+1}$ *if and only if the Toeplitz matrix* $\{\gamma_{k'-k}\}_{k,k'=0,\ldots,m}$ *is non-negative definite.*

Furthermore, $\mathbf{c} \in \mathrm{Int}(\mathcal{M}_{2m+1})$ *if and only if the Toeplitz matrix* $\{\gamma_{k-k'}\}_{k,k'=0,\ldots,m}$ *is positive definite.*

We also have

Theorem III.6 ([11], VI, Sec.2) *A point* $\boldsymbol{c} = \{\alpha_0, \alpha_1, \beta_1, \ldots, \alpha_m, \beta_m\}$ *is a boundary point of the moment space* $\mathcal{M}_{2m+1}$ *if and only if there is a unique representation*

$$\gamma_k = \sum_{j=1}^{m'} \omega_j \mathrm{e}^{\mathrm{i}\pi\theta_j k}, \tag{3.9}$$

where $m' \leq m$ *and* $-1 \leq \theta_j \leq 1$.

If $\mathbf{c} \in \mathrm{Int}(\mathcal{M}_{2m+1})$, *then for each* $\tau_0 \in [-1, 1]$ *there exists a unique representation with* $m+1$ *nodes including* τ_0 *as a node, that is*

$$\gamma_k = \sum_{j=1}^{m} \omega_j \mathrm{e}^{\mathrm{i}\pi\theta_j k} + \omega_0 \mathrm{e}^{\mathrm{i}\pi\tau_0 k}, \tag{3.10}$$

where $-1 \leq \theta_j \leq 1$.

Let us consider weights ω supported in a subinterval of $[-1, 1]$. We then prove

Theorem III.7 *Let ω be a weight supported in some interval $I = [a, b]$, $I \subseteq [-1, 1]$. Then, there exists a unique representation*

$$\int_{-1}^{1} \omega(t) \mathrm{e}^{\mathrm{i}\pi k t} dt = \sum_{j=1}^{m} \omega_j \mathrm{e}^{\mathrm{i}\pi\theta_j k} + \omega_0 (-1)^k \quad \textit{for} \quad |k| \leq m, \tag{3.11}$$

where $a < \theta_j < b$ and $\omega_j > 0$ for $j = 0, \ldots, m$.

Moreover, if $I = [-a, a]$, where $0 < a \leq 1/2$, then

$$\omega_0 \leq \frac{4 \int_{-\frac{1}{2}}^{\frac{1}{2}} \omega(t)\, dt}{2 + (2 + \sqrt{3})^m + (2 - \sqrt{3})^m}. \tag{3.12}$$

Proof

Let us start by considering the periodic T-system (3.5) and $\boldsymbol{c} = \{\alpha_0, \alpha_1, \beta_1, \ldots, \alpha_m, \beta_m\}$ the point in the moment space obtained from the measure $d\mu(t) = \omega(t)\, dt$. It is easy to show that the Toeplitz matrix $\{\gamma_{j-k}\}$, obtained for the moments in (3.8), is positive definite (see (4.7)). Thus, Theorem III.5 and (3.10) with $\tau_0 = 1$ imply a unique representation (3.11) with $-1 < \theta_j < 1$ and $k = 0, \cdots, m$. Since the weights are real, (3.11) also holds for $k = -m, \cdots, -1$. We want to show that, in fact, $a < \theta_j < b$.

Since the weight ω is supported in $[a, b] \subseteq [-1, 1]$, we can also consider $[a, 1]$ as its interval of definition. We note that the functions in (3.5) form a Chebyshev system on this interval (in fact, on any subinterval of $[-1, 1]$). Using Theorem III.3 we construct a representation which includes the boundary point 1 of the interval $[a, 1]$ as a node. However, this representation also holds on $[-1, 1]$ where (3.11) guarantees uniqueness. Thus, to avoid a contradiction, we conclude that $a < \theta_j \leq 1$ in (3.11). Similarly, let us consider the weight ω in $[-1, b]$. By the same argument we obtain that $-1 \leq \theta_j < b$ (the points -1 and 1 are identical on $[-1, 1]$). Therefore, we conclude that $a < \theta_j < b$ and (3.11) is established.

Let us now consider a periodic trigonometric polynomial

$$v_m(t) = T_m(1 - \cos(\pi t)), \tag{3.13}$$

where T_m is the Chebyshev polynomial of degree m. Since the degree of $v_m(t)$ does not exceed m, we have from (3.11)

$$\int_{-\frac{1}{2}}^{\frac{1}{2}} v_m(t)\, \omega(t)\, dt = \sum_{j=1}^{m} \omega_j v_m(\theta_j) + \omega_0 v_m(1), \tag{3.14}$$

where $-1/2 < \theta_j < 1/2$.

Let us compute $v_m(1) = T_m(2)$. Using the three-term recursion for the Chebyshev polynomials, we obtain

$$v_m(1) = ((2+\sqrt{3})^m + (2-\sqrt{3})^m)/2. \tag{3.15}$$

Since in the interval $[-1/2, 1/2]$ the absolute value of v_m does not exceed one,

$$\omega_0\, v_m(1) = \left| \int_{-\frac{1}{2}}^{\frac{1}{2}} v_m(t)\, \omega(t)\, dt - \sum_{j=1}^{m} \omega_j v_m(\theta_j) \right| \leq \int_{-\frac{1}{2}}^{\frac{1}{2}} \omega(t)\, dt + \sum_{j=1}^{m} \omega_j. \tag{3.16}$$

Setting $k = 0$ in (3.11), we obtain

$$\sum_{j=1}^{m} \omega_j = \int_{-\frac{1}{2}}^{\frac{1}{2}} \omega(t)\, dt - \omega_0 \tag{3.17}$$

and, combining with (3.16), we arrive at (3.12). □

Remark III.1 Since the numerator in (3.12) remains bounded and the denominator grows exponentially fast with m, the coefficient ω_0 is very small even for m of moderate size.

IV A new family of Gaussian-type quadratures

Let us consider the trigonometric moments of a weight $w(\tau)$,

$$t_k = \int_{-1}^{1} \mathrm{e}^{\mathrm{i}\pi\tau k} w(\tau)\, d\tau. \tag{4.1}$$

In our approach, it is essential to consider only weights supported inside $[-\frac{1}{2}, \frac{1}{2}]$. Only then can the moments t_k be viewed as values of a properly sampled bandlimited function (see (6.2) and (6.3)).

In this section we start by using Carathéodory representation and Theorem III.7 from the previous section, to construct two different Gaussian quadratures for integrals with weight w. These quadratures are exact for trigonometric polynomials of appropriate degree.

We then generalize these types of quadratures further and develop a new family of Gaussian-type quadratures. This family of quadrature formulas is parameterized by the eigenvalues of the Toeplitz matrix

$$\boldsymbol{T} = \{t_{l-k}\}_{0 \le k,l \le N}. \tag{4.2}$$

Among these new quadrature formulas, only those corresponding to eigenvalues of small size are of practical interest. In fact, the size of the eigenvalue determines the error of the quadrature formula. To compute the weights and nodes of these quadratures, we develop a new algorithm which may be viewed as a (major) modification of Algorithm II.1. The new algorithm is described in Section V. The main results of this section are gathered in Theorem IV.1.

We start by using Theorem III.7 to write

$$t_k = \sum_{j=1}^{N} \omega_j \mathrm{e}^{\mathrm{i}\pi\phi_j k} + \omega_0 (-1)^k \quad \text{for} \quad |k| \le N, \tag{4.3}$$

for unique positive weights ω_j and phases ϕ_j in $(-1, 1)$. Then, for any $A(z) = \sum_{|k|\le N} a_k z^k$ in Λ_N, the space of Laurent polynomials of degree at most N, we have

$$\int_{-1}^{1} A(\mathrm{e}^{\mathrm{i}\pi\tau}) w(\tau) d\tau = \sum_{|k|\le N} a_k t_k = \sum_{j=1}^{N} \omega_j A(\mathrm{e}^{\mathrm{i}\pi\phi_j}) + \omega_0 A(-1), \tag{4.4}$$

for unique positive weights ω_j and nodes $\mathrm{e}^{\mathrm{i}\pi\phi_j}$.

Alternatively, using Carathéodory representation (2.1) applied to the sequence $c_k = t_k, 1 \le k \le N$,

$$\int_{-1}^{1} A(\mathrm{e}^{\mathrm{i}\pi\tau}) w(\tau) d\tau \;=\; \sum_{j=1}^{M} \rho_j A(\mathrm{e}^{\mathrm{i}\pi\theta_j}) + (t_0 - c_0)\frac{1}{2}\int_{-1}^{1} A(\mathrm{e}^{\mathrm{i}\pi\tau}) d\tau$$

$$= \sum_{j=1}^{M} \rho_j A(\mathrm{e}^{\mathrm{i}\pi\theta_j}) + \lambda^{(N)} \frac{1}{2} \int_{-1}^{1} A(\mathrm{e}^{\mathrm{i}\pi\tau}) d\tau, \tag{4.5}$$

where $c_0 = \sum_{j=1}^{M} \rho_j$ and $\{\mathrm{e}^{\mathrm{i}\pi\theta_j}\}$ are the roots of the eigenpolynomial corresponding to the smallest eigenvalue $\lambda^{(N)}$ of $\boldsymbol{T}$.

Note that (4.5) is again valid for all $A(z)$ in Λ_N and that the positive weights ρ_j and phases θ_j in $(-1, 1]$ are unique.

Thus, we have two different quadratures that may not coincide. However, by considering $w(\tau)$ supported inside $(-\frac{1}{2}, \frac{1}{2})$, (3.12) implies that w_0 in (4.4) decreases exponentially fast with N and, since $\min w(\tau) = 0$ for $|\tau| \leq 1$, we have

$$\lim_{N \to \infty} \lambda^{(N)} = 0 \tag{4.6}$$

as shown in [7, page 65]. In consequence, for large N, the difference between these two quadratures can be made smaller than the accuracy sought.

A similar reasoning could be applied to other small eigenvalues of $\boldsymbol{T}$ provided we can generalize (4.5) to other eigenvalues and roots of the corresponding eigenpolynomials. For that purpose, we first describe some properties of these eigenpolynomials.

IV.1 Toeplitz matrices for trigonometric moments

We summarize in this section properties of eigenpolynomials of the Toeplitz matrix $\boldsymbol{T}$ with entries $\{t_{l-k}\}_{k,l=0,\cdots,N}$. The matrix $\boldsymbol{T}$ is self-adjoint and positive definite since, for all $\boldsymbol{x} \in \mathbb{C}^{N+1}$,

$$\langle \boldsymbol{T}\boldsymbol{x}, \boldsymbol{x} \rangle = \sum_{k,l=0,\ldots,N} t_{l-k} x_l \overline{x_k} = \int_{-1}^{1} |P_{\boldsymbol{x}}(\mathrm{e}^{\mathrm{i}\pi\tau})|^2 w(\tau) d\tau \tag{4.7}$$

where $\langle \boldsymbol{x}, \boldsymbol{y} \rangle = \sum_k x_k \overline{y_k}$ is the usual inner product of two vectors and $P_{\boldsymbol{x}}(z) = \sum_k x_k z^k$.

More generally, for all $\boldsymbol{x}, \boldsymbol{y} \in \mathbb{C}^{N+1}$, $\boldsymbol{T}$ induces a weighted inner product for trigonometric polynomials,

$$\langle \boldsymbol{T}\boldsymbol{x}, \boldsymbol{y} \rangle = \int_{-1}^{1} P_{\boldsymbol{x}}(\mathrm{e}^{\mathrm{i}\pi\tau}) \overline{P_{\boldsymbol{y}}(\mathrm{e}^{\mathrm{i}\pi\tau})} w(\tau) d\tau. \tag{4.8}$$

Since $\boldsymbol{T}$ is positive definite, there exist an orthonormal basis $\{\boldsymbol{v}^{(k)}\}_{k=0,\ldots,N}$ of eigenvectors of $\boldsymbol{T}$ corresponding to eigenvalues $\lambda^{(0)} \geq \lambda^{(1)} \geq \cdots \geq \lambda^{(N)} > 0$. The corresponding eigenpolynomials $V^{(k)}(z) = \sum_j \boldsymbol{v}_j^{(k)} z^j$ satisfy

$$\int_{-1}^{1} V^{(k)}(\mathrm{e}^{\mathrm{i}\pi t}) \overline{V^{(l)}(\mathrm{e}^{\mathrm{i}\pi t})} d\, t = 2\delta_{kl} \tag{4.9}$$

and, because of (4.8),

$$\int_{-1}^{1} V^{(k)}(\mathrm{e}^{\mathrm{i}\pi t})\overline{V^{(l)}(\mathrm{e}^{\mathrm{i}\pi t})}w(t)dt = \delta_{kl}\,\lambda^{(k)}. \tag{4.10}$$

For a vector $\boldsymbol{x} = (x_0, \cdots, x_N)$, let us define the *reciprocal vector* of $\boldsymbol{x}$ as

$$\boldsymbol{x}_\star = (\overline{x_N}, \cdots, \overline{x_0})$$

and, similarly, for a trigonometric polynomial $P(z)$, the *reciprocal polynomial* of P as

$$P_\star(z) = \overline{P}(z^{-1}) = \overline{P(\overline{z}^{-1})}. \tag{4.11}$$

Since $\boldsymbol{T}$ is Toeplitz Hermitian, we have

$$\boldsymbol{T}\boldsymbol{x}_\star = \lambda\boldsymbol{x}_\star, \quad \text{if} \quad \boldsymbol{T}\boldsymbol{x} = \lambda\boldsymbol{x}.$$

In particular, if λ is a simple eigenvalue, its corresponding eigenspace can be generated by a self-reciprocal eigenvector $\boldsymbol{x}$, i. e., $\boldsymbol{x}_\star = \boldsymbol{x}$ and the associated (self-reciprocal) eigenpolynomial will have roots in pairs $\{\gamma, \overline{\gamma}^{-1}\}$.

IV.2 Gaussian-type quadratures on the unit circle

In this section we present the main results of the paper. We derive new Gaussian-type quadratures valid for any eigenvalue of the matrix $\boldsymbol{T}$ rather than just the smallest eigenvalue λ_N. These quadratures allow us to select the desired accuracy and thus, to construct accuracy dependent families of quadratures.

The nodes of the quadrature in (4.5) are the roots of the eigenpolynomial corresponding to the least eigenvalue of $\boldsymbol{T}$ and, because of Carathéodory representation, we know that these roots are on the unit circle and that the weights are positive numbers. In our generalization, this standard property for the nodes and weights is no longer inforced. However, we will show that for nodes on the unit circle, the corresponding weights are real. Moreover, in all examples we have examined, for all small eigenvalues λ of $\boldsymbol{T}$, their negative weights are associated with the nodes outside the support of the weight and are comparable in size with λ. We believe this property to hold for a wide variety of weights.

We prove the following

Theorem IV.1 *Assume that the eigenpolynomial $V^{(s)}(z)$ corresponding to the eigenvalue $\lambda^{(s)}$ of $\boldsymbol{T}$ has distinct, nonzero roots $\{\gamma_j\}_{j=1}^N$. Then, there exist numbers $\{w_j\}_{j=1}^N$ such that*

i) *For all Laurent polynomials $P(z)$ of degree at most N,*

$$\int_{-1}^{1} P(\mathrm{e}^{\mathrm{i}\pi t})\,w(t)\,dt = \sum_{j=1}^{N} w_j P(\gamma_j) + \lambda^{(s)}\frac{1}{2}\int_{-1}^{1} P(\mathrm{e}^{\mathrm{i}\pi t})\,dt. \tag{4.12}$$

ii) *For each root γ_k with $|\gamma_k| = 1$, the corresponding weight w_k is a real number and*

$$w_k = \int_{-1}^{1} |L_k^s(\mathrm{e}^{\mathrm{i}\pi t})|^2 \, w(t)\, dt - \lambda^{(s)} \frac{1}{2} \int_{-1}^{1} |L_k^s(\mathrm{e}^{\mathrm{i}\pi t})|^2 \, dt, \tag{4.13}$$

where

$$L_k^s(z) = \frac{V^{(s)}(z)}{(V^{(s)})'(\gamma_k)\,(z - \gamma_k)} \tag{4.14}$$

is the Lagrange polynomial associated with the root γ_k.

iii) *If $\lambda^{(s)}$ is a simple eigenvalue, then for $k = 1, \cdots, N$ the weight w_k is nonzero and*

$$\frac{1}{w_k} = \sum_{\substack{0 \le l \le N \\ l \ne s}} \frac{V^{(l)}(\gamma_k)\, V_\star^{(l)}(\gamma_k)}{\lambda^{(l)} - \lambda^{(s)}}, \tag{4.15}$$

where $V_\star^{(l)}(z) = \overline{V^{(l)}}(z^{-1})$ is the reciprocal polynomial of $V^{(l)}(z)$.

In particular, for each γ_k with $|\gamma_k| = 1$,

$$\frac{1}{w_k} = \sum_{\substack{0 \le l \le N \\ l \ne s}} \frac{|V^{(l)}(\gamma_k)|^2}{\lambda^{(l)} - \lambda^{(s)}}. \tag{4.16}$$

iv) *If $\lambda^{(s)}$ is a simple eigenvalue and all roots γ_k are on the unit circle, then the set $\{w_k\}_{k=1}^N$ contains exactly s positive numbers and $N - s$ negative numbers.*

In particular, if $s = 0$ or $s = N$ then all w_k are negative or positive, respectively.

Remark IV.1 Our approach to obtain Gaussian quadratures does not use Szegő polynomials and is therefore substantially different than the one in [10]. We briefly explain the approach in [10]. Note that (4.9) and (4.10) show that the polynomials $\{V^{(k)}(z)\}$ are orthogonal with respect to both the usual inner product for trigonometric polynomials and the weighted inner product with weight $w(t)$. We can also construct Szegő polynomials $\{p_k(z)\}$ orthogonal with respect to $w(t)$ and such that each $p_k(z)$ has precise degree k [25]. For any k, the roots of $p_k(z)$ are all in $|z| < 1$ [7].

Szegő polynomials and their reciprocals induce para-orthogonal polynomials [10],

$$B_n(z) = p_n(z) + \xi_n \, z^n \, (p_n)_\star(z),$$

where ξ_n are complex constants, $|\xi_n| = 1$. The roots of $B_n(z)$ are on the unit circle and can be used as the nodes for Gaussian quadratures with respect to the weight $w(t)$.

Under appropriate assumptions to guarantee uniqueness, the quadratures in [10] should coincide with those obtained in Theorem III.7.

In contrast to these exact quadratures, in Theorem IV.1 we derive a new family of Gaussian-type quadratures where for each eigenvalue of the Toeplitz matrix (4.2) there is a corresponding quadrature formula. Even for the smallest eigenvalue $\lambda^{(N)}$, the quadratures in (4.12) and in III.7 are different because of the extra integral term in (4.12). The size of this extra term is controlled by the size of the corresponding eigenvalue and, thus, it is never exactly zero. However, in applications, this extra term can be made as small as desired via oversampling (see (6.1)–(6.3) and note that (4.6) is valid for all small eigenvalues, not just the smallest [7, page 65]).

Remark IV.2 For an eigenvalue $\lambda^{(s)}$ of small size, the integral term on the right hand side of (4.12) can be neglected. This is the case of practical interest.

Remark IV.3 Even though the weights w_k could be complex valued, an important consequence of Theorem IV.1 is that in many important cases w_k are, in fact, real.

Remark IV.4 We have observed (see Table 1) that the weights w_k corresponding to nodes outside the support of the weight $w(t)$ are small, negative, and roughly of the size of the eigenvalue $\lambda^{(s)}$. Although we now present a heuristic explanation of this behavior, we do not know if a proof can be obtained along this path.

Let us split the sum in (4.16),

$$\frac{1}{w_k} = \sum_{l:\lambda^{(l)}>\lambda^{(s)}} \frac{|V^{(l)}(\gamma_k)|^2}{\lambda^{(l)}-\lambda^{(s)}} - \sum_{l:\lambda^{(s)}>\lambda^{(l)}} \frac{|V^{(l)}(\gamma_k)|^2}{\lambda^{(s)}-\lambda^{(l)}}. \tag{4.17}$$

If $\lambda^{(s)}$ is in the range of the exponential decay of the eigenvalues, the first term in (4.17) turns out to be much smaller than the second term which is approximately

$$\frac{1}{\lambda^{(s)}} \sum_{l:\lambda^{(s)}>\lambda^{(l)}} |V^{(l)}(\gamma_k)|^2.$$

For γ_k outside the support of the measure we have observed (Figures 2, 3, and 5–8) that

$$\sum_{l:\lambda^{(s)}>\lambda^{(l)}} |V^{(l)}(\gamma_k)|^2$$

is a constant of moderate size.

Thus, the second term in (4.17) is $O(1/\lambda^{(s)})$ and the weight is indeed negative and roughly of the size of the eigenvalue.

Remark IV.5 For the weight with value 1 in $(-\frac{1}{2},\frac{1}{2})$ and 0 otherwise, the eigenpolynomials are the Discrete PSWF. For these functions we know that all eigenvalues are simple and that all eigenpolynomial roots are on the unit circle [22].

Corollary IV.1 *Under the assumptions of Theorem IV.1, it follows that the Toeplitz matrix* $\boldsymbol{T}$ *in* (4.2) *has the following representation as a sum of rank one Toeplitz matrices,*

$$(\boldsymbol{T} - \lambda^{(s)}\boldsymbol{I})_{kl} = \sum_{j=1}^{N} w_j \gamma_j^{l-k},$$

where $\lambda^{(s)}$, w_j, *and* γ_j *are as in* (4.12).

This corollary should be compared with Remark II.3 noting that, in the corollary, $\lambda^{(s)}$ is not necessarily the least eigenvalue of $\boldsymbol{T}$.

Proof of Theorem IV.1

1. For $\boldsymbol{x} = (x_0, \cdots, x_N) \in \mathbb{C}^{N+1}$ let us define

$$A_{\boldsymbol{x}}(z) = \begin{cases} \sum_{l=-L}^{L} x_{l+L} z^l & \text{if} \quad N = 2L \\ \sum_{l=-L+1}^{L} x_{l+L-1} z^l & \text{if} \quad N = 2L-1. \end{cases}$$

The values of $A_{\boldsymbol{x}}$ on the unit circle have a phase shift respect of those for $P_{\boldsymbol{x}}$. In fact, depending on the parity of N, $A_{\boldsymbol{x}}(\mathrm{e}^{\mathrm{i}\pi t})$ is either $P_{\boldsymbol{x}}(\mathrm{e}^{\mathrm{i}\pi t})\mathrm{e}^{-\mathrm{i}\pi tL}$ or $P_{\boldsymbol{x}}(\mathrm{e}^{\mathrm{i}\pi t})\mathrm{e}^{-\mathrm{i}\pi t(L-1)}$.

Hence, (4.8) holds replacing $P_{\boldsymbol{x}}$ by $A_{\boldsymbol{x}}$ and then (4.9) (4.10) also hold for the shifted eigenpolynomials.

We prove the Theorem for the case $N = 2L$. (The case $N = 2L-1$ is similar.) For this case, using the same notation $V^{(k)}$ for the shifted eigenpolynomials, we have

$$V^{(k)}(z) = \sum_{l=-L}^{L} \boldsymbol{v}_{l+L}^{(k)} z^l.$$

2. Since $\{\gamma_j\}$ are distinct, we define $\{w_j\}_{j=1}^{N}$ as the unique solution of the Vandermonde system

$$\sum_{j=1}^{N} \gamma_j^{-k} w_j = \int_{-1}^{1} \mathrm{e}^{-\mathrm{i}\pi tk} w(t)dt \quad \text{for} \quad k = 1, \cdots, N. \tag{4.18}$$

3. Let $P \in \Lambda_N$, then $z^N P(z)$ it is a polynomial of at most degree $2N$, and since $z^L V^{(s)}(z)$ it is a polynomial of degree N, by Euclidean division, there exist polynomials $q(z)$ and $r(z)$ of degrees at most N and $N-1$ such that,

$$z^N P(z) = z^L V^{(s)}(z) q(z) + r(z).$$

Thus,

$$P(z) = V^{(s)}(z)Q(z) + R(z), \tag{4.19}$$

where $Q(z) \in \Lambda_L$ and $R(z)$ has the form $R(z) = \sum_{k=1}^{N} r_k z^{-k}$ and hence $\int_{-1}^{1} R(\mathrm{e}^{\mathrm{i}\pi t})dt = 0$.

Using the fact that $\{V^{(l)}\}_{l=0}^{N}$ is a basis of Λ_L, we write

$$\overline{Q(\mathrm{e}^{\mathrm{i}\pi t})} = \sum_{l=0}^{N} d_l\, V^{(l)}(\mathrm{e}^{\mathrm{i}\pi t}),$$

where d_l are some complex coefficients.

Using (4.10) and (4.18), we multiply both sides of (4.19) by $w(t)$ and integrate to obtain

$$\begin{aligned}\int_{-1}^{1} P(\mathrm{e}^{\mathrm{i}\pi t})w(t)dt &= \sum_{l=0}^{N} \overline{d_l} \int_{-1}^{1} V^{(s)}(\mathrm{e}^{\mathrm{i}\pi t})\overline{V^{(l)}(\mathrm{e}^{\mathrm{i}\pi t})}w(t)dt + \int_{-1}^{1} R(\mathrm{e}^{\mathrm{i}\pi t})w(t)dt \\ &= \overline{d_s}\lambda^{(s)} + \sum_{j=1}^{N} w_j R(\gamma_j).\end{aligned}$$

Now, (4.19) implies that the last sum equals $\sum_{j=1}^{N} w_j P(\gamma_j)$. To find the constant d_s, we integrate both sides of (4.19) and use (4.9) to obtain

$$\int_{-1}^{1} P(\mathrm{e}^{\mathrm{i}\pi t})\, dt = \sum_{l=0}^{N} \overline{d_l} \int_{-1}^{1} V^{(s)}(\mathrm{e}^{\mathrm{i}\pi t})\overline{V^{(l)}(\mathrm{e}^{\mathrm{i}\pi t})}\, dt = 2\overline{d_s},$$

and thus (4.12).

4. Let us assume that the node γ_k has unit norm, $|\gamma_k| = 1$, and let $P(z) = L_k^s(z)\,(L_k^s)_\star(z)$. We have $P(\gamma_r) = \delta_{rk}$ and since $P \in \Lambda_{N-1}$, (4.12) implies

$$\int_{-1}^{1} |L_k^s(\mathrm{e}^{\mathrm{i}\pi t})|^2\, w(t)\, dt = \lambda^{(s)} \frac{1}{2} \int_{-1}^{1} |L_k^s(\mathrm{e}^{\mathrm{i}\pi t})|^2\, dt + w_k.$$

Clearly w_k is real.

5. We now show that for $1 \le k, j \le N$,

$$w_k \sum_{\substack{0 \le l \le N \\ l \ne s}} \frac{V^{(l)}(\gamma_j)\, V_\star^{(l)}(\gamma_k)}{\lambda^{(l)} - \lambda^{(s)}} = \delta_{kj} \tag{4.20}$$

and thus, considering $k = j$, (4.15) follows. Note that we need $\lambda^{(s)}$ to be simple to guarantee $\lambda^{(l)} - \lambda^{(s)} \neq 0, l \neq s$ in (4.20).

If we view the left hand side of (4.20) as the entries A_{kj} of a matrix A and let B be the matrix of entries

$$B_{lk} = V^{(l)}(\gamma_k) \quad \text{where} \quad 0 \leq l \leq N,\, l \neq s \quad \text{and} \quad 1 \leq k \leq N, \tag{4.21}$$

we can prove (4.20) by showing that $B\,A = B$ and that B is non-singular.

For the latter claim, we simply check that the columns of B are linearly independent. Indeed, let $a_l, l \neq s$, be constants such that

$$\sum_{l \neq s} a_l V^{(l)}(\gamma_k) = 0 \quad \text{for} \quad k = 1, \ldots, N.$$

It follows that the polynomial $P(z) = \sum_{l \neq s} a_l V^{(l)}(z) \in \Lambda_L$ has the $N = 2L$ distinct roots γ_k. Since P and $V^{(s)}$ have the same degree and the same N distinct roots, $P(z) = c\, V^{(s)}(z)$, for some constant c. By (4.9), $V^{(s)}(z)$ is orthogonal to all the other eigenpolynomials and so $a_l = 0$.

To show that $B\,A = B$, we first substitute $P(z) = V^{(l)}(z)V_\star^{(m)}(z)$ in (4.12) to obtain

$$\begin{aligned} \int_{-1}^{1} V^{(l)}(\mathrm{e}^{\mathrm{i}\pi t})\overline{V^{(m)}(\mathrm{e}^{\mathrm{i}\pi t})} w(t)\, dt &= \lambda^{(s)} \frac{1}{2} \int_{-1}^{1} V^{(l)}(\mathrm{e}^{\mathrm{i}\pi t})\overline{V^{(m)}(\mathrm{e}^{\mathrm{i}\pi t})}\, dt \\ &\quad + \sum_{j=1}^{N} w_j V^{(l)}(\gamma_j) V_\star^{(m)}(\gamma_j). \end{aligned}$$

Using (4.9)–(4.10), we rewrite the previous equation as

$$\delta_{lm}(\lambda^{(l)} - \lambda^{(s)}) = \sum_{j=1}^{N} w_j V^{(l)}(\gamma_j) V_\star^{(m)}(\gamma_j) \tag{4.22}$$

and thus,

$$\begin{aligned} (B\,A)_{mn} &= \sum_j V^{(m)}(\gamma_j) w_j \sum_{l \neq s} \frac{V^{(l)}(\gamma_n)\, V_\star^{(l)}(\gamma_j)}{\lambda^{(l)} - \lambda^{(s)}} \\ &= \sum_{l \neq s} \frac{V^{(l)}(\gamma_n)}{\lambda^{(l)} - \lambda^{(s)}} \sum_j w_j V^{(m)}(\gamma_j) V_\star^{(l)}(\gamma_j) \\ &= V^{(m)}(\gamma_n) = B_{mn}. \end{aligned}$$

6. To prove the last assertion of the theorem, we consider (4.20) when all γ_k have unit norm and thus all w_k are real. In this case,

$$V_\star^{(l)}(\gamma_k) = \overline{V^{(l)}((\gamma_k)_\star)} = \overline{V^{(l)}(\gamma_k)},$$

and we can rewrite (4.20) as a matrix identity

$$B^\star \Gamma B = W, \tag{4.23}$$

where B is the invertible matrix defined in (4.21), $B^\star$ is its adjoint and Γ and W are diagonal matrices with real entries $\left\{ \dfrac{1}{\lambda^{(l)} - \lambda^{(s)}} \right\}_{\substack{0 \le l \le N \\ l \ne s}}$ and $\left\{ \dfrac{1}{w_l} \right\}_{1 \le l \le N}$, respectively.

Using Sylvester's law of inertia [9, Theorem 4.5.8], (4.23) implies that Γ and W have the same inertia, that is, the same number of positive, negative, and zero eigenvalues. The result follows because we assumed $\lambda^{(s)}$ to be simple and then $\lambda^{(0)} \ge \cdots \ge \lambda^{(s-1)} > \lambda^{(s)} > \lambda^{(s+1)} \ge \cdots \ge \lambda^{(N)}$. □

Techniques similar to those used in the proof of Theorem IV.1 allow us to derive several results for eigenpolynomials corresponding to multiple eigenvalues or for the case where their roots lie outside the unit circle. Here we limit our attention to the case of simple eigenvalues or eigenpolynomials with all roots on the unit circle.

W. Trench [26] has shown that both the multiplicity of the eigenvalues and the number of the eigenpolynomial zeros outside of the unit circle depend on the oscillations of the weight function $w(\tau)$. We state two of the results in [26] for $\boldsymbol{T}$ as in (4.2),

Theorem IV.2 ([26], Theorem 2.1) *If λ is an eigenvalue of $\boldsymbol{T}$ with multiplicity m, then $w(\tau) - \lambda$ changes sign at least $2m - 1$ times in $(-1, 1)$.*

Theorem IV.3 ([26], Theorem 3.1) *Let $u(z)$ be a self-reciprocal eigenpolynomial corresponding to the eigenvalue λ of $\boldsymbol{T}$. If $u(z)$ has $2m\,(m \ge 1)$ zeros that are not on the unit circle, then $w(\tau) - \lambda$ changes sign at least $2m + 1$ times in $(-1, 1)$.*

IV.3 Examples

We consider three examples with different weights and construct the appropriate quadratures.

Example 1. First we consider the weight

$$w(t) = \begin{cases} 1 & t \in [-a, a],\ a \le \frac{1}{2} \\ 0 & \text{elsewhere.} \end{cases} \tag{4.24}$$

For this weight the eigenpolynomials $V^{(l)}(e^{i\pi t})$ of the $N+1 \times N+1$ Toeplitz matrix $\boldsymbol{T}$ are the discrete PSWF [22]. Thus the eigenpolynomial $V^{(l)}(e^{i\pi t})$ has all of its zeros on the unit circle. Moreover, it has exactly l zeros for t in the interval $(-a, a)$ and N zeros for t in $[-1, 1]$. In this example we have selected $N = 97$, $a = 1/6$, $c = 15\pi$. We then construct the matrix $\boldsymbol{T}$ and compute the eigenpolynomial corresponding to the eigenvalue

$$\lambda^{(30)} = 9.77306136381891632828 \cdot 10^{-16}. \tag{4.25}$$

The eigenpolynomial $V^{(30)}(e^{i\pi t})$ is shown in Figures 2 and 3. Locations of the zeros on the unit circle are displayed in Figure 4. We then use the quadrature formula corresponding to this eigenvalue and tabulate the weights in Table 1. Note that the weights for nodes inside the interval $[-1/6, 1/6]$ are positive and those for nodes outside this interval are negative and roughly of the size of $\lambda^{(30)}$.

Example 2. We consider the weight

$$w(t) = \begin{cases} \frac{|t|}{a} & t \in [-a, a],\ a \leq \frac{1}{2} \\ 0 & \text{elsewhere.} \end{cases} \tag{4.26}$$

In this example we have selected $N = 61$, $a = 1/4$, $c = 15\pi$. We then construct the matrix $\boldsymbol{T}$ and compute the eigenpolynomial corresponding to the eigenvalue

$$\lambda^{(28)} = 1.11598931688523706280 \cdot 10^{-14}. \tag{4.27}$$

The eigenpolynomial $V^{(28)}(e^{i\pi t})$ is shown in Figures 5 and 6 .

Example 3. We consider a non-symmetric weight

$$w(t) = \begin{cases} 1 + \frac{t}{a} & t \in [-a, a],\ a \leq \frac{1}{2} \\ 0 & \text{elsewhere.} \end{cases} \tag{4.28}$$

In this example we have selected $N = 61$, $a = 1/4$, $c = 15\pi$. We then construct the matrix $\boldsymbol{T}$ and compute the eigenpolynomial corresponding to the eigenvalue

$$\lambda^{(28)} = 4.68165338379692121389 \cdot 10^{-15}. \tag{4.29}$$

The eigenpolynomial $V^{(28)}(e^{i\pi t})$ is shown in Figures 7 and 8. Although we do not have a proof at the moment, it appears that there is a class of weights for which eigenpolynomials corresponding to small eigenvalues mimic the behavior of the discrete PSWF with respect to locations of zeros. In Example 3 we know that all zeros are on the unit circle due to Theorems IV.2 and IV.3.

In Table 2 we illustrate the performance of quadratures for different bandlimits c. This table should be compared with Table 1 in [28]. The performance of both sets of quadratures is very similar. Yet these quadratures are quite different as can be seen by comparing Table 3 with Table 5 in [28]. Although the accuracy is almost identical, approximately 10^{-7}, the positions of nodes and weights differ by approximately $10^{-3} - -10^{-4}$.

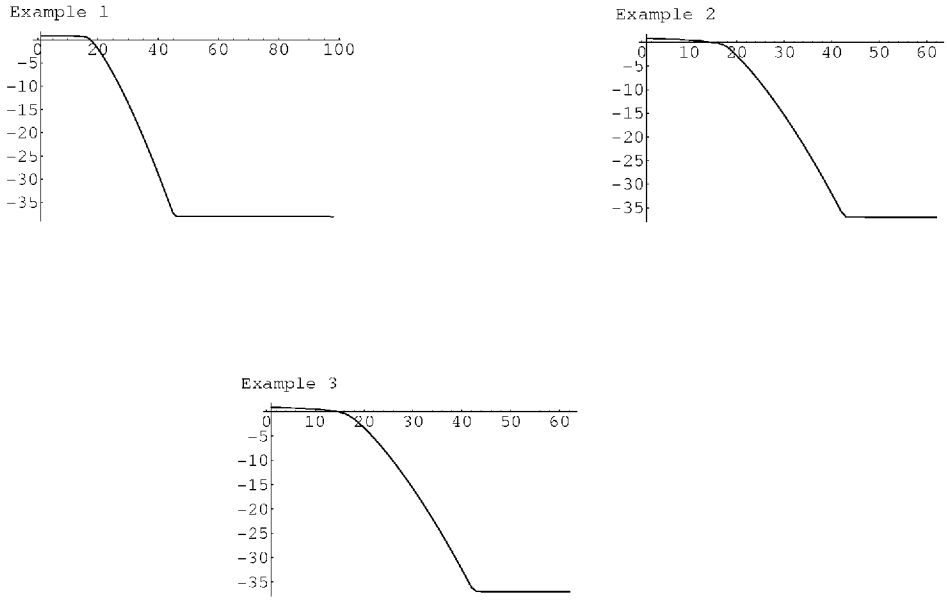

Figure 1: Decay of the eigenvalues of the matrix $\boldsymbol{T}$ in Examples 1-3. The scale of the vertical axes is logarithmic ($\log_{10}$), whereas the horizontal axes displays indices of eigenvalues. We note the exponential rate of decay. The flat portion of the graph for large indices is due to the limited precision of our computations. Thus, these graphs also illustrate the practical difficulty of finding the eigenpolynomial corresponding to the smallest eigenvalue.

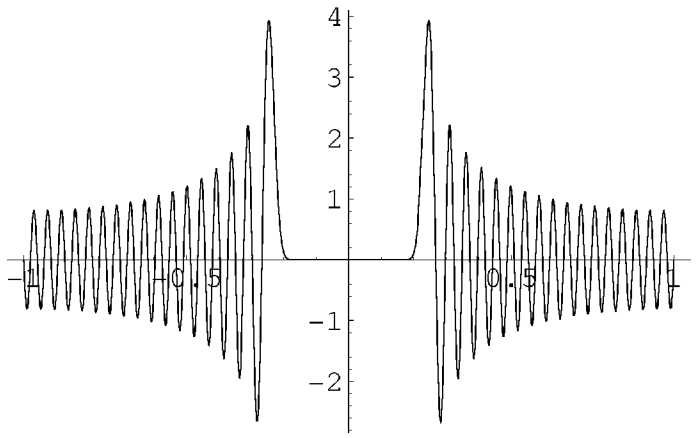

Figure 2: Modified eigenpolynomial $e^{-i\pi t\frac{N}{2}} V^{(30)}(e^{i\pi t})$ on the interval $[-1, 1]$, where $N = 97$ and $V^{(30)}(e^{i\pi t})$ is the eigenpolynomial corresponding to the eigenvalue $\lambda^{(30)}$ in Example 1. The phase factor $e^{-i\pi tN/2}$ is introduced to make this function real.

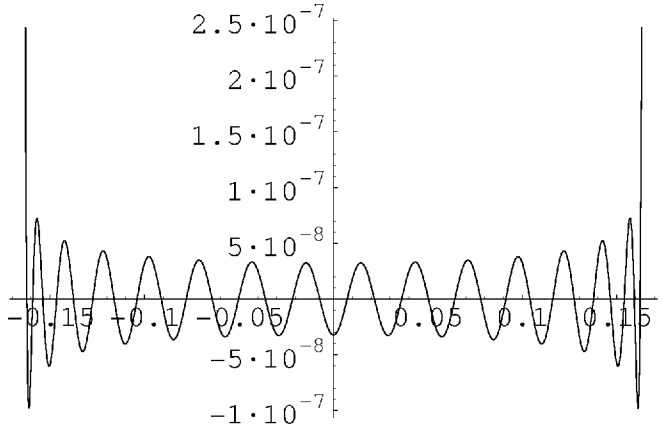

Figure 3: The same function as in Figure 2 on the interval $[-1/6, 1/6]$.

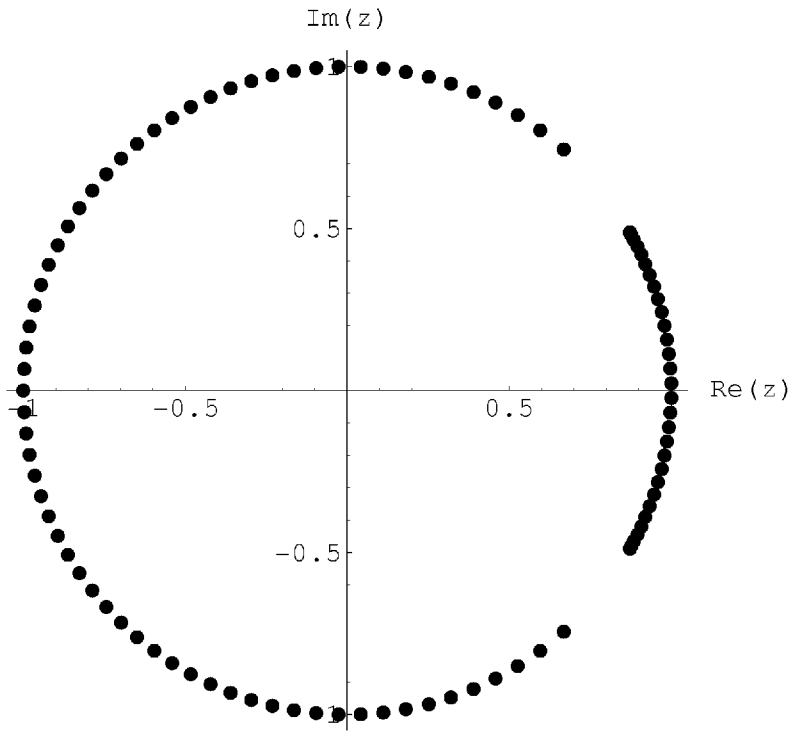

Figure 4: Location of the zeros on the unit circle for the eigenpolynomial $V^{(30)}$ in Example 1.

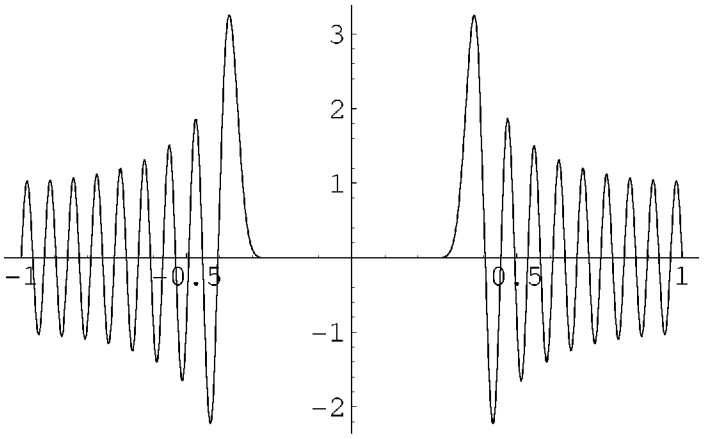

Figure 5: Modified eigenpolynomial (see Figure 2) on the interval $[-1, 1]$ corresponding to the eigenvalue $\lambda^{(28)}$ in Example 2.

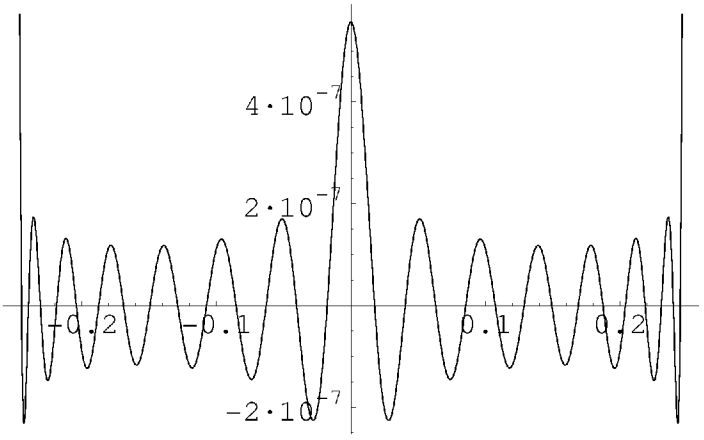

Figure 6: The same function of Figure 5 on the interval $[-1/4, 1/4]$.

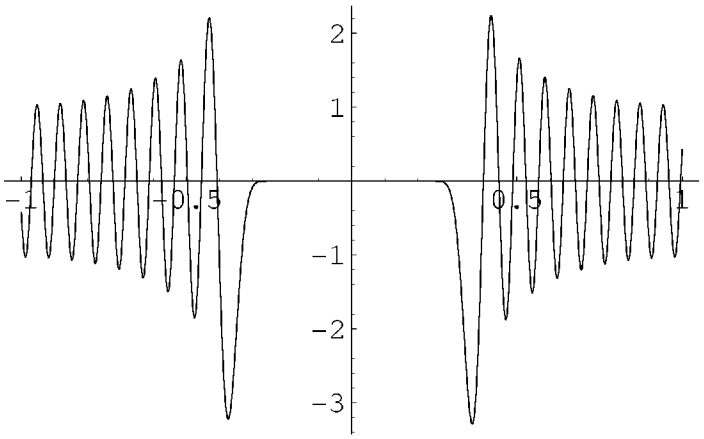

Figure 7: Modified eigenpolynomial (see Figure 2) on the interval $[-1, 1]$ corresponding to the eigenvalue $\lambda^{(28)}$ in Example 3.

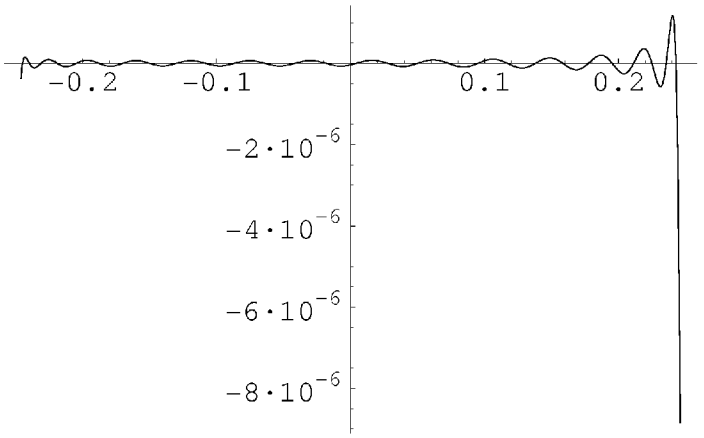

Figure 8: The same function of Figure 7 on the interval $[-1/4, 1/4]$.

#	weights
1	$-1.0328 \cdot 10^{-17}$
2	$-1.0328 \cdot 10^{-17}$
3	$-1.0329 \cdot 10^{-17}$
⋮	⋮
33	$-1.3518 \cdot 10^{-17}$
34	$-1.6030 \cdot 10^{-17}$
35	0.00580295532842819966
36	0.01310603337477264417
37	0.01959211245475268191
38	0.02506789313597245367
39	0.02954323947353217723
40	0.03313334531810570720
41	0.03598544514201341779
42	0.03823923547752508920
43	0.04001188663952018400
44	0.04139574827622469674
45	0.04246105337417774134
46	0.04325984471286061543
47	0.04382960375644760677
48	0.04419611220330997984
49	0.04437549133235668283

#	weights
50	0.04437549133235668283
51	0.04419611220330997984
52	0.04382960375644760677
53	0.04325984471286061543
54	0.04246105337417774134
55	0.04139574827622469674
56	0.04001188663952018400
57	0.03823923547752508920
58	0.03598544514201341779
59	0.03313334531810570720
60	0.02954323947353217723
61	0.02506789313597245367
62	0.01959211245475268191
63	0.01310603337477264417
64	0.00580295532842819966
65	$-1.6030 \cdot 10^{-17}$
66	$-1.3518 \cdot 10^{-17}$
⋮	⋮
96	$-1.0329 \cdot 10^{-17}$
97	$-1.0328 \cdot 10^{-17}$

Table 1: Table of weights for the quadrature formula with $\lambda^{(30)}$ in Example 1. The weight #1 corresponds to the node $\gamma_1 = -1$ (see Figure 4).

c	# of nodes	Maximum Errors
20	13	$1.2 \cdot 10^{-7}$
50	24	$1.1 \cdot 10^{-7}$
100	41	$1.6 \cdot 10^{-7}$
200	74	$1.8 \cdot 10^{-7}$
500	171	$1.4 \cdot 10^{-7}$
1000	331	$2.4 \cdot 10^{-7}$
2000	651	$1.2 \cdot 10^{-7}$
4000	1288	$3.7 \cdot 10^{-7}$

Table 2: Quadrature performance for varying band limits.

Node	Weight
−0.99041609489889	2.42209284787E−02
−0.95238829377394	5.04152570050E−02
−0.89243677566550	6.82109308489E−02
−0.81807124037876	7.96841731718E−02
−0.73438712699465	8.71710040243E−02
−0.64454148960251	9.22000859355E−02
−0.55050369342444	9.56668891250E−02
−0.45355265507507	9.80920675810E−02
−0.35456254990620	9.97843340729E−02
−0.25416536256280	1.00930070892E−01
−0.15284664158549	1.01641529848E−01
−0.05100535080412	1.01982696564E−01
0.05100535080412	1.01982696564E−01
0.15284664158549	1.01641529848E−01
0.25416536256280	1.00930070892E−01
0.35456254990620	9.97843340729E−02
0.45355265507507	9.80920675810E−02
0.55050369342444	9.56668891250E−02
0.64454148960251	9.22000859355E−02
0.73438712699465	8.71710040243E−02
0.81807124037876	7.96841731718E−02
0.89243677566550	6.82109308489E−02
0.95238829377394	5.04152570050E−02
0.99041609489889	2.42209284787E−02

Table 3: Quadrature nodes for exponentials with maximum bandlimit $c = 50$. The maximum error is $\approx 1.1 \cdot 10^{-7}$.

V A new algorithm for Carathéodory representation

V.1 Algorithm 2

We now describe an algorithm for computing quadratures via a Carathéodory-type approach based on Theorem IV.1. It is easy to see that, although there are similarities with Pisarenko's method, the algorithms are substantially different. We plan to address implications for signal processing in a separate paper.

1) Given t_k, the trigonometric moments of a measure, we construct the $(N+1)\times(N+1)$ Toeplitz matrix $\boldsymbol{T}_N$ with elements $(\boldsymbol{T}_N)_{kj} = t_{j-k}$. This matrix is positive definite and has a large number of small eigenvalues.

2) For a given accuracy ϵ, we compute the inverse of the Toeplitz matrix $\boldsymbol{T}_N - \epsilon\boldsymbol{I}$. For a selfadjoint Toeplitz matrix, it is sufficient to solve $(\boldsymbol{T}_N - \epsilon\boldsymbol{I})\boldsymbol{x_0} = \boldsymbol{e_0}$, where $\boldsymbol{e_0} = (1, 0, \ldots, 0)^t$. After $\boldsymbol{x_0}$ is found, we use the Gohberg-Semencul representation of the inverse of the Toeplitz matrix [6] (see also [5] for a modern perspective) in order to apply it to a vector. If ϵ is too close to an eigenvalue of $\boldsymbol{T}_N$, it might be necessary to slighty modify the value of ϵ and repeat this step.

This step requires $O(N^2)$ operations if we use the Levinson algorithm. However, we know how to build a stable $O(N(\log N)^2)$ algorithm for this purpose which we will present elsewhere.

3) Using the power method for $(\boldsymbol{T}_N - \epsilon\boldsymbol{I})^{-1}$, we find an eigenvalue $\lambda^{(q)}$ close to ϵ and the corresponding eigenvector $\boldsymbol{q}$. This step requires $O(N \log N)$ operations due to the Gohberg-Semencul representation of the inverse.

4) Next, compute all zeros on the unit circle of the eigenpolynomial corresponding to the eigenvector $\boldsymbol{q}$.

This requires $O(N \log N)$ operations since we use the unequally spaced fast Fourier transform ([4], [1]) to evaluate the trigonometric polynomial on the unit circle. We pick out the zeros within the support of the measure and denote their number by M.

5) Using the algorithm described below, we find the weights $\boldsymbol{\rho}$ by solving the Vandermonde system for all nodes (including those outside the support). This algorithm takes $O(N \log N)$ operations.

V.2 Solving Vandermonde systems using polynomial evaluation

To obtain the weights in step 5) of Algorithm V.1, we need to solve a $M \times M$ Vandermonde system with nodes on the unit circle. In this section we discuss an algorithm to obtain

the solution by evaluating certain polynomials on the Vandermonde matrix nodes. The algorithm can be derived from more general results [8, 15, 20]. Here we give a simpler presentation adapted to our particular application. Note that general algorithms to solve Vandermonde systems are unstable, unless there is a particular arrangement of the nodes.

Let $\{\gamma_1, \ldots, \gamma_M\}$ be distinct complex numbers and define

$$\boldsymbol{V} = \begin{bmatrix} 1 & \cdots & 1 \\ \gamma_1 & & \gamma_M \\ \vdots & & \vdots \\ \gamma_1^{M-1} & \cdots & \gamma_M^{M-1} \end{bmatrix} \in \mathbb{C}^{M\times M}.$$

Since the nodes $\{\gamma_r\}$ are distinct, $\det \boldsymbol{V} \neq 0$ and thus given $\boldsymbol{b} = (b_0, \cdots, b_{M-1})^t$, there is a unique $\boldsymbol{\rho} = (\rho_1, \cdots, \rho_M)^t$ such that

$$\boldsymbol{V}\boldsymbol{\rho} = \boldsymbol{b}. \tag{5.1}$$

If we define

$$Q(z) = \prod_{k=1}^{M}(z - \gamma_k) = \sum_{k=0}^{M} q_k z^k, \tag{5.2}$$

then, for any polynomial P of degree at most $M-1$,

$$\frac{P(z)}{Q(z)} = \sum_{r=1}^{M} \frac{P(\gamma_r)}{Q'(\gamma_r)(z-\gamma_r)}.$$

Thus, for $|z| < \min|\gamma_r|^{-1}$,

$$\frac{z^{M-1}}{z^M}\frac{P(z^{-1})}{Q(z^{-1})} = \sum_{r=1}^{M} \frac{P(\gamma_r)}{Q'(\gamma_r)} \sum_{k=0}^{+\infty} \gamma_r^k z^k = \sum_{k=0}^{+\infty} \left(\sum_{r=1}^{M} \frac{P(\gamma_r)}{Q'(\gamma_r)} \gamma_r^k \right) z^k. \tag{5.3}$$

Now choose P to be the unique polynomial with $P(\gamma_r) = \rho_r\, Q'(\gamma_r)$ for $1 \leq r \leq M$, and let $B(z) = \sum_{k=0}^{M-1} b_k z^k$. Substituting in (5.3),

$$\frac{z^{M-1}P(z^{-1})}{z^M Q(z^{-1})} = \sum_{k=0}^{M-1} \underbrace{\sum_{r=1}^{M} \rho(r)\gamma_r^k}_{b_k} z^k + \quad \text{higher powers} \quad = B(z) + z^M(\cdots).$$

If we denote

$$\tilde{P}(z) = z^{M-1}P(z^{-1}) \quad \text{and}$$
$$\tilde{Q}(z) = z^M Q(z^{-1}),$$

then

$$\tilde{P}(z) = \tilde{Q}(z)B(z) + z^M \tilde{Q}(z)(\cdots) \tag{5.4}$$

and thus the coefficients of $\tilde{P}$ correspond to the first M coefficients of $\tilde{Q}(z)B(z)$.

As a result, we have the following algorithm:

V.3 Algorithm to solve Vandermonde systems

1) Given $\{\gamma_k\}$ compute $\boldsymbol{q} = (q_0, \cdots, q_M)$.

2) Given $\boldsymbol{b}$ and $\boldsymbol{q}$ compute

$$\tilde{p}(s) = \sum_{l=0}^{s} \tilde{q}(s-l)b(l)$$

for $0 \leq s \leq M-1$.

3) Compute $\boldsymbol{\rho}$ as

$$\rho_r = \frac{P(\gamma_r)}{Q'(\gamma_r)} = -\frac{\gamma_r \tilde{P}(\frac{1}{\gamma_r})}{\tilde{Q}'(\frac{1}{\gamma_r})}$$

for $1 \leq r \leq M$.

This algorithm is equivalent to the following factorization of the inverse of the Vandermonde matrix in terms of a diagonal matrix, its transpose $\boldsymbol{V}^t$, and a triangular Hankel matrix,

$$\boldsymbol{V}^{-1} = \begin{bmatrix} \frac{1}{Q'(\gamma_1)} & \cdots & 0 \\ & \ddots & \\ 0 & \cdots & \frac{1}{Q'(\gamma_M)} \end{bmatrix} \boldsymbol{V}^t \begin{bmatrix} q_1 & q_2 & \cdots & q_M \\ q_2 & \cdots & q_M & 0 \\ \vdots & & & \vdots \\ & & \cdots & 0 \\ q_M & \cdots & 0 & 0 \end{bmatrix}. \tag{5.5}$$

This description is a particular case of the inversion formulae for Löwner-Vandermonde [20] or close to Vandermonde matrices [8, Corollary 2.1 p. 157]. We can state those results as (see [20, p. 548])

$$\boldsymbol{V}^{-1} = \begin{bmatrix} x_1 & \cdots & 0 \\ & \ddots & \\ 0 & \cdots & x_M \end{bmatrix} \boldsymbol{V}^t \begin{bmatrix} -y_2 & -y_3 & \cdots & 1 \\ -y_3 & \cdots & 1 & 0 \\ \vdots & & & \vdots \\ & & \cdots & 0 \\ 1 & \cdots & 0 & 0 \end{bmatrix},$$

where the vectors $\boldsymbol{x} = (x_1, \cdots, x_M)^t$ and $\boldsymbol{y} = (y_1, \cdots, y_M)^t$ are solutions of

$$\boldsymbol{V}\boldsymbol{x} = (0, \cdots, 1)^t \quad \text{and} \quad \boldsymbol{V}^t\boldsymbol{y} = [\gamma_r^M]_{r=1}^M.$$

Since γ_r are the roots of $Q(z)$ we can take $\boldsymbol{y} = -(q_0, \cdots, q_{M-1})^t$ and if $B(z) = z^M$ in (5.4), then $P(z) = 1$ and $\boldsymbol{x} = (\frac{1}{Q'(\gamma_1)}, \cdots, \frac{1}{Q'(\gamma_M)})^t$.

Remark V.1 For Algorithm V.1, we first obtained the eigenvector $\boldsymbol{q}$ corresponding to an eigenvalue close to ϵ. Thus, Step 1. of the Vandermonde algorithm is already accomplished and Step 2. can be performed using the FFT. Furthermore, the nodes γ_k belong to the unit circle and via the unequally spaced fast Fourier transform we have a fast algorithm to obtain the weights.

Remark V.2 As an example, we use this approach to derive the solution of the Vandermonde system with nodes at $\gamma_r = \mathrm{e}^{\mathrm{i}2\pi\frac{(r-1)}{M}}$, $1 \le r \le M$. In this case, $Q(z) = 1 - z^M$ and $\tilde{P}(z) = z^{M-1}P(z^{-1}) = \tilde{Q}(z)B(z) + z^M(\cdots) = -B(z) + z^M(\cdots)$. We conclude $P = -\tilde{B}(z)$ and thus

$$\begin{aligned} \rho_r &= \frac{P(\gamma_r)}{Q'(\gamma_r)} = \frac{-\gamma_r^{M-1}B(\overline{\gamma_r})}{-M\gamma_r^{M-1}} \\ &= \frac{1}{M}\sum_{k=0}^{M-1} b_k e^{-\mathrm{i}2\pi rk/M}. \end{aligned}$$

As expected, we obtained the inverse of the discrete Fourier transform matrix.

VI Approximation of bandlimited functions

Let us consider the problem stated in (1.3)–(1.5), that is, given

$$u(x) = \int_{-1}^{1} w(\tau)\, \mathrm{e}^{\mathrm{i}\, c\tau\, x}\, d\tau, \tag{6.1}$$

construct the function $\tilde{u}(x)$ in (1.4) such that (1.5) holds. We show in this section that the approximation obtained with exponential sums holds in any subinterval of $(-1, 1)$. In fact, in Theorem VI.1, we prove the existence of such an approximation even though our proof does not provide a practical method to obtain the nodes and weights in the exponential sum. In practice we obtain them using Algorithm V.1.

We assume that we have access to values of $u(x)$ for x uniformly sampled. We select the sampling rate to be at least twice the Nyquist sampling rate for $u(x)$. We have observed that this is the minimal rate for which our method works properly.

In fact, let us discretize $u(x)$ at nodes $x_k = \frac{k}{N}$, for $|k| \leq N$ and pick N such that $N \geq \frac{2c}{\pi}$. The value of N determines our sampling rate. The resulting values are

$$u_k = u(x_k) = \int_{-1}^{1} w(\tau) \mathrm{e}^{\mathrm{i}\, c\tau\, \frac{k}{N}}\, d\,\tau. \tag{6.2}$$

Defining $\nu = \frac{c}{\pi N}$, then $\nu \leq 1/2$ and by changing variables $t = \nu\tau$,

$$u_k = \int_{-\nu}^{\nu} \sigma(t) \mathrm{e}^{\mathrm{i}\pi t k}\, dt \quad \text{for} \quad |k| \leq N \tag{6.3}$$

are the trigonometric moments of a new weight $\sigma(t) = \frac{1}{\nu} w(\frac{t}{\nu})$ supported in $(-\nu, \nu) \subseteq [-\frac{1}{2}, \frac{1}{2}]$.

Now, assume we can approximate $\int_{-1}^{1} \sigma(t)\, \mathrm{e}^{\mathrm{i}\pi t y}\, dt$ by $\sum_{j=1}^{N} w_j \mathrm{e}^{\mathrm{i}\pi\theta_j y}$ for $|y| \leq N$. Then, since

$$u(x) = \int_{-1}^{1} w(\tau)\, \mathrm{e}^{\mathrm{i}\, c\tau\, x}\, d\tau = \int_{-\nu}^{\nu} \sigma(t)\, \mathrm{e}^{\mathrm{i}\pi t N x}\, dt,$$

we can appproximate $u(x)$ for $|x| \leq 1$.

Indeed, we now show that for any d, $0 < d < 1$, we can approximate $u(x)$ for $|x| \leq d$.

Theorem VI.1 *Let σ be a weight supported in $[-\nu, \nu]$, $0 < \nu \leq \frac{1}{2}$ and let ϵ and d be positive numbers with $d < 1$. Then, for N sufficiently large, there exist real constants $\{w_1, \cdots, w_N\}$ and $\{\theta_1, \cdots, \theta_N\}$, with $w_j > 0$ and $|\theta_j| < \nu$ such that*

$$\left| \int_{-1}^{1} \sigma(t)\, \mathrm{e}^{\mathrm{i}\pi t y}\, dt - \sum_{j=1}^{N} w_j\, \mathrm{e}^{\mathrm{i}\pi\theta_j y} \right| < \epsilon, \quad \textit{for} \quad |y| \leq dN + 1. \tag{6.4}$$

For the proof, we will use the fact that exponential functions can be well approximated by splines interpolating them at integer values.

For fixed $t \in [-\pi, \pi]$ and positive integer m, consider the exponential Euler spline of order $2m-1$,

$$S_{2m-1}(x, \mathrm{e}^{\mathrm{i}t}) = \sum_{k \in \mathbb{Z}} \mathrm{e}^{\mathrm{i}tk} L_{2m-1}(x-k), \tag{6.5}$$

where $L_n(x)$ is the fundamental cardinal spline of order n, $L_n(r) = \delta_{r0}$, for all $r \in \mathbb{Z}$.

We will use the following properties (see [21, pages 29, 30, and 35]) valid for all $x, t \in \mathbb{R}$,

$$\left|S_{2m-1}(x, \mathrm{e}^{\mathrm{i}t})\right| \leq 1, \tag{6.6}$$

$$\left|\mathrm{e}^{\mathrm{i}\pi tx} - S_{2m-1}(x, \mathrm{e}^{\mathrm{i}\pi t})\right| < 3|t|^{2m}, \tag{6.7}$$

and $$|L_{2m-1}(x)| \leq d_m \, \mathrm{e}^{-\alpha_m |x|}, \tag{6.8}$$

for positive constants d_m and α_m.

Proof of Theorem VI.1 Let

$$u(y) = \int_{-1}^{1} \sigma(t) \, \mathrm{e}^{\mathrm{i}\,\pi\, t y} \, dt$$

and for each m define the spline of order $2m-1$ interpolating $u(y)$ at the integers,

$$\begin{aligned} a(y) &= \sum_k u(k) L_{2m-1}(y-k) \\ &= \int_{-1}^{1} \sigma(t) \, S_{2m-1}(y, \mathrm{e}^{\mathrm{i}\pi t}) \, dt. \end{aligned}$$

By (6.7),

$$|u(y) - a(y)| \leq 3 \int_{-\nu}^{\nu} \sigma(t) \, |t|^{2m} \, dt \leq 3\nu^{2m} \|\sigma\|_1,$$

where $\|\sigma\|_1 = \int_{-1}^{1} \sigma(t) \, dt$. We choose m such that $3\nu^{2m}\|\sigma\|_1 < \frac{\epsilon}{4}$.

On the other hand, for each N, Theorem III.7 allow us to represent the moments $u(k)$, $|k| \leq N$,

$$u(k) = \int_{-1}^{1} \sigma(t) \, \mathrm{e}^{\mathrm{i}\,\pi\, k\, t} \, dt = \sum_{j=1}^{N} w_j \mathrm{e}^{\mathrm{i}\,\pi\,\theta_j\, k} + \omega_0 \, (-1)^k, \tag{6.9}$$

where

$$w_0 \leq \frac{4\|\sigma\|_1}{2 + (2+\sqrt{3})^N + (2-\sqrt{3})^N}. \tag{6.10}$$

Let

$$\tilde{u}(y) = \sum_{j=1}^{N} w_j \mathrm{e}^{\mathrm{i}\,\pi\,\theta_j\,y}$$

then $u(k) = \tilde{u}(k) + \omega_0\,(-1)^k$ for $|k| \le N$, and defining

$$\begin{aligned} \tilde{a}(y) &= \sum_k \tilde{u}(k) L_{2m-1}(y-k) \\ &= \sum_{j=1}^{N} w_j S_{2m-1}(y, \mathrm{e}^{\mathrm{i}\pi\,\theta_j}), \end{aligned}$$

(6.7) gives the estimate

$$|\tilde{u}(y) - \tilde{a}(y)| \le 3 \sum_{j=1}^{N} w_j |\theta_j|^{2m} \le 3\nu^{2m}(u(0) - w_0) \le 3\nu^{2m} \|\sigma\|_1 < \frac{\epsilon}{4}.$$

We have shown that $u(y)$ is close to $a(y)$ and $\tilde{u}(y)$ to $\tilde{a}(y)$. To finish the proof, we need to show that $|a(y) - \tilde{a}(y)| < \frac{\epsilon}{2}$, for $|y| \le dN + 1$. Now,

$$\begin{aligned} a(y) - \tilde{a}(y) &= \sum_{|k| \le N} \omega_0\,(-1)^k L_{2m-1}(y-k) + \sum_{|k|>N} (u(k) - \tilde{u}(k)) L_{2m-1}(y-k) \\ &= w_0 S_{2m-1}(y, \mathrm{e}^{\mathrm{i}\pi}) + \sum_{|k|>N} (u(k) - \tilde{u}(k) - \omega_0\,(-1)^k) L_{2m-1}(y-k) \end{aligned}$$

and

$$\begin{aligned} |u(k) - \tilde{u}(k) - \omega_0\,(-1)^k| &\le |u(k)| + |\tilde{u}(k)| + \omega_0 \le \sum_{j=0}^{N} w_j + \sum_{j=1}^{N} w_j + \omega_0 \\ &\le 2u(0) = 2\|\sigma\|_1, \end{aligned}$$

where we used (6.9).

Using (6.6) and (6.8),

$$|a(y) - \tilde{a}(y)| \le w_0 + 2\,\|\sigma\|_1\, d_m \sum_{|k|>N} \mathrm{e}^{-\alpha_m |y-k|}.$$

Hence, for large N, we can estimate w_0 using (6.10) and for the last sum, when $|y| \le dN + 1$,

$$\begin{aligned} \sum_{|k|>N} \mathrm{e}^{-\alpha_m|y-k|} &= \sum_{k=N+1}^{\infty} (\mathrm{e}^{-\alpha_m(k-y)} + \mathrm{e}^{-\alpha_m(k+y)}) \\ &= \frac{\mathrm{e}^{\alpha_m y} + \mathrm{e}^{-\alpha_m y}}{1 - \mathrm{e}^{-\alpha_m}} \mathrm{e}^{-\alpha_m(N+1)} \\ &\le \frac{2}{1 - \mathrm{e}^{-\alpha_m}} \mathrm{e}^{-\alpha_m(1-d)N}. \quad \square \end{aligned}$$

Remark VI.1 In the proof of Theorem VI.1 we used Theorem III.7 to represent the moments (6.3) as

$$\int_{-\nu}^{\nu} \sigma(t)\, \mathrm{e}^{\mathrm{i}\pi t k}\, dt = \sum_{j=1}^{N} w_j \mathrm{e}^{\mathrm{i}\pi\theta_j k} + w_0(-1)^k,$$

where w_0 decreases exponentially with N. The approximation in (6.4) is obtained using these w_j and θ_j. Nevertheless, in practice, we use instead the weights and nodes from the quadratures in (4.12). We also note that, as the proof of the theorem indicates, for (1.5) to hold on most of the interval $(-1, 1)$, we should appropriately oversample the function u in (1.3).

VII Approximation of integrals by linear combinations of exponentials

In this section we show that by solving the problem (1.3)–(1.5) for $x \in [-1,1]$, we also find quadratures for functions that can be considered as a linear combination of exponentials with bandlimit c. We provide two examples with Bessel functions and with PSWF.

Proposition VII.1 *For $x \in [-1,1]$ let us consider*

$$v(x) = \int_0^1 w(\tau) J_{2n}(c\,x\tau)\,d\tau, \tag{7.1}$$

where $w \geq 0$ is a weight, J_{2n} is the Bessel function of order $2n$, $n \geq 0$ and c is a positive real constant. Then we have

$$|v(x) - \tilde{v}(x)| \leq \frac{2}{\pi}\,\epsilon, \tag{7.2}$$

where

$$\tilde{v}(x) = \sum_{k=1}^{M} w_k J_{2n}(c\,x\,\theta_k), \tag{7.3}$$

and the nodes θ_k and the weights w_k are as in (1.4) but for the weight $\tilde{w}$ defined as $\tilde{w}(\tau) = w(\tau)/2$ for $0 \leq \tau \leq 1$ and $\tilde{w}(\tau) = w(-\tau)/2$, $-1 \leq \tau \leq 0$.

Since J_{2n} is an even function, we have

$$v(x) = \int_{-1}^1 \tilde{w}(\tau) J_{2n}(c\,x\tau)\,d\tau. \tag{7.4}$$

Using

$$J_{2n}(\xi) = \frac{(-1)^n}{\pi} \int_{-1}^1 \frac{T_{2n}(y)}{\sqrt{1-y^2}}\,\mathrm{e}^{\mathrm{i}y\xi}\,dy, \tag{7.5}$$

we obtain

$$v(x) - \tilde{v}(x) = \frac{(-1)^n}{\pi} \int_{-1}^1 \frac{T_{2n}(y)}{\sqrt{1-y^2}} \left[\int_{-1}^1 \tilde{w}(\tau) \mathrm{e}^{\mathrm{i}cxy\tau} d\tau - \sum_{k=1}^{M} w_k \mathrm{e}^{\mathrm{i}cxy\theta_k} \right] dy. \tag{7.6}$$

Since $|y| \leq 1$, we have (by selecting nodes and weights as in (1.4))

$$\left| \int_{-1}^1 \tilde{w}(\tau) \mathrm{e}^{\mathrm{i}cxy\tau} d\tau - \sum_{k=1}^{M} w_k \mathrm{e}^{\mathrm{i}cxy\theta_k} \right| \leq \epsilon \tag{7.7}$$

for $x \in [-1,1]$. Thus, we obtain

$$|v(x) - \tilde{v}(x)| \leq \frac{\epsilon}{\pi} \int_{-1}^{1} \frac{|T_{2n}(y)|}{\sqrt{1-y^2}} dy = \frac{\epsilon}{\pi} \int_0^{\pi} |\cos(2nx)| dx = \begin{cases} \frac{2}{\pi}\epsilon & \text{if} \quad n \neq 0 \\ \epsilon & \text{if} \quad n = 0. \end{cases} \tag{7.8}$$

A similar result holds for the PSWF which are defined as the eigenfunctions of the operator

$$F_c(\phi)(x) = \int_{-1}^{1} \mathrm{e}^{\mathrm{i}cxt} \phi(t) dt, \tag{7.9}$$

where c is a positive real constant (bandlimit) and $F_c : L^2[-1,1] \to L^2[-1,1]$. These bandlimited functions satisfy

$$\lambda_j \psi_j(x) = \int_{-1}^{1} \mathrm{e}^{\mathrm{i}cxt} \psi_j(t) dt, \tag{7.10}$$

where the eigenvalues λ_j, $j = 0, 1, \ldots$, are all non-zero and simple, and are arranged so that $|\lambda_{j-1}| > |\lambda_j|$, $j = 1, 2, \ldots$.

Proposition VII.2 *For all non-negative integers j, let us consider integrals*

$$v_j = \int_{-1}^{1} w(\tau) \psi_j(\tau)\, d\tau, \tag{7.11}$$

where $w \geq 0$ is a weight and ψ_j is the PSWF corresponding to the band limit $c > 0$. Then

$$|v_j - \tilde{v}_j| \leq \frac{\sqrt{2}}{|\lambda_j|} \epsilon, \tag{7.12}$$

where

$$\tilde{v}_j = \sum_{k=1}^{M} w_k \psi_j(\theta_k), \tag{7.13}$$

and the nodes θ_k and the weights w_k are the same as in (1.4).

For large c, the spectrum of F_c can be divided into three groups. The first group contains approximately $2c/\pi$ eigenvalues with absolute value very close to one. They are followed by order $\log c$ eigenvalues whose absolute values make an exponentially fast transition from 1 to 0. The third group consists of exponentially decaying eigenvalues that are very close to zero. For precise statements see [23], [24], [13] and [28].

Therefore, it follows from (7.12) that, for the first $\approx 2c/\pi$ eigenfunctions, the integrals in (7.11) are well approximated by the quadratures in (7.13). To prove (7.12), use (7.10), to write

$$v_j - \tilde{v}_j = \frac{1}{\lambda_j} \int_{-1}^{1} \left(\int_{-1}^{1} w(\tau) \mathrm{e}^{\mathrm{i}c\tau t} d\tau - \sum_{k=1}^{M} w_k \mathrm{e}^{\mathrm{i}c\theta_k t} \right) \psi_j(t) dt. \tag{7.14}$$

Since $|t| \leq 1$, we have

$$\left| \int_{-1}^{1} w(\tau) \mathrm{e}^{\mathrm{i}c\tau t} d\tau - \sum_{k=1}^{M} w_k \mathrm{e}^{\mathrm{i}c\theta_k t} \right| \leq \epsilon, \tag{7.15}$$

and $\|\psi_j\|_2 = 1$ implies $\int_{-1}^{1} |\psi_j(t)| dt \leq \sqrt{2}$. □

Remark VII.1 If the weight function w is chosen as in (8.40), then the eigenpolynomials are the discrete PSWF [22] (see Example 1 in Section IV.3). In this case, the nodes $\{\theta_k\}$ are zeros of a discrete PSWF corresponding to a small eigenvalue. Therefore, these nodes are Gaussian nodes for PSWF (appropriately scaled to the interval $[-1, 1]$) as stated in Proposition VII.2.

VIII Interpolating Bases for Bandlimited Functions

In this section we construct bases for bandlimited functions with bandlimit $c > 0$ using exponentials $\{e^{ict_l x}\}_{l=1}^M$, where $\{t_l\}$ are some quadrature nodes with $|t_l| < 1$. In particular, we derive interpolating bases as linear combinations of such exponentials.

We start by constructing, for some $\epsilon > 0$ and bandlimit $2c > 0$, the nodes $|t_l| < 1$ and the weights $w_l > 0$, $l = 1, \ldots, M$, where $M = M(c, \epsilon)$, such that for all $x \in [-1, 1]$,

$$\left| \int_{-1}^{1} e^{2icxt}\, dt - \sum_{l=1}^{M} w_l e^{2icxt_l} \right| < \epsilon^2, \tag{8.1}$$

where, for each l there exists l' such that $t_{l'} = -t_l$ and $w_{l'} = w_l$.

Since $\int_{-1}^{1} e^{2icxt}\, dt = \sin(2cx)/cx$, we have from (8.1)

$$\left| \frac{\sin c(x-t)}{c(x-t)} - \tfrac{1}{2} \sum_{l=1}^{M} w_l e^{ic(x-t)t_l} \right| < \frac{\epsilon^2}{2}, \tag{8.2}$$

where $|x|, |t| \le 1$.

In considering bandlimited functions we will use the PSWF (see [23], [14], and a more recent paper [28]). The PSWF are real eigenfunctions of the operator F_c in (7.9) with eigenvalues λ_j, $j = 0, 1, \ldots$, such that $|\lambda_0| > |\lambda_1| > \ldots > 0$. They are also eigenfunctions of the operator $Q_c = \frac{c}{2\pi} F_c^* F_c$, namely,

$$\frac{1}{\pi} \int_{-1}^{1} \frac{\sin c(x-t)}{(x-t)}\, \psi_j(t) dt = \mu_j\, \psi_j(x), \tag{8.3}$$

with eigenvalues

$$\mu_j = \frac{c}{2\pi} |\lambda_j|^2, \quad j = 0, 1, \ldots. \tag{8.4}$$

We prove

Theorem VIII.1 *For x in $[-1, 1]$ and for any $|b| \le c$ and $\epsilon > 0$ there exist coefficients $\{\alpha_l\}_{l=1}^M$ and constants A_1, A_2 such that*

$$\left\| e^{ibx} - \sum_{l=1}^{M} \alpha_l e^{ict_l x} \right\|_\infty \le A_1\, \epsilon, \tag{8.5}$$

and

$$\left\| e^{ibx} - \sum_{l=1}^{M} \alpha_l e^{ict_l x} \right\|_2 \le A_2\, \epsilon, \tag{8.6}$$

where the nodes $|t_l| < 1$, $l = 1, \ldots, M$ are the same as in (8.1) and do not depend on b.

In other words, for a given precision ϵ, the functions $\{e^{ict_l x}\}_{l=1}^{M}$ form an approximate basis for bandlimited functions.

The proof of this theorem uses the fact that the PSWF are uniformly bounded

$$\|\psi_j\|_\infty \leq C_\infty, \quad j = 0, 1, \ldots, \tag{8.7}$$

where C_∞ does not depend on j. Through direct numerical examination it is not difficult to verify that C_∞ is a fairly small constant that weakly depends on the bandlimit c. However, we are not aware of a proof that provides a tight bound in (8.7). A proof that C_∞ exists can be constructed using the fact that for $j \gg c$, the functions ψ_j approach the Legendre polynomials. In order to obtain appropriate estimates, one can use the recurrence relations derived in [28].

Proof of Theorem VIII.1 Let us start by expanding e^{ibx} into the basis $\{\psi_j\}_{j=0}^{\infty}$ corresponding to the bandlimit c. We have

$$e^{ibx} = e^{ic(b/c)x} = \sum_{j=0}^{\infty} \lambda_j \psi_j(b/c)\psi_j(x), \tag{8.8}$$

where $|b/c| \leq 1$, and by (8.7)

$$\left| e^{ibx} - \sum_{j=0}^{M-1} \lambda_j \psi_j(b/c)\psi_j(x) \right| \leq \sum_{j=M}^{\infty} |\lambda_j| \, |\psi_j(b/c)| \, |\psi_j(x)| \leq C_\infty \sum_{j=M}^{\infty} |\lambda_j| \, |\psi_j(x)|. \tag{8.9}$$

Thus we obtain

$$\left\| e^{ibx} - \sum_{j=0}^{M-1} \lambda_j \psi_j(b/c)\psi_j(x) \right\|_\infty \leq C_\infty^2 \sum_{j=M}^{\infty} |\lambda_j|, \tag{8.10}$$

and, using (8.8) and the orthonormality of ψ_j on $[-1, 1]$,

$$\left\| e^{ibx} - \sum_{j=0}^{M-1} \lambda_j \psi_j(b/c)\psi_j(x) \right\|_2 = \sqrt{\sum_{j=M}^{\infty} |\lambda_j|^2 \, |\psi_j(b/c)|^2} \leq C_\infty \sqrt{\sum_{j=M}^{\infty} |\lambda_j|^2}. \tag{8.11}$$

From (7.10), we have

$$\int_{-1}^{1} e^{-i\,c\,t\,t_l} \, \psi_j(t) dt = \bar{\lambda}_j \psi_j(t_l), \tag{8.12}$$

and, using (8.2)–(8.3) and the relationship between μ_j and λ_j in (8.4), we obtain

$$\left| \sum_{l=1}^{M} w_l \, e^{i\,c\,x\,t_l} \bar{\lambda}_j \, \psi_j(t_l) - |\lambda_j|^2 \psi_j(x) \right| \leq \epsilon^2 \int_{-1}^{1} |\psi_j(t)| \, dt \leq \sqrt{2}\,\epsilon^2. \tag{8.13}$$

Thus, we arrive at

$$\left\| \sum_{l=1}^{M} w_l \mathrm{e}^{\mathrm{i}\, c\, x\, t_l}\, \psi_j(t_l) - \lambda_j\, \psi_j(x) \right\|_\infty \leq \sqrt{2} \frac{\epsilon^2}{|\lambda_j|}, \tag{8.14}$$

and

$$\left\| \sum_{l=1}^{M} w_l \mathrm{e}^{\mathrm{i}cxt_l} \psi_j(t_l) - \lambda_j \psi_j(x) \right\|_2 \leq 2 \frac{\epsilon^2}{|\lambda_j|}. \tag{8.15}$$

Combining (8.10) and (8.14), we have

$$\left\| \mathrm{e}^{\mathrm{i}bx} - \sum_{l=1}^{M} \sum_{j=0}^{M-1} w_l \mathrm{e}^{\mathrm{i}cxt_l} \psi_j(b/c) \psi_j(t_l) \right\|_\infty \leq C_\infty^2 \sum_{j=M}^{\infty} |\lambda_j| + \sqrt{2}\, C_\infty \sum_{j=0}^{M-1} \frac{\epsilon^2}{|\lambda_j|}. \tag{8.16}$$

Similarly, combining (8.11) and (8.15), we obtain

$$\left\| \mathrm{e}^{\mathrm{i}bx} - \sum_{l=1}^{M} \sum_{j=0}^{M-1} w_l \mathrm{e}^{\mathrm{i}cxt_l} \psi_j(b/c) \psi_j(t_l) \right\|_2 \leq C_\infty \sqrt{\sum_{j=M}^{\infty} |\lambda_j|^2} + 2\, C_\infty \sum_{j=0}^{M-1} \frac{\epsilon^2}{|\lambda_j|}, \tag{8.17}$$

By setting

$$\alpha_l = w_l \sum_{j=0}^{M-1} \psi_j(b/c)\, \psi_j(t_l), \tag{8.18}$$

and observing that $|\lambda_M| \approx \epsilon$ and that $|\lambda_j| \ll |\lambda_M|$ for $j > M$, we obtain (8.5) and (8.6). □

We now construct two useful bases as linear combinations of the functions $\{\mathrm{e}^{\mathrm{i}ct_l x}\}_{l=1}^{M}$. First, let us consider the following algebraic eigenvalue problem:

$$\sum_{l=1}^{M} w_l \mathrm{e}^{\mathrm{i}ct_m t_l} \Psi_j(t_l) = \eta_j \Psi_j(t_m), \tag{8.19}$$

where t_l and w_l are the same as in (8.1). By solving (8.19), we find η_j and $\Psi_j(t_l)$. We then consider functions Ψ_j, $j = 1, \ldots, M$, defined for any x as

$$\Psi_j(x) = \frac{1}{\eta_j} \sum_{l=1}^{M} w_l \mathrm{e}^{\mathrm{i}cxt_l} \Psi_j(t_l). \tag{8.20}$$

The functions Ψ_j in (8.20) are linear combinations of the exponentials $\{\mathrm{e}^{\mathrm{i}\, c\, x\, t_l}\}_{l=1}^{n}$. We will show that the functions Ψ_j are nearly orthonormal and we will use them as an approximate basis for weighted bandlimited functions with bandlimit c.

Remark VIII.1 The functions Ψ_j mimic the PSWF. However, one has to be careful relating ψ_j and Ψ_j. Since a large number of eigenvalues λ_j satisfy both $|\lambda_j|$ is close to $\sqrt{2\pi/c}$ and $\eta_j - \lambda_j = O(\epsilon^2)$, then, in solving (8.19), we also obtain a large number of eigenvalues η_j with absolute value close to $\sqrt{2\pi/c}$. Therefore, in spite of the fact that all λ_j are distinct, we may obtain a group of eigenvalues that are identical within the precision of the computation. In this case the functions Ψ_j correspond to linear combinations of the PSWF. In other words, we need to impose additional conditions in (8.19) to maintain a proper correspondence with the PSWF. However, in many applications there is no apparent need to make such an identification since in all cases the resulting functions span the same subspace.

Proposition VIII.1 *The functions Ψ_j, $j = 1, \ldots, M$, are nearly orthogonal and satisfy*

$$\left| \int_{-1}^{1} \Psi_j(t)\, \Psi_{j'}(t) dt - \delta_{jj'} \right| < \frac{\epsilon^2 \sum_{k=1}^{M} w_k}{|\eta_j|\, |\eta_{j'}|}. \tag{8.21}$$

Proof We start by defining $q_l^j = \sqrt{w_l}\Psi_j(t_l)$. We substitute in (8.19) to obtain

$$\sum_{l=1}^{M} \sqrt{w_m} \mathrm{e}^{\mathrm{i}ct_m t_l} \sqrt{w_l}\, q_l^j = \eta_j\, q_m^j. \tag{8.22}$$

The vectors $\{\boldsymbol{q}^j\}$ are eigenvectors of the matrix S, $S_{ml} = \sqrt{w_m}\mathrm{e}^{\mathrm{i}ct_m t_l}\sqrt{w_l}$. If we take into account the symmetry of nodes t_l and weights w_l in (8.1), we obtain that the matrix S is normal, $SS^* = S^*S$, and, in addition, $\bar{S} = S^*$. In Proposition VIII.2 we show that for such matrices there exists an orthonormal basis of real eigenvectors. Thus, computed via (8.22), we assume q_l^j to be a real orthogonal matrix and then

$$\sum_{j=1}^{M} \sqrt{w_l}\, \Psi_j(t_l)\, \Psi_j(t_m)\, \sqrt{w_m} = \delta_{lm}, \tag{8.23}$$

and

$$\sum_{l=1}^{M} \Psi_j(t_l)\, w_l\, \Psi_{j'}(t_l) = \delta_{jj'}. \tag{8.24}$$

We have

$$\int_{-1}^{1} \Psi_j(t)\, \Psi_{j'}(t) dt = \frac{1}{\eta_j\, \eta_{j'}} \sum_{l,l'=1}^{M} w_l\, w_{l'}\, \Psi_j(t_l)\, \Psi_{j'}(t_{l'}) \int_{-1}^{1} \mathrm{e}^{\mathrm{i}ct(t_l + t_{l'})}\, dt \tag{8.25}$$

and, from (8.1), we obtain

$$\left| \int_{-1}^{1} \Psi_j(t)\,\Psi_{j'}(t)dt - \frac{1}{\eta_j\,\eta_{j'}} \sum_{l,l'=1}^{M} w_l\,w_{l'}\,\Psi_j(t_l)\,\Psi_{j'}(t_{l'}) \sum_{k=1}^{M} w_k \mathrm{e}^{\mathrm{i}ct_k(t_l+t_{l'})} \right| \leq \frac{\epsilon^2 \sum_{k=1}^{M} w_k}{|\eta_j|\,|\eta_{j'}|}. \tag{8.26}$$

For the last inequality we also used Schwarz inequality and (8.24) to estimate

$$\begin{aligned} \left| \sum_{l,l'=1}^{M} w_l\,w_{l'}\,\Psi_j(t_l)\,\Psi_{j'}(t_{l'}) \right| &\leq \sum_{l} w_l\,|\Psi_j(t_l)| \sum_{l} w_l\,|\Psi_{j'}(t_l)| \\ &\leq (\sum_{l=1}^{M} w_l\,|\Psi_j(t_l)|)^2 \leq (\sum_{l=1}^{M} w_l)(\sum_{l=1}^{M} w_l\,|\Psi_j(t_l)|^2) = \sum_{l=1}^{M} w_l. \end{aligned}$$

To finish, using (8.19) and (8.24) we simplify (8.26) and arrive at (8.21). □

We still need to prove

Proposition VIII.2 *Let S be a normal matrix such that $\bar{S} = S^*$. Then there exist an orthonormal basis of real eigenvectors of S.*

Proof First, since S is normal, eigenspaces corresponding to different eigenvalues are orthogonal. Thus, it is sufficient to prove the proposition for any eigenspace $E(\lambda) = \{\boldsymbol{x} : S\boldsymbol{x} = \lambda\boldsymbol{x}\}$. Also, normality of S implies that for any $\boldsymbol{x} \in E(\lambda)$ we have $\bar{\boldsymbol{x}} \in E(\lambda)$. Indeed, from $S^*\boldsymbol{x} = \bar{\lambda}\boldsymbol{x}$ and $\bar{S} = S^*$ it follows that $S\bar{\boldsymbol{x}} = \lambda\bar{\boldsymbol{x}}$. Consequently, if $\{\boldsymbol{v_k}\}_{k=1}^{m}$ is a basis of $E(\lambda)$, then $E(\lambda)$ can be spanned by the real and imaginary parts of $\boldsymbol{v_k}$,

$$\mathcal{A} = \{\mathrm{Re}(\boldsymbol{v_k}), \mathrm{Im}(\boldsymbol{v_k})\}_{k=1}^{m},$$

where for any vector $\boldsymbol{x} = (x_1, \ldots, x_M)$, $\mathrm{Re}(\boldsymbol{x}) = (\mathrm{Re}(x_1), \ldots, \mathrm{Re}(x_m))$, and similarly for $\mathrm{Im}(\boldsymbol{x})$. By Gram-Schmidt orthonormalization of the $2m$ (linearly dependent) vectors $\mathcal{A}$, we obtain the desired result. See another proof in [9, Theorem 4.4.7] □

Let us now construct interpolating bases as linear combinations of the exponentials $\{\mathrm{e}^{\mathrm{i}cxt_l}\}_{l=1}^{n}$. We define functions R_k, $k = 1, \ldots, M$ as

$$R_k(x) = \sum_{l=1}^{M} r_{kl} \mathrm{e}^{\mathrm{i}cxt_l}, \tag{8.27}$$

where

$$r_{kl} = \sum_{j=1}^{M} w_k\,\Psi_j(t_k)\,\frac{1}{\eta_j}\,\Psi_j(t_l)\,w_l = \sum_{j=1}^{M} \sqrt{w_k}\,q_k^j\,\frac{1}{\eta_j}\,q_l^j\,\sqrt{w_l}. \tag{8.28}$$

By direct evaluation in (8.19) and (8.23), we verify that functions R_k are interpolating,

$$R_k(t_m) = \delta_{km}. \tag{8.29}$$

Let us show that the integration of $R_k(t)\,\mathrm{e}^{\mathrm{i}\,a\,t}$, where $|a| \le c$, yields a one point quadrature rule of accuracy $O(\epsilon)$.

Proposition VIII.3 *For $|a| \le c$ let*

$$\Delta_k = \int_{-1}^{1} R_k(t)\mathrm{e}^{\mathrm{i}at}\,dt - w_k\,\mathrm{e}^{\mathrm{i}at_k}. \tag{8.30}$$

Then we have

$$|\Delta_k| \le \|\Delta\|_2 \le \sqrt{M}\,\frac{\max_{k=1,\cdots,M}|w_k|}{\min_{k=1,\cdots,M}|\eta_k|}\,\epsilon^2, \tag{8.31}$$

where $\|\Delta\|_2 = \sqrt{\sum_{k=1}^{M}|\Delta_k|^2}$.

Proof For functions $\mathrm{e}^{\mathrm{i}ax}$, where $|a| < c$, we have

$$\int_{-1}^{1} R_k(t)\mathrm{e}^{\mathrm{i}at}\,dt - \sum_{l=1}^{M} r_{kl}\sum_{m=1}^{M} w_m\mathrm{e}^{\mathrm{i}ct_m(t_l+a/c)} = \sum_{l=1}^{M} r_{kl}s_l, \tag{8.32}$$

where

$$s_l = \int_{-1}^{1} \mathrm{e}^{\mathrm{i}ct(t_l+a/c)}\,dt - \sum_{m=1}^{M} w_m\mathrm{e}^{\mathrm{i}ct_m(t_l+a/c)}. \tag{8.33}$$

We obtain using (8.27) and (8.29),

$$\sum_{l=1}^{M} r_{kl}\sum_{m=1}^{M} w_m\mathrm{e}^{\mathrm{i}ct_m(t_l+a/c)} = \sum_{m=1}^{M} w_m\,R_k(t_m)\mathrm{e}^{\mathrm{i}at_m} = w_k\,\mathrm{e}^{\mathrm{i}at_k}, \tag{8.34}$$

and, therefore, Δ_k in (8.30) can be written as a matrix-vector multiplication, $\Delta_k = \sum_{l=1}^{M} r_{kl}s_l$. The inequality (8.31) is then obtained via the usual l^2-norm estimates, taking into account that the matrices q_k^j and q_l^j in (8.28) are orthogonal. □

We have observed (via computation) that $\max_{k=1,\cdots,M}|w_k| = O(1)$ and $\min_{k=1,\cdots,M}|\eta_k| = O(\epsilon^{-1})$ in (8.31), thus resulting in $\|\Delta\|_2 = O(\epsilon)$. Next we derive a weak estimate showing that the functions R_k are close to be an interpolating basis for bandlimited exponentials.

Proposition VIII.4 *For every b, $|b| \le c$ let us consider the function*

$$\Omega_b(t) = \mathrm{e}^{\mathrm{i}bt} - \sum_{k=1}^{M} \mathrm{e}^{\mathrm{i}bt_k}\,R_k(t). \tag{8.35}$$

Then, for every $|a| \le c$, we have

$$\left|\int_{-1}^{1} \Omega_b(t)\,\mathrm{e}^{\mathrm{i}at}\,dt\right| \le (1 + M\,\frac{\max_{k=1,\cdots,M}|w_k|}{\min_{k=1,\cdots,M}|\eta_k|})\,\epsilon^2. \tag{8.36}$$

Proof Using (8.30), we have

$$\int_{-1}^{1} \Omega_b(t)\, \mathrm{e}^{\mathrm{i}at}\, dt = \int_{-1}^{1} \mathrm{e}^{\mathrm{i}(b+a)t}\, dt - \sum_{k=1}^{M} w_k\, \mathrm{e}^{\mathrm{i}(b+a)t_k} - \sum_{k=1}^{M} \mathrm{e}^{\mathrm{i}bt_k}\, \Delta_k, \tag{8.37}$$

where

$$\Delta_k = \int_{-1}^{1} R_k(t) \mathrm{e}^{\mathrm{i}at}\, dt - w_k\, \mathrm{e}^{\mathrm{i}at_k}\,. \tag{8.38}$$

Applying (8.1), we obtain

$$\left| \int_{-1}^{1} \Omega_b(t)\, \mathrm{e}^{\mathrm{i}at}\, dt \right| \leq \epsilon^2 + \sqrt{M}\, \|\Delta\|_2. \tag{8.39}$$

The estimate (8.36) then follows from Proposition VIII.3. □

Remark VIII.2 Using the functions R_k, $k = 1, \ldots, M$, on a hierarchy of intervals, it is possible to construct a multiresolution basis (for a finite number of scales) similar to multiwavelet bases. We will consider such construction and its applications elsewhere.

VIII.1 Examples

For the weight

$$\omega(t) = \begin{cases} 1 & t \in [-a, a],\ a \leq \frac{1}{2} \\ 0 & \text{otherwise.} \end{cases} \tag{8.40}$$

we construct a 30-node quadrature formula so that (8.1) is satisfied with $\epsilon^2 \approx 10^{-15}$. We display the error in Figure 9. For bandlimit $c = 7.5\,\pi$, we construct an interpolating basis $\{R_k\}_{k=1}^{30}$ and display one of the functions in Figure 10. We then demonstrate the performance of the interpolation using this basis for three examples,

$$g_1(t) = \cos(ct), \tag{8.41}$$

$$g_2(t) = t, \tag{8.42}$$

$$g_3(t) = P_9(t)\,, \tag{8.43}$$

where P_9 is the Legendre polynomial of degree 9. These three functions are not periodic and we use

$$\tilde{g}_1(t) = \sum_{l=1}^{30} \cos(ct_l) R_l(t), \tag{8.44}$$

$$\tilde{g}_2(t) = \sum_{l=1}^{30} t_l R_l(t), \quad \text{and} \tag{8.45}$$

$$\tilde{g}_3(t) = \sum_{l=1}^{30} P_9(t_l) R_l(t) \tag{8.46}$$

as approximations. We display the function g_1 in Figure 11 and the error of approximation by $\tilde{g}_1$ in Figure 12. Similarly, we display the function g_2 in Figure 13 and the error of approximation by $\tilde{g}_2$ in Figure 14, the function g_3 in Figure 15 and the error of approximation by $\tilde{g}_3$ in Figure 16.

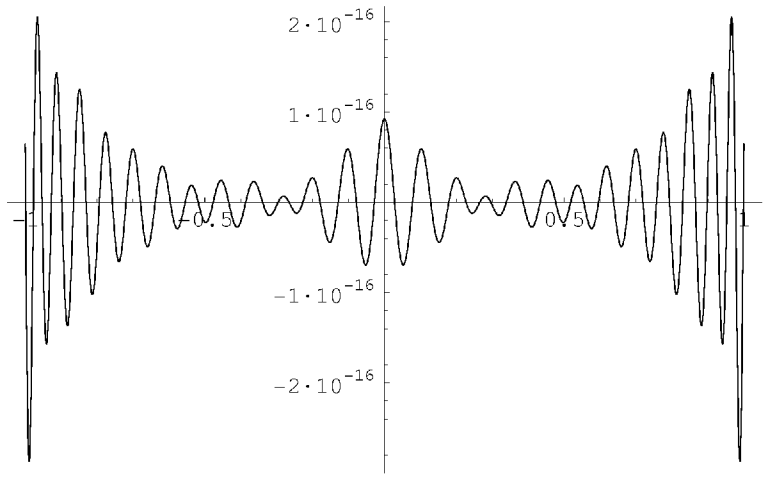

Figure 9: Error in (8.1) for Example 1.

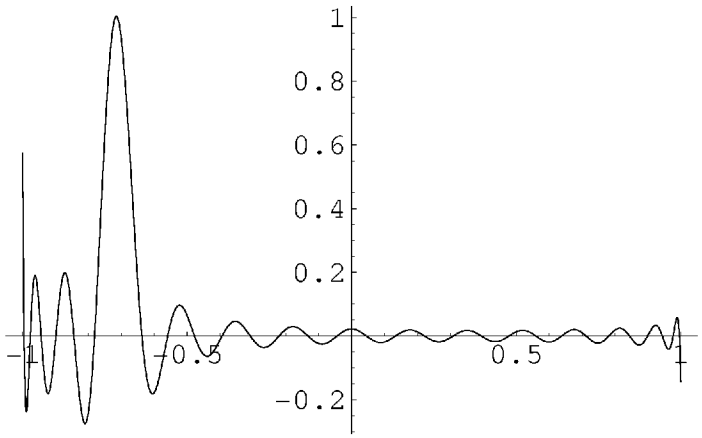

Figure 10: Interpolating function $R_7(t)$ on the interval $[-1, 1]$.

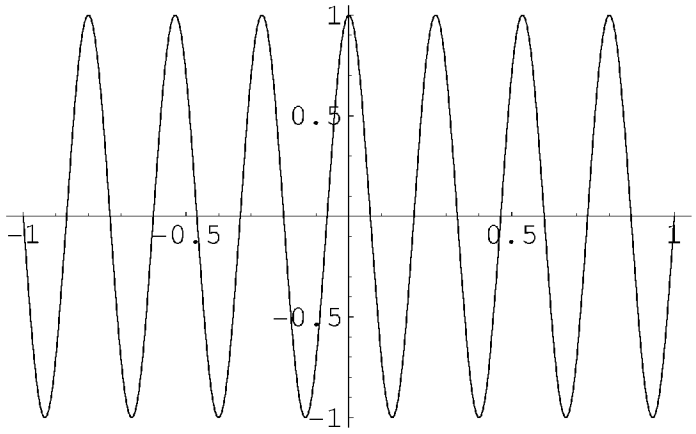

Figure 11: Function $g_1(t)$ on the interval $[-1, 1]$.

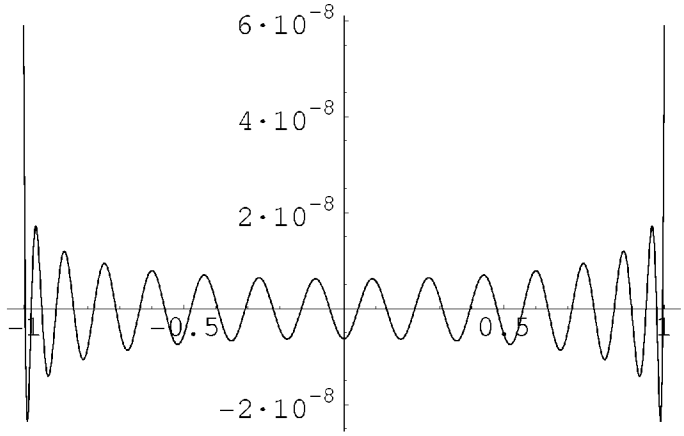

Figure 12: Difference $g_1(t) - \tilde{g}_1(t)$ on the interval $[-1, 1]$.

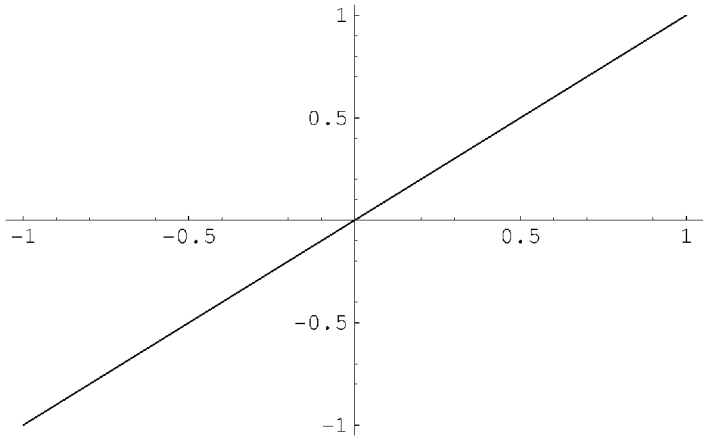

Figure 13: Function $g_2(t)$ on the interval $[-1, 1]$.

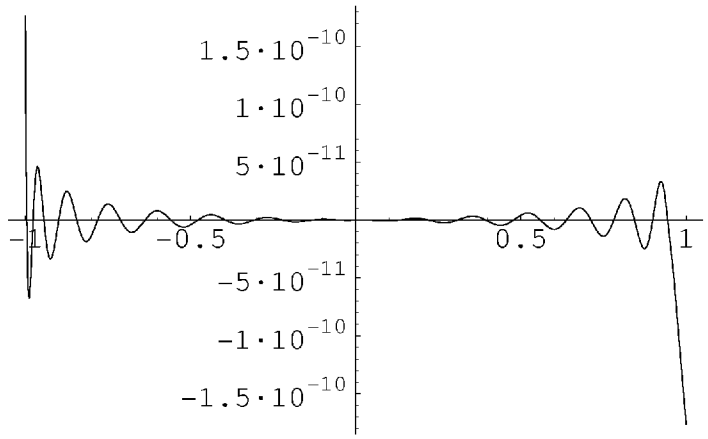

Figure 14: Difference $g_2(t) - \tilde{g}_2(t)$ on the interval $[-1, 1]$.

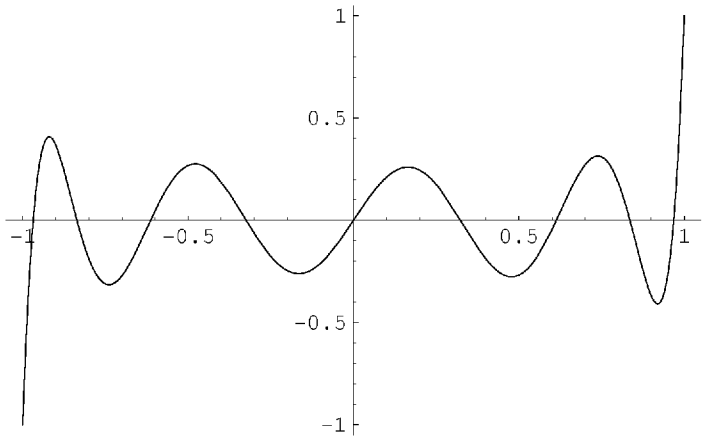

Figure 15: Function $g_3(t)$ on the interval $[-1, 1]$.

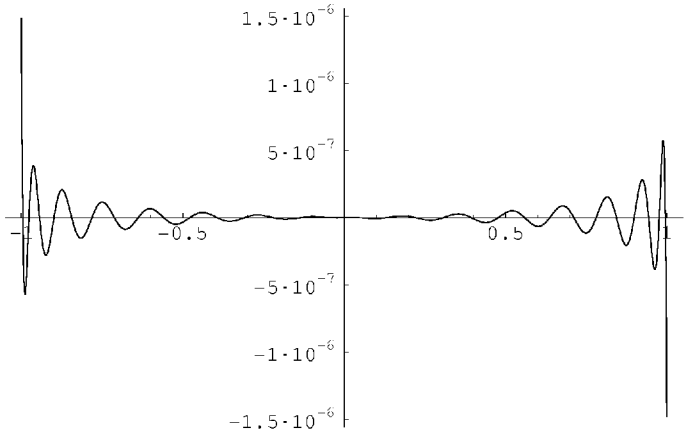

Figure 16: Difference $g_3(t) - \tilde{g}_3(t)$ on the interval $[-1, 1]$.

IX Conclusions

In this paper we have introduced a new family of Gaussian-type quadratures for weighted integrals of exponentials. These quadratures are parameterized by the eigenvalues of the positive definite Toeplitz matrix constructed from the trigonometric moments of the weight. The eigenvalues of this matrix accumulate towards zero and appear to have exponential decay (see Figure 1). For small eigenvalues, these quadratures are of practical interest.

The remarkable feature of these quadratures is that they have nodes outside the support of the measure and, as it turns out, the corresponding weights are negative and small, roughly of the size of the eigenvalue. The case corresponding to the smallest eigenvalue is equivalent to the classical Carathéodory representation.

As an application of the new quadratures, we show how to approximate and integrate several (essentially) bandlimited functions. We also have constructed using quadrature nodes and for a given precision, an interpolating basis for bandlimited functions on an interval.

In the paper we made a number of observations for which we do not have proofs. Let us finish by stating two unresolved issues. First, it is desirable to have tight uniform estimates for the $L_\infty-$norm of the PSWF (with a fixed bandlimiting constant) or, ideally, for the eigenfunctions associated with more general weights. Second, we conjecture that in Theorem IV.1, it is not necessary to require distinct roots for the eigenpolynomial since it might be a consequence of the eigenvalue being simple. We neither have a proof nor a counterexample at this time.

A Appendix

To prove Theorem II.2, we use a technique that goes back to [2] (see [27, Theorem 7.3] and [18, Chapter 5] for more details) which involves the Fejér kernel,

$$F_L(x) = \sum_{|k|\le L} (1 - \frac{|k|}{L+1}) \mathrm{e}^{\mathrm{i}\pi kx} = \frac{\sin^2((L+1)\frac{\pi x}{2})}{(L+1)\sin^2\frac{\pi x}{2}}, \tag{1.1}$$

for real x.

We need the following result,

Theorem A.1 ([18], Theorem 8, Chapter 5) *For $|k| \le N$ let*

$$c_k = \sum_{j=1}^{M} \rho_j z_j^k,$$

where $\rho_j \ge 0$ and $|z_j| = 1$. Then, for all L, $0 \le L \le N$,

$$(L+1)\,\|\boldsymbol{\rho}\|_2^2 \le c_0^2 + 2\sum_{k=1}^{L} |c_k|^2.$$

Proof Let $a_k = 1 - \frac{|k|}{L+1}$ be the coefficients of the Fejér kernel F_L and write $z_j = \mathrm{e}^{\mathrm{i}\pi\theta_j}$. Since $\rho_j \ge 0$ and $F_L(\theta) \ge 0$ for all θ,

$$\begin{aligned}
\sum_{|k|\le L} a_k |c_k|^2 &= \sum_{|k|\le L} a_k \sum_{j,l} \rho_j \rho_l (\frac{z_j}{z_l})^k \\
&= \sum_{j,l} \rho_j \rho_l F_L(\theta_j - \theta_l) \ge F_L(0) \sum_{j=1}^{M} \rho_j^2 \\
&= (L+1) \sum_{j=1}^{M} \rho_j^2.
\end{aligned}$$

The theorem follows because $a_0 = 1$ and $a_k \le 1$. □

Proof of Theorem II.2 We first use (2.1) to extend the definition of c_k as $c_{-k} = \overline{c_k}$ for $k = 1, \cdots, N$ and $c_0 = \sum_{j=1}^{M} \rho_j$. We then define the Toeplitz matrix $\boldsymbol{T}_N$, $(\boldsymbol{T}_N)_{kj} = (c_{j-k})_{0\le k,j\le N}$ and the polynomial

$$Q(z) = \prod_{j=1}^{M} (z - \mathrm{e}^{\mathrm{i}\pi\theta_j}) = \sum_{k=0}^{M} q_k z^k.$$

Then, $\boldsymbol{q} = (q_0, \cdots, q_M, 0, \cdots, 0)^t$ belongs to the null subspace of $\boldsymbol{T}_N$ because for all l

$$\sum_{k=0}^{M} \sum_{j=1}^{M} \rho_j \mathrm{e}^{\mathrm{i}\pi\theta_j(k-l)} q_k = \sum_{j=1}^{M} \rho_j \mathrm{e}^{-\mathrm{i}\pi\theta_j l} Q(\mathrm{e}^{\mathrm{i}\pi\theta_j}) = 0,$$

since, for all j, $Q(\mathrm{e}^{\mathrm{i}\pi\theta_j}) = 0$.

The matrix $\boldsymbol{A} = \boldsymbol{T}_N - c_0 \boldsymbol{I}$ has the eigenvalue $-c_0$ because $\boldsymbol{T}_N$ is singular. We can bound c_0^2 by the Frobenius norm of $\boldsymbol{A}$ to obtain

$$c_0^2 \leq 2 \sum_{j=1}^{N} j |c_{N+1-j}|^2 \leq 2N \|\boldsymbol{c}\|_2^2.$$

To finish the proof, we use Theorem A.1 with $L = N$. □

ACKNOWLEDGMENT

We would like to thank Dr. Martin Mohlenkamp for a number of useful suggestions.

References

[1] G. Beylkin. On the fast Fourier transform of functions with singularities. *Appl. Comput. Harmon. Anal.*, 2(4):363–381, 1995.

[2] J. W. S. Cassels. On the sums of powers of complex numbers. *Acta Math. Acad. Sci. Hungar.*, 7:283 289, 1956.

[3] H. Cheng, L. Greengard, and V. Rokhlin. A fast adaptive multipole algorithm in three dimensions. *J. Comput. Phys.*, 155(2):468–498, 1999.

[4] A. Dutt and V. Rokhlin. Fast Fourier transforms for nonequispaced data. *SIAM J. Sci. Comput.*, 14(6):1368 1393, 1993.

[5] I. Gohberg and V. Olshevsky. Circulants, displacements and decompositions of matrices. *Integral Equations Operator Theory*, 15(5):730–743, 1992.

[6] I. C. Gohberg and A. A. Semencul. The inversion of finite Toeplitz matrices and their continual analogues. *Mat. Issled.*, 7(2(24)):201–223, 290, 1972.

[7] U. Grenander and G. Szegő. *Toeplitz forms and their applications.* Chelsea Publishing Co., New York, second edition, 1984.

[8] G. Heinig and K. Rost. *Algebraic methods for Toeplitz-like matrices and operators.* Birkhäuser Verlag, Basel, 1984.

[9] R. A. Horn and C. R. Johnson. *Topics in matrix analysis.* Cambridge University Press, Cambridge, 1994. Corrected reprint of the 1991 original.

[10] W. B. Jones, O. Njåstad, and W. J. Thron. Moment theory, orthogonal polynomials, quadrature, and continued fractions associated with the unit circle. *Bull. London Math. Soc.*, 21(2):113–152, 1989.

[11] S. Karlin and W. J. Studden. *Tchebycheff systems: With applications in analysis and statistics.* Interscience Publishers John Wiley & Sons, New York-London-Sydney, 1966. Pure and Applied Mathematics, Vol. XV.

[12] M. G. Kreĭn and A. A. Nudel'man. *The Markov moment problem and extremal problems.* American Mathematical Society, Providence, R.I., 1977. Ideas and problems of P. L. Čebyšev and A. A. Markov and their further development, Translations of Mathematical Monographs, Vol. 50.

[13] H. J. Landau. The eigenvalue behavior of certain convolution equations. *Trans. Amer. Math. Soc.*, 115:242–256, 1965.

[14] H. J. Landau and H. O. Pollak. Prolate spheroidal wave functions, Fourier analysis and uncertainty II. *Bell System Tech. J.*, 40:65 84, 1961.

[15] H. Lu. Fast solution of confluent Vandermonde linear systems. *SIAM J. Matrix Anal. Appl.*, 15(4):1277–1289, 1994.

[16] A. A. Markov. On the limiting values of integrals in connection with interpolation. *Zap. Imp. Akad. Nauk. Fiz.-Mat. Otd.*, 8(6), 1898. In Russian. Also in [17, pp. 146-230].

[17] A. A. Markov. *Selected Papers on Continued Fractions and the Theory of Functions Deviating Least from Zero.* OGIZ, Moscow-Leningrad, 1948.

[18] H. L. Montgomery. *Ten lectures on the interface between analytic number theory and harmonic analysis.* Published for the Conference Board of the Mathematical Sciences, Washington, DC, 1994.

[19] V. F. Pisarenko. The retrieval of harmonics from a covariance function. *Geophys. J. R. Astr. Soc.*, 33:347–366, 1973.

[20] K. Rost and Z. Vavřín. Inversion formulas and fast algorithms for Löwner-Vandermonde matrices. In *Proceedings of the Sixth Conference of the International Linear Algebra Society (Chemnitz, 1996)*, volume 275/276, pages 537 549, 1998.

[21] I. J. Schoenberg. *Cardinal spline interpolation.* SIAM, Philadelphia, Pa., 1973. Conference Board of the Mathematical Sciences Regional Conference Series in Applied Mathematics, No. 12.

[22] D. Slepian. Prolate spheroidal wave functions, Fourier analysis and uncertainty V. The discrete case. *Bell System Tech. J.*, 57:1371 1430, 1978.

[23] D. Slepian and H. O. Pollak. Prolate spheroidal wave functions, Fourier analysis and uncertainty I. *Bell System Tech. J.*, 40:43–63, 1961.

[24] David Slepian. Some asymptotic expansions for prolate spheroidal wave functions. *J. Math. and Phys.*, 44:99 140, 1965.

[25] Gabor Szegö. *Orthogonal Polynomials.* AMS, Providence, RI, 4th edition, 1975.

[26] W. F. Trench. Some spectral properties of Hermitian Toeplitz matrices. *SIAM J. Matrix Anal. Appl.*, 15(3):938 942, 1994.

[27] P. Turán. *On a new method of analysis and its applications.* John Wiley & Sons Inc., New York, 1984. With the assistance of G. Halász and J. Pintz, A Wiley-Interscience Publication.

[28] H. Xiao, V. Rokhlin, and N. Yarvin. Prolate spheroidal wavefunctions, quadrature and interpolation. *Inverse Problems*, 17(4):805 838, 2001.

[29] N. Yarvin and V. Rokhlin. Generalized Gaussian quadratures and singular value decompositions of integral operators. *SIAM J. Sci. Comput.*, 20(2):699–718 (electronic), 1999.

[30] N. Yarvin and V. Rokhlin. An improved fast multipole algorithm for potential fields on the line. *SIAM J. Numer. Anal.*, 36(2):629 666 (electronic), 1999.

INSTITUTE OF PHYSICS PUBLISHING INVERSE PROBLEMS

Inverse Problems **17** (2001) 805–838 www.iop.org/Journals/ip PII: S0266-5611(01)17291-6

Prolate spheroidal wavefunctions, quadrature and interpolation

H Xiao, V Rokhlin and N Yarvin

Department of Computer Science, Yale University, PO Box 208285 Yale Station, New Haven, CT 06520-8285, USA

E-mail: xiao-hong@cs.yale.edu, rokhlin-vladimir@cs.yale.edu and yarvin-norman@cs.yale.edu

Received 20 September 2000

Abstract

Polynomials are one of the principal tools of classical numerical analysis. When a function needs to be interpolated, integrated, differentiated, etc, it is assumed to be approximated by a polynomial of a certain fixed order (though the polynomial is almost never constructed explicitly), and a treatment appropriate to such a polynomial is applied. We introduce analogous techniques based on the assumption that the function to be dealt with is band-limited, and use the well developed apparatus of prolate spheroidal wavefunctions to construct quadratures, interpolation and differentiation formulae, etc, for band-limited functions. Since band-limited functions are often encountered in physics, engineering, statistics, etc, the apparatus we introduce appears to be natural in many environments. Our results are illustrated with several numerical examples.

1. Introduction

Numerical quadrature and interpolation are a well developed part of numerical analysis; polynomials are the classical tool for the design of such schemes. Conceptually speaking, one assumes that the function is well approximated by expressions of the form

$$\sum_{j=0}^{n} a_j x^j, \tag{1}$$

with reasonably small n, and one designs algorithms that are effective for functions of the form (1)—needless to say, one almost never actually computes the coefficients $\{a_i\}$; one only uses the fact of their existence. Obviously, the polynomial approach is only effective for functions that are well approximated by polynomials.

When one has to handle functions that are well behaved on the whole line (for example, in signal processing), polynomials are not an appropriate tool. In such cases, trigonometric polynomials are used; existing tools are very satisfactory for dealing with functions defined

0266-5611/01/040805+34$30.00

and well behaved on the whole of $\mathbb{R}^1$. Such tools, in effect, make the assumption that the functions are band-limited or nearly so; a function $f : \mathbb{R} \to \mathbb{R}$ is said to be band-limited if there exist a positive real c and a function $\sigma \in L^2[-1, 1]$ such that

$$f(x) = \int_{-1}^{1} e^{icxt} \sigma(t)\, dt. \tag{2}$$

However, in many cases, we are confronted with band-limited functions defined on intervals (or, more generally, on compact regions in $\mathbb{R}^n$). Wave phenomena are a rich source of such functions, both in the engineering and computational contexts; they are also encountered in fluid dynamics, signal processing, and many other areas. Often, such functions can be effectively approximated by polynomials via standard tools of classical analysis. However, even when such approximations are feasible, they are usually not optimal. Smooth periodic functions are a good illustration of this observation: while they *can* be approximated by polynomials (for example, via Chebyshev or Legendre expansions), they are more efficiently approximated by Fourier expansions, both for analytical and numerical purposes. It would appear that an approach explicitly based on trigonometric polynomials could be more efficient in dealing with band-limited functions.

In the engineering context, such an apparatus was constructed more than 30 years ago (see [8–10, 21, 22]). The natural tool for analysing band-limited functions on $\mathbb{R}^1$ is the Fourier transform, unless the functions are periodic, in which case the natural tool is the Fourier series. The authors of [21, 22] observe that, for the analysis of band-limited functions on the interval, prolate spheroidal wavefunctions (PSWFs) are likewise a natural approach. The authors also construct a multi-dimensional version of the theory, though their apparatus is only complete for the case of spherical regions.

The present paper constructs tools for using the approach of [21, 22] in the modern computational environment. We construct a class of quadratures for band-limited functions that closely parallel the Gaussian quadratures for polynomials. The nodes are very close to being roots of appropriately chosen PSWFs, the resulting quadratures are stable, and all weights are positive. As in the case of polynomials, there are interpolation, differentiation and indefinite integration schemes associated with the obtained quadratures, exact on certain classes of band-limited functions. These procedures are the main tools necessary for the numerical use of spectral discretizations based on PSWFs, instead of on the usual polynomial bases. When dealing with band-limited functions, the number of nodes required by these procedures to obtain a prescribed accuracy is much less than that required by their polynomial-based counterparts. An additional bonus is the fact that the condition number of differentiation of PSWFs is less than that of differentiation of the usual polynomial basis functions (see section 8).

This paper is organized as follows. Section 2 summarizes various standard mathematical facts used in the remainder of the paper. Section 3 contains derivations of various results used in the algorithms described in later sections. Section 4 describes algorithms for evaluation of PSWFs and associated eigenvalues. Section 5 describes a construction of quadratures for band-limited functions. Section 6 describes an alternative approach to arriving at such quadratures; it shows that roots of appropriately chosen PSWFs can serve as quadrature nodes. Section 7 analyses the use of PSWFs for interpolation. Section 8 contains results of our numerical experiments with quadratures and interpolation. Section 9 contains a number of miscellaneous properties of PSWFs, and section 10 contains generalizations and conclusions.

2. Mathematical preliminaries

As a matter of convention, in this paper the norm of a function is, unless stated otherwise, its L^2 norm:

$$\|f\| = \sqrt{\int |f(x)|^2 \, \mathrm{d}x}. \tag{3}$$

2.1. Chebyshev systems

Definition 2.1. *A sequence of functions $\phi_1, \ldots, \phi_n$ will be referred to as a Chebyshev system on the interval $[a, b]$ if each of them is continuous and the determinant*

$$\begin{vmatrix} \phi_1(x_1) & \cdots & \phi_1(x_n) \\ \vdots & & \vdots \\ \phi_n(x_1) & \cdots & \phi_n(x_n) \end{vmatrix} \tag{4}$$

is nonzero for any sequence of points $x_1, \ldots, x_n$ such that $a \leqslant x_1 < x_2 \cdots < x_n \leqslant b$.

An alternative definition of a Chebyshev system is that any linear combination of the functions with nonzero coefficients must have fewer than n zeros.

Examples of Chebyshev and extended Chebyshev systems include the following. (Additional examples can be found in [12].)

Example 2.1. *The powers $1, x, x^2, \ldots, x^n$ form an extended Chebyshev system on the interval $(-\infty, \infty)$.*

Example 2.2. *The exponentials $\mathrm{e}^{\lambda_1 x}, \mathrm{e}^{\lambda_2 x}, \ldots, \mathrm{e}^{\lambda_n x}$ form an extended Chebyshev system for any $\lambda_1, \ldots, \lambda_n > 0$ on the interval $[0, \infty)$.*

Example 2.3. *The functions $1, \cos x, \sin x, \cos 2x, \sin 2x, \ldots, \cos nx, \sin nx$ form a Chebyshev system on the interval $[0, 2\pi]$.*

2.2. Generalized Gaussian quadratures

A quadrature rule is an expression of the form

$$\sum_{j=1}^{n} w_j \phi(x_j), \tag{5}$$

where the points $x_j \in \mathbb{R}$ and coefficients $w_j \in \mathbb{R}$ are referred to as the nodes and weights of the quadrature, respectively. They serve as approximations to integrals of the form

$$\int_a^b \phi(x)\, \omega(x) \, \mathrm{d}x, \tag{6}$$

with ω being an integrable non-negative function.

Quadratures are typically chosen so that the quadrature (5) is equal to the desired integral (6) for some set of functions, commonly polynomials of some fixed order. Of these, the classical Gaussian quadrature rules consist of n nodes and integrate polynomials of order $2n - 1$ exactly. In [14], the notion of a Gaussian quadrature was generalized as follows.

Definition 2.2. *A quadrature formula will be referred to as Gaussian with respect to a set of $2n$ functions $\phi_1, \ldots, \phi_{2n} : [a, b] \to \mathbb{R}$ and a weight function $\omega : [a, b] \to \mathbb{R}^+$ if it consists of n weights and nodes, and integrates the functions ϕ_i exactly with the weight function ω for all $i = 1, \ldots, 2n$. The weights and nodes of a Gaussian quadrature will be referred to as Gaussian weights and nodes, respectively.*

The following theorem appears to be due to Markov [15, 16]; proofs of it can also be found in [13] and [12] (in a somewhat different form).

Theorem 2.1. *Suppose that the functions $\phi_1, \ldots, \phi_{2n} : [a, b] \to \mathbb{R}$ form a Chebyshev system on $[a, b]$. Suppose in addition that $\omega : [a, b] \to \mathbb{R}$ is a non-negative integrable function $[a, b] \to \mathbb{R}$. Then there exists a unique Gaussian quadrature for the functions $\phi_1, \ldots, \phi_{2n}$ on $[a, b]$ with respect to the weight function ω. The weights of this quadrature are positive.*

While the existence of generalized Gaussian quadratures was observed more than 100 years ago, the constructions found in [7, 11–13, 15, 16], do not easily yield numerical algorithms for the design of such quadrature formulae; such algorithms have been constructed recently (see [2, 14, 27]).

Remark 2.1. It might be worthwhile to observe here that when a generalized Gaussian quadrature is to be constructed, the determination of its nodes tends to be the critical step (though the procedure of [2, 14, 27] determines the nodes and weights simultaneously). Indeed, once the nodes $x_1, x_2, \ldots, x_n$ have been found, the weights $w_1, w_2, \ldots, w_n$ can be determined easily as the solution of the $n \times n$ system of linear equations

$$\sum_{j=1}^{n} w_j \cdot \phi_i(x_j) = \int_a^b \omega(x)\phi_i(x)\,\mathrm{d}x, \tag{7}$$

with $i = 1, 2, \ldots, n$.

2.3. Legendre polynomials

In agreement with standard practice, we will be denoting by P_n the classical Legendre polynomials, defined by the three-term recursion

$$P_{n+1}(x) = \frac{2n+1}{n+1}\, x\, P_n(x) - \frac{n}{n+1}\, P_{n-1}(x), \tag{8}$$

with the initial conditions

$$P_0(x) = 1, \qquad P_1(x) = x; \tag{9}$$

as is well known,

$$P_k(1) = 1 \tag{10}$$

for all $k = 0, 1, 2, \ldots$, and each of the polynomials P_k satisfies the differential equation

$$(1 - x^2)\,\frac{\mathrm{d}^2 P_k(x)}{\mathrm{d}x^2} - 2x\,\frac{\mathrm{d}P_k(x)}{\mathrm{d}x} + k \cdot (k+1)\, P_k(x) = 0. \tag{11}$$

The polynomials defined by the formulae (8) and (9) are orthogonal on the interval $[-1, 1]$; however, they are not orthonormal, since for each $n \geqslant 0$,

$$\int_{-1}^{1} (P_n(x))^2\,\mathrm{d}x = \frac{1}{n + 1/2}; \tag{12}$$

the normalized version of the Legendre polynomials will be denoted by $\overline{P_n}$, so that

$$\overline{P_n}(x) = P_n(x) \cdot \sqrt{n + 1/2}. \tag{13}$$

The following lemma follows immediately from the Cauchy–Schwartz inequality and from the orthogonality of the Legendre polynomials on the interval $[-1, 1]$.

Lemma 2.2. *For all integer $k \geqslant n$,*

$$\left| \int_{-1}^{1} x^k \overline{P_n}(x)\,\mathrm{d}x \right| < \sqrt{\frac{2}{k+1}}. \tag{14}$$

For all integer $0 \leqslant k < n$,

$$\left| \int_{-1}^{1} x^k \overline{P_n}(x)\,\mathrm{d}x \right| = 0. \tag{15}$$

2.4. Convolutional Volterra equations

A convolutional Volterra equation of the second kind is an expression of the form

$$\varphi(x) = \int_a^x K(x-t)\,\varphi(t)\,\mathrm{d}t + \sigma(x) \tag{16}$$

where a, b are a pair of numbers such that $a < b$, the functions $\sigma, K : |a, b| \to \mathbb{C}$ are square-integrable and $\varphi : [a, b] \to \mathbb{C}$ is the function to be determined. Proofs of the following theorem can be found in [4], as well as in many other sources.

Theorem 2.3. *Equation (16) always has a unique solution on the interval $[a, b]$. If both functions K, σ are k times continuously differentiable, the solution φ is also k times continuously differentiable.*

2.5. Prolate spheroidal wavefunctions

In this subsection, we summarize certain facts about the PSWFs. Unless stated otherwise, all these facts can be found in [18, 21].

Given a real $c > 0$, we will denote by F_c the operator $L^2|-1, 1| \to L^2|-1, 1|$ defined by the formula

$$F_c(\varphi)(x) = \int_1^1 \mathrm{e}^{\mathrm{i}cxt}\,\varphi(t)\,\mathrm{d}t. \tag{17}$$

Obviously, F_c is compact; we will denote by $\lambda_0, \lambda_1, \ldots, \lambda_n, \ldots$ the eigenvalues of F_c ordered so that $|\lambda_{j-1}| \geqslant |\lambda_j|$ for all natural j. For each non-negative integer j, we will denote by ψ_j the eigenfunctions corresponding to λ_j, so that

$$\lambda_j \psi_j(x) = \int_1^1 \mathrm{e}^{\mathrm{i}cxt}\,\psi_j(t)\,\mathrm{d}t, \tag{18}$$

for all $x \in |-1, 1|$; we adopt the convention that the functions are normalized such that $\|\psi_j\|_{L^2[-1,1]} = 1$, for all j[1]. The following theorem is a combination of several lemmas from [7, 12, 21].

Theorem 2.4. *For any positive real c, the eigenfunctions $\psi_0, \psi_1, \ldots,$ of the operator F_c are purely real, are orthonormal and are complete in $L^2[-1, 1]$. The even-numbered eigenfunctions are even, and the odd-numbered ones are odd. All eigenvalues of F_c are non-zero and simple; the even-numbered eigenvalues are purely real and the odd-numbered ones are purely imaginary; in particular, $\lambda_j = i^j |\lambda_j|$. The functions ψ_i constitute a Chebyshev system on the interval $[-1, 1]$; in particular, the function ψ_i has exactly i zeros on that interval, for any $i = 0, 1, \ldots$.*

[1] This convention differs from that used in [21]; however, this paper is concerned almost exclusively with the approximation of functions on $[-1, 1]$, and in that context, the convention that the functions $\{\psi_j\}$ have unit norm on that interval is by far the most convenient.

We will define the self-adjoint operator $Q_c : L^2[-1, 1] \to L^2[-1, 1]$ by the formula

$$Q_c(\varphi) = \frac{1}{\pi} \int_{-1}^{1} \frac{\sin(c \cdot (x - t))}{x - t} \varphi(t)\, dt; \tag{19}$$

a simple calculation shows that

$$Q_c = \frac{c}{2\pi} \cdot F_c^* \cdot F_c, \tag{20}$$

that Q_c has the same eigenfunctions as F_c, and that the jth (in descending order) eigenvalue μ_j of Q_c is connected with λ_j by the formula

$$\mu_j = \frac{c}{2\pi} \cdot |\lambda_j|^2. \tag{21}$$

The operator Q_c is obviously closely related to the operator $P_c : L^2[-\infty, \infty] \to [-\infty, \infty]$ defined by the formula

$$P_c(\varphi) = \frac{1}{\pi} \cdot \int_{\infty}^{\infty} \frac{\sin(c \cdot (x - t))}{x - t} \cdot \varphi(t)\, dt, \tag{22}$$

which, as is well known, is the orthogonal projection operator onto the space of functions of band limit c on $(-\infty, \infty)$.

For large c, the spectrum of Q_c consists of three parts: about $2c/\pi$ eigenvalues that are very close to 1, followed by order $\log(c)$ eigenvalues which decay exponentially from 1 to nearly 0; the remaining eigenvalues are all very close to zero. The following theorem, proven (in a slightly different form) in [20], describes the spectrum of Q_c more precisely.

Theorem 2.5. *For any positive real c and $0 < \alpha < 1$ the number N of eigenvalues of the operator Q_c that are greater than α satisfies the equation*

$$N = \frac{2c}{\pi} + \left(\frac{1}{\pi^2} \log \frac{1 - \alpha}{\alpha} \right) \log(c) + O(\log(c)). \tag{23}$$

By a remarkable coincidence, the eigenfunctions $\psi_0, \psi_1, \ldots, \psi_n$ of the operator Q_c turn out to be the PSWFs, well known from classical mathematical physics (see, e.g., [17]). The following theorem formalizes this statement; it is proven in a considerably more general form in [22].

Theorem 2.6. *For any $c > 0$, there exists a strictly increasing sequence of positive real numbers $\chi_0, \chi_1, \ldots$ such that, for each $j \geqslant 0$, the differential equation*

$$(1 - x^2)\, \psi''(x) - 2x\, \psi'(x) + (\chi_j - c^2 x^2)\, \psi(x) = 0 \tag{24}$$

has a solution that is continuous on the interval $[-1, 1]$. For each $j \geqslant 0$, the function ψ_j (defined in theorem 2.4) is the solution of (24).

3. Analytical apparatus

3.1. Prolate series

Since the functions $\psi_0, \psi_1, \ldots, \psi_n, \ldots$ are a complete orthonormal basis in $L^2[-1, 1]$, any formula for the inner product of PSWFs with another function f is also a formula for the coefficients of an expansion of f into PSWFs (which we will refer to as the prolate expansion of f). Thus the following theorem provides the coefficients of the prolate expansion of the derivative of a prolate spheroidal function, and also the coefficients of the prolate expansion of a PSWF multiplied by x. Those coefficients are also the entries of the matrix for differentiation

of a prolate expansion (producing another prolate expansion), and the entries of the matrix for multiplication of a prolate expansion by x, respectively. (These formulae are not, however, suitable for producing such matrices numerically, since in many cases they exhibit catastrophic cancellation.)

Theorem 3.1. *Suppose that c is real and positive, and that the integers m and n are non-negative. If $m = n \pmod 2$, then*

$$\int_{-1}^{1} \psi_n'(x)\,\psi_m(x)\,\mathrm{d}x = \int_{-1}^{1} x\,\psi_n(x)\,\psi_m(x)\,\mathrm{d}x = 0. \tag{25}$$

If $m \neq n \pmod 2$, then

$$\int_{-1}^{1} \psi_n'(x)\,\psi_m(x)\,\mathrm{d}x = \frac{2\lambda_m^2}{\lambda_m^2 + \lambda_n^2}\,\psi_m(1)\,\psi_n(1), \tag{26}$$

$$\int_{-1}^{1} x\,\psi_n(x)\,\psi_m(x)\,\mathrm{d}x = \frac{2}{\mathrm{i}c}\,\frac{\lambda_m\lambda_n}{\lambda_m^2 + \lambda_n^2}\,\psi_m(1)\,\psi_n(1). \tag{27}$$

Proof. Since the functions ψ_j are alternately even and odd, (25) is obvious. In order to prove (26), we start with the identity

$$\lambda_n\psi_n = \int_{-1}^{1} \mathrm{e}^{\mathrm{i}cxt}\,\psi_n(t)\,\mathrm{d}t \tag{28}$$

(see (18) in section 2.5). Differentiating (28) with respect to x, we obtain

$$\lambda_n\psi_n'(x) = \mathrm{i}\,c\int_{-1}^{1} t\,\mathrm{e}^{\mathrm{i}cxt}\,\psi_n(t)\,\mathrm{d}t. \tag{29}$$

Projecting both sides of (29) on ψ_m and using the identity (28) (with n replaced with m) again, we have

$$\begin{aligned}\lambda_n\int_{-1}^{1} \psi_n'(x)\,\psi_m(x)\,\mathrm{d}x &= \mathrm{i}\,c\int_{-1}^{1} \psi_m(x)\int_{-1}^{1} t\,\mathrm{e}^{\mathrm{i}cxt}\,\psi_n(t)\,\mathrm{d}t\,\mathrm{d}x\\ &= \mathrm{i}\,c\int_{-1}^{1} t\,\psi_n(t)\int_{-1}^{1} \mathrm{e}^{\mathrm{i}cxt}\,\psi_m(x)\,\mathrm{d}x\,\mathrm{d}t\\ &= \mathrm{i}\,c\,\lambda_m\int_{-1}^{1} t\,\psi_n(t)\,\psi_m(t)\,\mathrm{d}t.\end{aligned} \tag{30}$$

Obviously, the above calculation can be repeated with m and n exchanged, yielding the identity

$$\lambda_m\int_{-1}^{1} \psi_m'(x)\,\psi_n(x)\,\mathrm{d}x = \mathrm{i}\,c\,\lambda_n\int_{-1}^{1} t\,\psi_n(t)\,\psi_m(t)\,\mathrm{d}t; \tag{31}$$

combining (30) with (31), we have

$$\int_{-1}^{1} \psi_m'(x)\,\psi_n(x)\,\mathrm{d}x = \frac{\lambda_n^2}{\lambda_m^2}\int_{-1}^{1} \psi_m(x)\,\psi_n'(x)\,\mathrm{d}x. \tag{32}$$

On the other hand, integrating the left side of (32) by parts, we have

$$\int_{-1}^{1} \psi_m'(x)\,\psi_n(x)\,\mathrm{d}x = \psi_m(1)\,\psi_n(1) - \psi_m(-1)\,\psi_n(-1) - \int_{-1}^{1} \psi_n'(x)\,\psi_m(x)\,\mathrm{d}x. \tag{33}$$

Since $m \neq n \pmod 2$, we rewrite (33) as

$$\int_{-1}^{1} \psi_m'(x)\,\psi_n(x)\,\mathrm{d}x = 2\,\psi_m(1)\,\psi_n(1) - \int_{-1}^{1} \psi_n'(x)\,\psi_m(x)\,\mathrm{d}x. \tag{34}$$

Now, combining (32) and (34) and rearranging terms, we get

$$\int_1^1 \psi_n'(x)\,\psi_m(x)\,\mathrm{d}x = \frac{2\lambda_m^2}{\lambda_m^2+\lambda_n^2}\,\psi_m(1)\,\psi_n(1). \tag{35}$$

Substituting (30) into (35), we get

$$\begin{aligned}\int_1^1 x\,\psi_n(x)\,\psi_m(x)\,\mathrm{d}x &= \frac{1}{\mathrm{i}c}\,\frac{\lambda_n}{\lambda_m}\int_1^1 \psi_n'(x)\,\psi_m(x)\,\mathrm{d}x \\ &= \frac{1}{\mathrm{i}c}\,\frac{\lambda_n}{\lambda_m}\,\frac{2\lambda_m^2}{\lambda_m^2+\lambda_n^2}\,\psi_m(1)\,\psi_n(1) \\ &= \frac{2}{\mathrm{i}c}\,\frac{\lambda_m\lambda_n}{\lambda_m^2+\lambda_n^2}\,\psi_m(1)\,\psi_n(1). \end{aligned}\tag{36}$$

□

The following corollary, which is an immediate consequence of (32), finds use in the numerical evaluation of the eigenvalues $\{\lambda_j\}$.

Corollary 3.2. *Suppose that c is real and positive, and that the integers m and n are non-negative. If $m \neq n \pmod 2$, then*

$$\frac{\lambda_m^2}{\lambda_n^2} = \frac{\int_{-1}^1 \psi_n'(x)\,\psi_m(x)\,\mathrm{d}x}{\int_{-1}^1 \psi_m'(x)\,\psi_n(x)\,\mathrm{d}x}. \tag{37}$$

3.2. Decay of Legendre coefficients of prolate spheroidal wavefunctions

Since each of the functions ψ_j is analytic on $\mathbb{C}$, on the interval $[-1, 1]$ it can be expanded in a Legendre series of the form

$$\psi_j(x) = \sum_{k=0}^{\infty} \beta_k \overline{P_k}(x), \tag{38}$$

with the coefficients β_k decaying superalgebraically; the following two theorems establish bounds for the decay rate.

Lemma 3.3. *Let $\overline{P_n}(x)$ be the nth normalized Legendre polynomial (defined in (13)). Then for any real a,*

$$\int_{-1}^1 \mathrm{e}^{\mathrm{i}ax}\,\overline{P_n}(x)\,\mathrm{d}x = \sum_{k=k_0}^{\infty} \alpha_k \int_{-1}^1 x^{2k}\,\overline{P_n}(x)\,\mathrm{d}x + \mathrm{i}\sum_{k=k_0}^{\infty} \beta_k \int_{-1}^1 x^{2k+1}\,\overline{P_n}(x)\,\mathrm{d}x \tag{39}$$

where

$$\alpha_k = (-1)^k \frac{a^{2k}}{(2k)!}, \tag{40}$$

$$\beta_k = (-1)^k \frac{a^{2k+1}}{(2k+1)!}, \tag{41}$$

$$k_0 = \lfloor n/2 \rfloor. \tag{42}$$

Furthermore, for all integer $m \geqslant \lfloor e\cdot|a|\rfloor + 1$,

$$\left|\int_{-1}^1 \mathrm{e}^{\mathrm{i}ax}\,\overline{P_n}(x)\,\mathrm{d}x - \sum_{k=k_0}^{m-1} \alpha_k \int_{-1}^1 x^{2k}\,\overline{P_n}(x)\,\mathrm{d}x - \mathrm{i}\sum_{k=k_0}^{m-1} \beta_k \int_{-1}^1 x^{2k+1}\,\overline{P_n}(x)\,\mathrm{d}x\right| < (\tfrac{1}{2})^{2m}. \tag{43}$$

In particular, if

$$n \geqslant 2\,(\lfloor e \cdot |a| \rfloor + 1), \tag{44}$$

then

$$\left| \int_{-1}^{1} e^{i\alpha x}\, \overline{P_n}(x)\, dx \right| < (\tfrac{1}{2})^{n-1}. \tag{45}$$

Proof. Formula (39) follows immediately from lemma 2.2 and Taylor's expansion of $e^{i\alpha x}$. In order to prove (43), we assume that m is an integer such that

$$m \geqslant \lfloor e \cdot |a| \rfloor + 1. \tag{46}$$

Introducing the notation

$$R_m = \sum_{k=m}^{\infty} \alpha_k \int_1^1 x^{2k}\, \overline{P_n}(x)\, dx + i \sum_{k=m}^{\infty} \beta_k \int_1^1 x^{2k+1}\, \overline{P_n}(x)\, dx, \tag{47}$$

we immediately observe that, due to lemma 2.2 and the triangle inequality,

$$|R_m| \leqslant \sum_{k=2m}^{\infty} \left(\frac{|a|^k}{k!} \cdot \sqrt{\frac{2}{k+1}} \right) < \sum_{k=2m}^{\infty} \frac{|a|^k}{k!}. \tag{48}$$

Since (46) implies that

$$\frac{|a|}{2m+k} < \frac{|a|}{2m} < \frac{1}{2e} < \frac{1}{2}, \tag{49}$$

for all integer $m, k > 0$, we rewrite (48) as

$$|R_m| < \frac{|a|^{2m}}{(2m)!} \cdot \left(1 + \frac{1}{2} + \frac{1}{4} + \cdots \right) < 2\, \frac{|a|^{2m}}{(2m)!} \tag{50}$$

and obtain (43) immediately using Stirling's formula. Finally, we obtain (45) by choosing

$$m = \lfloor e \cdot |a| \rfloor + 1. \tag{51}$$

□

Theorem 3.4. *Let $\psi_m(x)$ be the mth prolate spheroidal function with band limit c, let $\overline{P_k}(x)$ be the kth normalized Legendre polynomial (defined in (13)) and let λ_m be the eigenvalue which corresponds to $\psi_m(x)$ (as in theorem 2.4). Then for all integer $m \geqslant 0$ and all real positive c, if*

$$k \geqslant 2\,(\lfloor e \cdot c \rfloor + 1), \tag{52}$$

then

$$\left| \int_1^1 \psi_m(x)\, \overline{P_k}(x)\, dx \right| < \frac{1}{\lambda_m} \cdot \left(\frac{1}{2} \right)^{k-1}. \tag{53}$$

Moreover, given any $\varepsilon > 0$, if

$$k \geqslant 2\,(\lfloor e \cdot c \rfloor + 1) + \log_2\left(\frac{1}{\varepsilon} \right) + \log_2\left(\frac{1}{\lambda_m} \right), \tag{54}$$

then

$$\left| \int_{-1}^{1} \psi_m(x)\, \overline{P_k}(x)\, dx \right| < \varepsilon. \tag{55}$$

Proof. Obviously

$$\left|\int_{-1}^{1}\psi_m(x)\,\overline{P_k}(x)\,\mathrm{d}x\right| = \frac{1}{|\lambda_m|}\cdot\left|\int_{-1}^{1}\psi_m(x)\left(\int_{-1}^{1}\mathrm{e}^{\mathrm{i}cxt}\,\overline{P_k}(t)\,\mathrm{d}t\right)\mathrm{d}x\right|$$
$$< \frac{1}{|\lambda_m|}\int_{-1}^{1}|\psi_m(x)|\cdot\left|\int_{-1}^{1}\mathrm{e}^{\mathrm{i}cxt}\,\overline{P_k}(t)\,\mathrm{d}t\right|\mathrm{d}x. \tag{56}$$

Introducing the notation

$$a = cx, \tag{57}$$

and remembering that the prolate functions have unit norm, so that

$$\int_{1}^{1}|\psi_m(x)|\,\mathrm{d}x \leqslant \sqrt{2}, \tag{58}$$

we observe that the combination of (56)–(58) and lemma 3.3 implies that

$$\left|\int_{1}^{1}\psi_m(x)\,\overline{P_k}(x)\,\mathrm{d}x\right| < \frac{1}{|\lambda_m|}\cdot\left(\frac{1}{2}\right)^{k-1}\int_{1}^{1}|\psi_m(x)|\,\mathrm{d}x \leqslant \frac{1}{|\lambda_m|}\left(\frac{1}{2}\right)^{k-1/2}. \tag{59}$$

Substituting (54) into (53), we immediately see (55). □

4. Numerical evaluation of prolate spheroidal wavefunctions

Both the classical Bouwkamp algorithm (see, e.g., [1]) for the evaluation of the functions ψ_j, and the algorithm presented in this paper for the same task, are based on the expression of those functions as a Legendre series of the form

$$\psi_j(x) = \sum_{k=0}^{\infty}\alpha_k P_k(x); \tag{60}$$

since the functions ψ_j are smooth, the coefficients α_k decay superalgebraically (with bounds for that decay being given in theorem 3.4). Substituting (60) into (24), and using (8) and (11), we obtain the well-known three-term recursion

$$\frac{(k+2)(k+1)}{(2k+3)(2k+5)}\cdot c^2\cdot\alpha_{k+2} + \left(k(k+1) + \frac{2k(k+1)-1}{(2k+3)(2k-1)}\cdot c^2 - \chi_j\right)\cdot\alpha_k$$
$$+\frac{k(k-1)}{(2k-3)(2k-1)}\cdot c^2\cdot\alpha_{k-2} = 0. \tag{61}$$

Combining (61) with (13), we obtain the three-term recursion

$$\frac{(k+2)(k+1)}{(2k+3)\sqrt{(2k+5)(2k+1)}}\cdot c^2\cdot\beta_{k+2}^j + \left(k(k+1) + \frac{2k(k+1)-1}{(2k+3)(2k-1)}\cdot c^2 - \chi_j\right)\cdot\beta_k^j$$
$$+\frac{k(k-1)}{(2k-1)\sqrt{(2k-3)(2k+1)}}\cdot c^2\cdot\beta_{k-2}^j = 0 \tag{62}$$

for the coefficients $\beta_0^j, \beta_1^j, \ldots$ of the expansion

$$\psi_j(x) = \sum_{k=0}^{\infty}\beta_k^j\cdot\overline{P_k}(x); \tag{63}$$

for each $j = 0, 1, 2, \ldots$, we will denote by β^j the vector in l^2 defined by the formula

$$\beta^j = (\beta_0^j, \beta_1^j, \beta_2^j, \ldots). \tag{64}$$

The following theorem restates the recursion (62) in a slightly different form.

Theorem 4.1. *The coefficients χ_i are the eigenvalues and the vectors β^i are the corresponding eigenvectors of the operator $l^2 \to l^2$ represented by the symmetric matrix A given by the formulae*

$$A_{k,k} = k(k+1) + \frac{2k(k+1)-1}{(2k+3)(2k-1)} \cdot c^2, \tag{65}$$

$$A_{k,k+2} = \frac{(k+2)(k+1)}{(2k+3)\sqrt{(2k+1)(2k+5)}} \cdot c^2, \tag{66}$$

$$A_{k+2,k} = \frac{(k+2)(k+1)}{(2k+3)\sqrt{(2k+1)(2k+5)}} \cdot c^2, \tag{67}$$

for all $k = 0, 1, 2, \ldots$, with the remainder of the entries of the matrix being zero.

In other words, the recursion (62) can be rewritten in the form

$$(A - \chi_j \cdot I)(\beta^j) = 0, \tag{68}$$

where A is separable into two symmetric tridiagonal matrices A_{even} and A_{odd}, the first consisting of the elements of A with even-numbered rows and columns and the second consisting of the elements of A with odd-numbered rows and columns. While these two matrices are infinite, and their entries do not decay much with increasing row or column number, the eigenvectors $\{\beta^j\}$ of interest (those corresponding to the first m prolate spheroidal functions) lie almost entirely in the leading rows and columns of the matrices (as shown by theorem 3.4). Thus the evaluation of prolate spheroidal functions can be performed by the following procedure:

- Generate the leading k rows and columns of A, where k is given by (54).
- Split the generated portion of A into A_{even} and A_{odd}, and use a solver for the symmetric tridiagonal eigenproblem (such as that in LAPACK) to compute their eigenvectors $\{\beta^j\}$ and eigenvalues $\{\chi_j\}$.
- Use the obtained values of the coefficients $\beta_0^j, \beta_1^j, \beta_2^j, \ldots$ in the expansion (63) to evaluate the function ψ_j at arbitrary points on the interval $[-1, 1]$.

Obviously steps 1 and 2 can be performed as a precomputation, for any given value of c. As a numerical diagonalization of a positive definite tridiagonal matrix with well-separated eigenvalues, this precomputation stage is numerically robust and efficient, requiring $O(c\,m)$ operations to construct the Legendre expansions of the form (64) for the first m prolate spheroidal functions; each subsequent evaluation of a prolate spheroidal function takes $O(c)$ operations.

4.1. Numerical evaluation of eigenvalues

Although the above algorithm for the evaluation of PSWFs also produces the eigenvalues $\{\chi_j\}$ of the differential operator (24), it does not produce the eigenvalues $\{\lambda_j\}$ of the integral operator F_c (defined in (17)). Some of those eigenvalues can be computed using the formula

$$\lambda_j \psi_j(x) = \int_{-1}^{1} \mathrm{e}^{\mathrm{i}cxt} \psi_j(t)\,\mathrm{d}t, \tag{69}$$

evaluating the integral on the right-hand side numerically; however, that evaluation obviously has a condition number of about $1/\lambda_j$, and is thus inappropriate for computing small λ_j. A well-conditioned procedure is as follows:

- Use (69) to calculate λ_0, evaluating the right-hand side numerically, and with $x = 0$ (so that $\psi_0(x)$ is not small).

- Use the calculated λ_0, together with corollary 3.2, to compute the absolute values $|\lambda_j|$, for $j = 1, 2, \ldots, m$, computing each $|\lambda_j|$ from $|\lambda_{j-1}|$ (and again, evaluating the required integrals numerically).
- Use the fact that $\lambda_j = \mathrm{i}^j |\lambda_j|$ (see theorem 2.4) to finish the computation.

5. Quadratures for band-limited functions

Since the PSWFs $\psi_0, \psi_1, \ldots, \psi_n, \ldots$ constitute a complete orthonormal basis in $L^2[-1, 1]$ (see theorem 2.4),

$$\mathrm{e}^{\mathrm{i}cxt} = \sum_{j=0}^{\infty} \left(\int_{-1}^{1} \mathrm{e}^{\mathrm{i}cx\tau}\, \psi_j(\tau)\, \mathrm{d}\tau \right) \psi_j(t), \tag{70}$$

for all $x, t \in [-1, 1]$; substituting (18) into (70) yields

$$\mathrm{e}^{\mathrm{i}cxt} = \sum_{j=0}^{\infty} \lambda_j\, \psi_j(x)\, \psi_j(t). \tag{71}$$

Thus if a quadrature integrates exactly the first n eigenfunctions, that is, if

$$\sum_{k=1}^{m} w_k \psi_j(x_k) = \int_{1}^{1} \psi_j(x)\, \mathrm{d}x, \tag{72}$$

for all $j = 0, 1, \ldots, n-1$, then the error of the quadrature when applied to a function $f(x) = \mathrm{e}^{\mathrm{i}cax}$, with $a \in [-1, 1]$, is given by

$$\sum_{k-1}^{m} w_k \mathrm{e}^{\mathrm{i}cax_k} - \int_{-1}^{1} \mathrm{e}^{\mathrm{i}cax}\, \mathrm{d}x = \sum_{k-1}^{m} w_k \left(\sum_{j-0}^{\infty} \lambda_j\, \psi_j(a)\, \psi_j(x_k) \right) - \int_{-1}^{1} \left(\sum_{j-0}^{\infty} \lambda_j\, \psi_j(a)\, \psi_j(x) \right) \mathrm{d}x$$

$$= \sum_{k=1}^{m} w_k \left(\sum_{j=n}^{\infty} \lambda_j\, \psi_j(a)\, \psi_j(x_k) \right) - \int_{-1}^{1} \left(\sum_{j=n}^{\infty} \lambda_j\, \psi_j(a)\, \psi_j(x) \right) \mathrm{d}x. \tag{73}$$

Due to the orthonormality of the functions $\{\psi_j\}$,

$$\left\| \sum_{j-n}^{\infty} \lambda_j\, \psi_j(a)\, \psi_j(x) \right\| = \sqrt{\sum_{j-n}^{\infty} |\lambda_j|^2}. \tag{74}$$

From (74), it is obvious that the error of integration (73) is of roughly the same magnitude as λ_n, provided that n is in the range where the eigenvalues $\{\lambda_j\}$ are decreasing exponentially (as is the case for quadratures of any useful accuracy; see theorem 2.5) and provided in addition that the weights $\{w_k\}$ are not large.

Now, the existence of an $n/2$-point quadrature that is exact for the first n PSWFs follows from the combination of theorems 2.1 and 2.4; an algorithm for the numerical evaluation of nodes and weights of such quadratures can be found in [2]. An alternative procedure for the construction of quadrature formulae for band-limited functions (leading to slightly different nodes and weights) is described in the following section; a numerical comparison of the two can be found in section 8 below.

Remark 5.1. The above text considers only the error of integration of a single exponential. For a band-limited function $g : [-1, 1] \to \mathbb{C}$ given by the formula

$$g(x) = \int_{-1}^{1} G(t) \mathrm{e}^{\mathrm{i}cxt}\, \mathrm{d}t, \tag{75}$$

for some function $G : [-1, 1] \to \mathbb{C}$, the error is obviously bounded by the formula

$$\left| \sum_{k=1}^{m} w_k g(x_k) - \int_{-1}^{1} g(x)\,\mathrm{d}x \right| \leqslant \varepsilon \cdot \|G\|, \tag{76}$$

where ε is the maximum error of integration (73) of a single exponential, for any $t \in [-1, 1]$. While $\|G\|$ might be much larger than $\|g\|_{[-1,1]}$ (as it is if, for instance, $g = \psi_{30,n}$), if the same equation (75) is used to extend g to the rest of the real line, then by Parseval's formula $\|G\| = \|g\|_{(-\infty,\infty)}$; that is to say, although the error of such a quadrature when applied to a band-limited function is not bounded proportional to the norm of that function on the interval of integration, it is bounded proportional to the norm of that function on the entire real line.

6. Quadrature nodes from roots of prolate functions

An alternative to the approach of the previous section is to use roots of appropriate PSWFs as quadrature nodes, with the weights determined via the procedure described in remark 2.1. The following theorems provide a basis for this; numerically (see section 8) the resulting quadrature nodes tend to be inferior to those produced by the optimization scheme of [2, 14, 27]; however, they are useful as starting points for that scheme, or as somewhat less efficient nodes which can be computed much more quickly.

6.1. Euclid division algorithm for band-limited functions

The following two theorems constitute a straightforward extension to band-limited functions of Euclid's division algorithm for polynomials. Their proofs are quite simple, and are provided here for completeness, since the author failed to find them in the literature.

Theorem 6.1. *Suppose that $\sigma, \varphi : [0, 1] \to \mathbb{C}$ are a pair of c^2-functions such that*

$$\varphi(1) \neq 0, \tag{77}$$

c is a positive real number and the functions f, p are defined by the formulae

$$f(x) = \int_0^1 \sigma(t) \mathrm{e}^{2\mathrm{i}cxt}\,\mathrm{d}t, \tag{78}$$

$$p(x) = \int_0^1 \varphi(t) \mathrm{e}^{\mathrm{i}cxt}\,\mathrm{d}t. \tag{79}$$

Then there exist two c^1-functions $\eta, \xi : [0, 1] \to \mathbb{C}$ such that

$$f(x) = p(x)\,q(x) + r(x) \tag{80}$$

for all $x \in \mathbb{R}$, with the functions $q, r : [0, 1] \to \mathbb{R}$ defined by the formulae

$$q(x) = \int_0^1 \eta(t) \mathrm{e}^{\mathrm{i}cxt}\,\mathrm{d}t, \tag{81}$$

$$r(x) = \int_0^1 \xi(t) \mathrm{e}^{\mathrm{i}cxt}\,\mathrm{d}t. \tag{82}$$

Proof. Obviously, for any functions p, q given by (79) and (81),

$$p(x)q(x) = \int_0^1 \varphi(t)\,\mathrm{e}^{\mathrm{i}cxt}\,\mathrm{d}t \cdot \int_0^1 \eta(\tau)\,\mathrm{e}^{\mathrm{i}cx\tau}\,\mathrm{d}\tau = \int_0^1 \int_0^1 \varphi(t)\,\eta(\tau)\,\mathrm{e}^{\mathrm{i}cx(t+\tau)}\,\mathrm{d}\tau\,\mathrm{d}t. \tag{83}$$

Defining the new independent variable u by the formula

$$u = t + \tau, \tag{84}$$

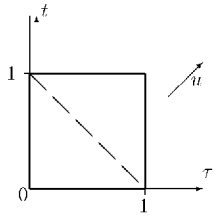

Figure 1. The split of integration range that yields (85).

we rewrite (83) as

$$p(x)q(x) = \int_0^1 e^{icux} \int_0^u \varphi(u-\tau)\eta(\tau)\,d\tau\,du + \int_1^2 e^{icux} \int_{u-1}^1 \varphi(u-\tau)\,\eta(\tau)\,d\tau\,du \tag{85}$$

(see figure 1). Substituting (78), (82) and (85) into (80), we get

$$\int_0^1 e^{icux} \int_0^u \varphi(u-\tau)\,\eta(\tau)\,d\tau\,du + \int_1^2 e^{icux} \int_{u-1}^1 \varphi(u-\tau)\,\eta(\tau)\,d\tau\,du + \int_0^1 \xi(t)\,e^{icxt}\,dt$$
$$= \int_0^{1/2} \sigma(t)\,e^{2icxt}\,dt + \int_{1/2}^1 \sigma(t)\,e^{2icxt}\,dt. \tag{86}$$

Due to the well-known uniqueness of the Fourier transform, (86) is equivalent to two independent equations:

$$\int_0^1 e^{icux} \int_0^u \varphi(u-\tau)\,\eta(\tau)\,d\tau\,du + \int_0^1 \xi(t)\,e^{icxt}\,dt = \int_0^{1/2} \sigma(t)\,e^{2icxt}\,dt, \tag{87}$$

$$\int_1^2 e^{icux} \int_{u-1}^1 \varphi(u-\tau)\,\eta(\tau)\,d\tau\,du = \int_{1/2}^1 \sigma(t)\,e^{2icxt}\,dt. \tag{88}$$

Now, we observe that (88) does not contain ξ and use it to obtain an expression for η as a function of φ and σ. After that, we will view (87) as an expression for ξ via φ, σ and η.

From (88) and the uniqueness of the Fourier transform, we obtain

$$\int_{u-1}^1 \varphi(u-\tau)\,\eta(\tau)\,d\tau = \frac{1}{2}\sigma\left(\frac{u}{2}\right), \tag{89}$$

for all $u \in [1, 2]$. Introducing the new variable v via the formula

$$v = u - 1, \tag{90}$$

we convert (89) into

$$\int_v^1 \varphi(v+1-\tau)\,\eta(\tau)\,d\tau = \frac{1}{2}\sigma\left(\frac{v+1}{2}\right), \tag{91}$$

which is a Volterra equation of the first kind with respect to η; differentiating (91) with respect to v, we get

$$-\varphi(1)\,\eta(v) + \int_v^1 \varphi'(v+1-\tau)\,\eta(\tau)\,d\tau = \frac{1}{4}\sigma'\left(\frac{v+1}{2}\right). \tag{92}$$

which is a Volterra equation of the second kind. Now, the existence and uniqueness of the solution of (92) (and, therefore, of (89) and (88)) follows from theorem 2.3 of section 2.

With η defined as the solution of (89), we use (87) together with the uniqueness of the Fourier transform, to finally obtain

$$\xi(u) = \frac{1}{2}\sigma\left(\frac{u}{2}\right) - \int_0^u \varphi(u-\tau)\,\eta(\tau)\,\mathrm{d}\tau, \tag{93}$$

for all $u \in [0, 1]$. □

The following theorem is a consequence of the preceding one.

Theorem 6.2. *Suppose that $\sigma, \varphi : [-1, 1] \to \mathbb{C}$ are a pair of c^2-functions such that $\varphi(-1) \neq 0$, $\varphi(1) \neq 0$, c is a positive real number and the functions f, p are defined by the formulae*

$$f(x) = \int_{-1}^{1} \sigma(t)\,\mathrm{e}^{2\mathrm{i}cxt}\,\mathrm{d}t, \tag{94}$$

$$p(x) = \int_{-1}^{1} \varphi(t)\,\mathrm{e}^{\mathrm{i}cxt}\,\mathrm{d}t. \tag{95}$$

Then there exist two functions $\eta, \xi : [-1, 1] \to \mathbb{C}$ such that

$$f(x) = p(x)\,q(x) + r(x) \tag{96}$$

for all $x \in \mathbb{R}$, with the functions $q, r : [-1, 1] \to \mathbb{R}$ defined by the formulae

$$q(x) = \int_{1}^{1} \eta(t)\,\mathrm{e}^{\mathrm{i}cxt}\,\mathrm{d}t, \tag{97}$$

$$r(x) = \int_{-1}^{1} \xi(t)\,\mathrm{e}^{\mathrm{i}cxt}\,\mathrm{d}t. \tag{98}$$

Proof. Defining the functions f_+, f_-, p_+, p_-, by the formulae

$$f_+(x) = \int_{0}^{1} \sigma(t)\,\mathrm{e}^{2\mathrm{i}cxt}\,\mathrm{d}t, \tag{99}$$

$$f\ (x) = \int_{-1}^{0} \sigma(t)\,\mathrm{e}^{2\mathrm{i}cxt}\,\mathrm{d}t, \tag{100}$$

$$p_+(x) = \int_{0}^{1} \varphi(t)\,\mathrm{e}^{\mathrm{i}cxt}\,\mathrm{d}t, \tag{101}$$

$$p_-(x) = \int_{1}^{0} \varphi(t)\,\mathrm{e}^{\mathrm{i}cxt}\,\mathrm{d}t, \tag{102}$$

we observe that, for all $x \in \mathbb{R}^1$,

$$f(x) = f_+(x) + f_-(x). \tag{103}$$

$$p(x) = p_+(x) + p_-(x). \tag{104}$$

Due to theorem 6.1, there exist such η_+, η , ξ_+, ξ , that

$$f_+(x) = p_+(x)\,q_+(x) + r_+(x), \tag{105}$$

$$f_-(x) = p_-(x)\,q_-(x) + r_-(x), \tag{106}$$

with the functions q_+, q_-, r_+, r_- defined by the formulae

$$q_+(x) = \int_0^1 \eta_+(t)\, e^{icxt}\, dt, \tag{107}$$

$$q_-(x) = \int_{-1}^0 \eta_-(t)\, e^{icxt}\, dt, \tag{108}$$

$$r_+(x) = \int_0^1 \xi_+(t)\, e^{icxt}\, dt, \tag{109}$$

$$r_-(x) = \int_{-1}^0 \xi_-(t)\, e^{icxt}\, dt. \tag{110}$$

Now, defining q by the formula

$$q(x) = q_-(x) + q_+(x) \tag{111}$$

for all $x \in [-1, 1]$, we have

$$\begin{aligned} p(x)\, q(x) &= (p_-(x) + p_+(x)) \cdot (q_-(x) + q_+(x)) \\ &= p_+(x)\, q_+(x) + p_-(x)\, q_-(x) + p_-(x)\, q_+(x) + p_+(x)\, q_-(x) \end{aligned} \tag{112}$$

and we define $r(x)$ by the obvious formula

$$r(x) = r_-(x) + r_+(x) - (p_-(x)\, q_+(x) + p_+(x)\, q_-(x)). \tag{113}$$

The product $p_+(x)q_-(x)$ is given by the formula

$$p_+(x)q_-(x) = \int_0^1 \int_{-1}^0 \varphi(t)\eta_+(t) e^{icx(t+\tau)}\, dt\, d\tau; \tag{114}$$

since $-1 \leqslant t+\tau \leqslant 1$ is the integral in that formula, the product $p_+(x)q_-(x)$ has the appropriate band limits; likewise for $p_-(x)q_+(x)$. □

6.2. *Quadrature nodes from the division theorem*

In much the same way that the division theorem for polynomials can be used to provide a constructive proof of Gaussian quadratures, theorem 6.2 provides a method of constructing generalized Gaussian quadratures for band-limited functions. The method is as follows.

To construct a quadrature for functions of a bandwidth $2c$, PSWF's corresponding to a bandwidth c are used. (Thus the eigenvalues $\{\lambda_j\}$ and eigenfunctions $\{\psi_j\}$ are in this section, as elsewhere in the paper, those corresponding to bandwidth c.) The following theorem provides a bound of the error of a quadrature whose nodes are the roots of the nth prolate function ψ_n, when applied to a function f which satisfies the conditions of the division theorem, in terms of the norms of the quotient and remainder of f divided by ψ_n:

Theorem 6.3. *Suppose that $x_1, x_2, \ldots, x_n \in \mathbb{R}$ are the roots of ψ_n. Let the numbers $w_1, w_2, \ldots, w_n \in \mathbb{R}$ be such that*

$$\sum_{k=1}^n w_k \psi_j(x_k) = \int_{-1}^1 \psi_j(x)\, dx, \tag{115}$$

for all $j = 0, 1, \ldots, n-1$. Then for any function $f : [-1, 1] \to \mathbb{C}$ which satisfies the conditions of theorem 6.2,

$$\left| \sum_{k=1}^n w_k f(x_k) - \int_{-1}^1 f(x)\, dx \right| \leqslant |\lambda_n| \cdot \|\eta\| + \|\xi\| \cdot \sum_{j=n}^{\infty} |\lambda_j| \cdot \|\psi_j\|_\infty^2 \cdot \left(2 + \sum_{k=1}^n |w_k|\right), \tag{116}$$

where the functions $\eta, \xi : [-1, 1] \to \mathbb{C}$ are as defined in theorem 6.2.

Proof. Since f satisfies the conditions of theorem 6.2, there exist functions $q, r : [-1, 1] \to \mathbb{R}$ defined by (97) and (98) such that

$$f(x) = \psi_n(x)\, q(x) + r(x). \tag{117}$$

Then, defining the error of integration E_f for the function f by

$$E_f = \left| \sum_{k=1}^{n} w_k f(x_k) - \int_1^1 f(x)\,\mathrm{d}x \right| \tag{118}$$

we have

$$\begin{aligned} E_f &= \left| \sum_{k=1}^{n} w_k \left(\psi_n(x_k)\, q(x_k) + r(x_k)\right) - \int_1^1 \left(\psi_n(x)\, q(x) + r(x)\right) \mathrm{d}x \right| \\ &\leqslant \left| \sum_{k=1}^{n} w_k\, \psi_n(x_k)\, q(x_k) - \int_{-1}^{1} \psi_n(x)\, q(x)\,\mathrm{d}x \right| + \left| \sum_{k=1}^{n} w_k r(x_k) - \int_{-1}^{1} r(x)\,\mathrm{d}x \right|. \end{aligned} \tag{119}$$

Since the nodes $\{x_k\}$ are the roots of ψ_n,

$$\sum_{k=1}^{n} w_k\, \psi_n(x_k)\, q(x_k) = 0. \tag{120}$$

Thus

$$E_f \leqslant \left| \int_{-1}^{1} \psi_n(x)\, q(x)\,\mathrm{d}x \right| + \left| \sum_{k=1}^{n} w_k r(x_k) - \int_{-1}^{1} r(x)\,\mathrm{d}x \right|. \tag{121}$$

Now

$$\begin{aligned} \int_1^1 \psi_n(x) q(x)\,\mathrm{d}x &= \int_1^1 \psi_n(x) \int_1^1 \eta(t) \mathrm{e}^{\mathrm{i}cxt}\,\mathrm{d}t\,\mathrm{d}x \\ &= \int_{-1}^{1} \eta(t) \int_{-1}^{1} \psi_n(x)\, \mathrm{e}^{\mathrm{i}cxt}\,\mathrm{d}x\,\mathrm{d}t \\ &= \int_{-1}^{1} \eta(t)\, \lambda_n\, \psi_n(t)\,\mathrm{d}t. \end{aligned} \tag{122}$$

Using the Cauchy–Schwartz inequality and the fact that the function ψ_n has unit norm, we get from (122) that

$$\left| \int_{-1}^{1} \psi_n(x)\, q(x)\,\mathrm{d}x \right| \leqslant |\lambda_n| \cdot \|\eta\|. \tag{123}$$

Also,

$$\begin{aligned} \sum_{k=1}^{n} w_k r(x_k) - \int_{-1}^{1} r(x)\,\mathrm{d}x &= \sum_{k=1}^{n} w_k \left(\int_{-1}^{1} \xi(t)\, \mathrm{e}^{\mathrm{i}cx_k t}\,\mathrm{d}t \right) - \int_{-1}^{1} \left(\int_{-1}^{1} \xi(t)\, \mathrm{e}^{\mathrm{i}cxt}\,\mathrm{d}t \right) \mathrm{d}x \\ &= \int_{-1}^{1} \xi(t) \left(\sum_{k=1}^{n} w_k \mathrm{e}^{\mathrm{i}cx_k t} - \int_{-1}^{1} \mathrm{e}^{\mathrm{i}cxt}\,\mathrm{d}x \right) \mathrm{d}t. \end{aligned} \tag{124}$$

Substituting (73) into (124), and using the Cauchy–Schwartz inequality, we get

$$\begin{aligned} \sum_{k=1}^{n} w_k r(x_k) - \int_{-1}^{1} r(x)\,\mathrm{d}x &= \int_{-1}^{1} \xi(t) \left(\sum_{k=1}^{m} w_k \left(\sum_{j=n}^{\infty} \lambda_j\, \psi_j(t)\, \psi_j(x_k) \right) \right. \\ &\quad \left. - \int_{-1}^{1} \left(\sum_{j=n}^{\infty} \lambda_j\, \psi_j(t)\, \psi_j(x) \right) \mathrm{d}x \right) \mathrm{d}t \\ &\leqslant \|\xi\| \cdot \sum_{j-n}^{\infty} |\lambda_j| \cdot \|\psi_j\|_\infty^2 \cdot \left(2 + \sum_{k-1}^{n} |w_k| \right). \end{aligned} \tag{125}$$

Combining (121), (123) and (125), we get

$$E_f \leqslant |\lambda_n| \cdot \|\eta\| + \|\xi\| \cdot \sum_{j=n}^{\infty} |\lambda_j| \cdot \|\psi_j\|_\infty^2 \cdot \left(2 + \sum_{k=1}^{n} |w_k|\right). \tag{126}$$

□

Remark 6.1. The use of theorem 6.3 for the construction of quadrature rules for band-limited functions depends on the fact that the norms of the band-limited functions q and r in (117) are not large compared to the norm of f (both sets of norms being on $[-\infty, \infty]$). Such estimates have been obtained for all $n > 2c/\pi + 10\log(c)$. The proofs are quite involved, and will be reported at a later date. In this paper, we demonstrate the performance of the obtained quadrature formulae numerically (see section 8 below).

Remark 6.2. It is natural to view (117) as an analogue for band-limited functions of the Euclid division theorem for polynomials. However, there are certain differences. In particular, theorem 6.1 admits extensions to band-limited functions of several variables, while the classical Euclid algorithm does not. Such extensions (together with several applications) will be reported at a later date.

7. Interpolation via prolate spheroidal wavefunctions

Interpolation is usually performed by the following general procedure: assuming that the function $f : [a, b] \to \mathbb{C}$ to be interpolated is given by the formula

$$f(x) = c_1\phi_1(x) + c_2\phi_2(x) + \cdots + c_n\phi_n(x), \tag{127}$$

where $\phi_1, \phi_2, \ldots, \phi_n : [a, b] \to \mathbb{C}$ are a fixed sequence of functions (often polynomials), solve an $n \times n$ linear system to determine the coefficients $c_1, c_2, \ldots, c_n$ from the values of f at the n interpolation nodes, then use (127) to evaluate f wherever needed. As is well known, if f is well approximated by a linear combination of the interpolation functions, and if the linear system to be solved is well conditioned, then this procedure is accurate.

As shown in section 5 in the context of quadratures, a linear combination of the first n prolate spheroidal functions $\psi_0, \psi_1, \ldots, \psi_{n-1}$ for a band limit c can provide a good approximation to functions of the form e^{icxt}, with $t \in [-1, 1]$ (see (71) and (74)); in the regime where the accuracy is numerically useful, the error is of the same order of magnitude as $|\lambda_n|$. This, in turn, shows that they provide a good approximation (in the same sense as in remark 5.1) to any band-limited function of band limit c. Thus, if $\psi_0, \psi_1, \ldots, \psi_{n-1}$ are used as the interpolation functions in this procedure, they can be expected to yield an accurate interpolation scheme for band-limited functions, provided that the matrix to be inverted is well conditioned. The following theorem shows that, if the interpolation nodes are chosen to be quadrature nodes accurate up to twice the bandwidth of interpolation, with the quadrature formula being accurate to more than twice as many digits as the interpolation formula is to be accurate to, then the matrix inverted in the procedure is close to being a scaled version of an orthogonal matrix.

Theorem 7.1. *Suppose the numbers $w_1, w_2, \ldots, w_n \in \mathbb{R}$ and $x_1, x_2, \ldots, x_n \in \mathbb{R}$ are such that*

$$\left| \int_{-1}^{1} e^{2icax}\, dx - \sum_{j=1}^{n} w_j e^{2icax_j} \right| < \varepsilon, \tag{128}$$

for all $a \in [-1, 1]$, *and for some* $c > 0$. *Let the matrix* A *be given by the formula*

$$A = \begin{pmatrix} \psi_0(x_1) & \psi_1(x_1) & \cdots & \psi_{n-1}(x_1) \\ \psi_0(x_2) & \psi_1(x_2) & \cdots & \psi_{n-1}(x_2) \\ \vdots & \vdots & & \vdots \\ \psi_0(x_n) & \psi_1(x_n) & \cdots & \psi_{n-1}(x_n) \end{pmatrix}, \tag{129}$$

let the matrix W *be the diagonal matrix whose diagonal entries are* $w_1, w_2, \ldots, w_n$, *and let the matrix* $E = [e_{jk}]$ *be given by the formula*

$$E = I - A^* W A. \tag{130}$$

Then

$$|e_{jk}| < \left| \frac{2\varepsilon}{\lambda_{j-1}\lambda_{k-1}} \right|. \tag{131}$$

Proof. Clearly

$$e_{jk} = \delta_{jk} - \sum_{l=1}^{n} w_l \, \psi_{j-1}(x_l) \, \psi_{k-1}(x_l), \tag{132}$$

where δ_{ij} is the Kronecker delta function. Using (18), this becomes

$$\begin{aligned} e_{jk} &= \delta_{jk} - \sum_{l-1}^{n} w_l \cdot \left(\frac{1}{\overline{\lambda}_{j-1}} \int_1^1 \mathrm{e}^{-\mathrm{i}cx_l t} \, \psi_{j-1}(t) \, \mathrm{d}t \right) \cdot \left(\frac{1}{\lambda_{k-1}} \int_1^1 \mathrm{e}^{\mathrm{i}cx_l \tau} \, \psi_{k-1}(\tau) \, \mathrm{d}\tau \right) \\ &= \delta_{jk} - \frac{1}{\overline{\lambda}_{j-1}\lambda_{k-1}} \int_{-1}^1 \int_{-1}^1 \psi_{j-1}(t) \, \psi_{k-1}(\tau) \sum_{l-1}^{n} w_l \mathrm{e}^{-\mathrm{i}cx_l t} \, \mathrm{e}^{\mathrm{i}cx_l \tau} \, \mathrm{d}t \, \mathrm{d}\tau. \end{aligned} \tag{133}$$

Using (128), this becomes

$$e_{jk} = \delta_{jk} - \frac{1}{\overline{\lambda}_{j-1}\lambda_{k-1}} \int_{-1}^1 \int_{-1}^1 \psi_{j-1}(t) \, \psi_{k-1}(\tau) \cdot \left(\int_{-1}^1 \mathrm{e}^{\ \mathrm{i}cst} \, \mathrm{e}^{\mathrm{i}cs\tau} \, \mathrm{d}s - f_c(t+\tau) \right) \mathrm{d}t \, \mathrm{d}\tau. \tag{134}$$

where $f_c : [-2, 2] \to \mathbb{C}$ is a function which satisfies the relation

$$|f_c(x)| < \varepsilon, \tag{135}$$

for all $x \in [-2, 2]$. Thus

$$\begin{aligned} e_{jk} = \delta_{jk} &- \frac{1}{\overline{\lambda}_{j-1}\lambda_{k-1}} \int_{-1}^1 \int_{-1}^1 \psi_{j-1}(t) \, \psi_{k-1}(\tau) \int_{-1}^1 \mathrm{e}^{-\mathrm{i}cst} \, \mathrm{e}^{\mathrm{i}cs\tau} \, \mathrm{d}s \, \mathrm{d}t \, \mathrm{d}\tau \\ &+ \frac{1}{\overline{\lambda}_{j-1}\lambda_{k-1}} \int_1^1 \int_1^1 \psi_{j-1}(t) \, \psi_{k-1}(\tau) \, f_c(t+\tau) \, \mathrm{d}t \, \mathrm{d}\tau. \end{aligned} \tag{136}$$

Using (18), this becomes

$$e_{jk} = \delta_{jk} - \int_{-1}^1 \psi_{j\ \ 1}(s) \, \psi_{k\ \ 1}(s) \, \mathrm{d}s + \frac{1}{\overline{\lambda}_{j-1}\lambda_{k-1}} \int_{-1}^1 \psi_{k\ \ 1}(\tau) \int_{-1}^1 \psi_{j\ \ 1}(t) \, f_c(t+\tau) \, \mathrm{d}t \, \mathrm{d}\tau. \tag{137}$$

Due to the orthonormality of the functions $\{\psi_j\}$, this becomes

$$e_{jk} = \frac{1}{\overline{\lambda}_{j-1}\lambda_{k-1}} \int_1^1 \psi_{k-1}(\tau) \int_1^1 \psi_{j-1}(t) \, f_c(t+\tau) \, \mathrm{d}t \, \mathrm{d}\tau. \tag{138}$$

Using the Cauchy–Schwartz inequality, this becomes

$$\begin{aligned} |e_{jk}| &\leqslant \left|\frac{1}{\lambda_{j-1}\lambda_{k-1}}\right| \|\psi_{k-1}\| \sqrt{\int_{-1}^{1} \left| \int_{-1}^{1} \psi_{j-1}(t)\, f_\varepsilon(t+\tau)\, \mathrm{d}t \right|^2 \mathrm{d}\tau} \\ &\leqslant \left|\frac{1}{\lambda_{j-1}\lambda_{k-1}}\right| \sqrt{\int_{-1}^{1} \|\psi_{j\ \ 1}\|^2 \int_{-1}^{1} |f_\varepsilon(t+\tau)|^2 \,\mathrm{d}t\, \mathrm{d}\tau} \\ &= \left|\frac{1}{\lambda_{j-1}\lambda_{k-1}}\right| \sqrt{\int_{-1}^{1}\int_{-1}^{1} |f_\varepsilon(t+\tau)|^2 \,\mathrm{d}t\, \mathrm{d}\tau} < \left|\frac{2\varepsilon}{\lambda_{j-1}\lambda_{k-1}}\right|. \end{aligned} \tag{139}$$

□

From inspection of theorem 2.5, it can easily be seen that the number N of eigenvalues needed for a bandwidth of $2c$ and an accuracy of ε^2 is roughly twice the number of eigenvalues needed for a bandwidth of c and an accuracy of ε. Thus a generalized Gaussian quadrature for a bandwidth $2c$ and an accuracy ε^2 has roughly the same number of nodes as are needed for interpolation of accuracy ε. In our numerical experiments, this correspondence was found to be much closer than the rough bounds in theorem 2.5 indicate; in the results tabulated in section 8, the number of nodes for an interpolation formula of a desired accuracy ε was always chosen to be the number of quadrature nodes for a desired accuracy ε^2 for twice the band limit (that number, in turn, being chosen as indicated in section 5); the correspondence between the desired accuracy and the experimentally measured maximum error can be seen in tables 3 and 4.

The coefficients $c_1, c_2, \ldots, c_n$ produced by this interpolation procedure (see (127)) can, of course, just as easily be used for evaluating derivatives or indefinite integrals of the interpolated function as they can for computing the function itself.

8. Numerical results

The algorithms of sections 5–7 have been implemented in double precision (64-bit floating point) arithmetic, with the results shown in tables 1–4. Tables 1 and 2 show the performance of quadrature nodes produced by the schemes of sections 5 and 6, when used as quadrature nodes; Tables 3 and 4 show their performance when used as interpolation nodes. These are not actually the same sets of nodes; even with the bandwidth c for interpolation being half of the bandwidth for quadrature (as it is in the tables), more nodes are needed to achieve a given accuracy of interpolation than are needed to achieve a given accuracy of quadrature, as can be seen by comparing the number of nodes (printed in the column labeled n in each table). The error figures in the tables are approximations of the maximum error of interpolation or of the quadrature, when applied to functions of the form $\cos(ax)$ and $\sin(ax)$, with $0 \leqslant a \leqslant c$; they were computed by measuring the error at a large number of points in a (for interpolation, in both a and x), including the extremes. The column labeled 'Roots' contains the errors for the nodes produced by the scheme of section 6; the column labeled 'Refined' contains the errors after those nodes, used as a starting point, have been run through the scheme of section 5. The variable ε which appears in the tables is the requested accuracy, used to determine the number of nodes in the ways described in sections 5 and 7.

Also tabulated are the numbers of Legendre nodes required to achieve the same accuracy ε using polynomial interpolation or quadrature schemes. Since Chebyshev nodes are generally known to be superior for interpolation, for that case the numbers of Chebyshev nodes required to achieve the same accuracy are also tabulated.

Table 1. Quadrature performance for varying band limits for $\varepsilon = 10^{-7}$.

		Maximum errors		
c	n	Roots	Refined	N_{pol}
10.0	9	0.96E 05	0.51E 07	13
20.0	13	0.17E 04	0.94E 07	19
30.0	17	0.12E–04	0.50E–07	25
40.0	20	0.70E–05	0.30E–06	31
50.0	24	0.35E–05	0.83E–07	37
60.0	27	0.25E–04	0.27E–06	43
70.0	31	0.11E–04	0.66E–07	48
80.0	34	0.48E–05	0.17E–06	54
90.0	38	0.21E–05	0.40E–07	59
100.0	41	0.12E 04	0.91E 07	65
200.0	74	0.24E 05	0.86E 07	118
300.0	106	0.32E–05	0.21E–06	171
400.0	139	0.52E–05	0.62E–07	223
500.0	171	0.56E–05	0.88E–07	275
600.0	203	0.58E–05	0.11E–06	326
700.0	235	0.57E–05	0.12E–06	377
800.0	267	0.55E–05	0.13E–06	428
900.0	299	0.53E–05	0.14E–06	479
1000.0	331	0.50E 05	0.14E 06	530
1200.0	395	0.44E 05	0.13E 06	632
1400.0	459	0.38E 05	0.11E 06	734
1600.0	523	0.31E–05	0.97E–07	835
1800.0	587	0.28E–05	0.80E–07	937
2000.0	651	0.23E–05	0.64E–07	1038
2400.0	778	0.29E–05	0.15E–06	1240
2800.0	906	0.19E–05	0.84E–07	1442
4000.0	1288	0.37E–05	0.17E–06	2047

Table 2. Quadrature performance for varying precisions for $c = 50$.

		Maximum errors		
ε	n	Roots	Refined	N_{pol}
0.10E 01	19	0.45E 01	0.10E 01	30
0.10E 02	20	0.70E 02	0.13E 02	32
0.10E 03	21	0.91E 03	0.14E 03	33
0.10E–04	22	0.82E–04	0.13E–04	34
0.10E–05	23	0.54E–04	0.11E–05	36
0.10E–06	24	0.35E–05	0.83E–07	37
0.10E–07	25	0.33E–05	0.57E–08	38
0.10E–08	26	0.18E–06	0.36E–09	39
0.10E–09	26	0.18E–06	0.36E–09	40
0.10E–10	27	0.17E–06	0.21E–10	42
0.10E 11	28	0.79E 08	0.11E 11	43
0.10E 12	29	0.78E 08	0.56E 13	45
0.10E–13	30	0.31E–09	0.27E–14	55

Figure 2 contains the maximum norm of the derivative of each prolate function $\psi_j(x)$, for $c = 200$ and $x \in [-1, 1]$, as a function of j; also plotted, for comparison, is the maximum

Table 3. Interpolation performance for varying band limits for $\varepsilon = 10^{-7}$.

		Maximum errors		N_{pol}	
c	n	Roots	Refined	Cheb.	Leg.
5.0	13	0.12E 06	0.12E 06	17	17
10.0	18	0.12E 06	0.13E 06	24	25
15.0	22	0.24E–06	0.25E–06	31	32
20.0	26	0.26E–06	0.28E–06	37	39
25.0	30	0.22E–06	0.23E–06	43	45
30.0	33	0.67E–06	0.73E–06	49	51
35.0	37	0.42E–06	0.46E–06	55	57
40.0	41	0.25E–06	0.27E–06	61	63
45.0	44	0.54E–06	0.60E–06	67	69
50.0	48	0.29E 06	0.33E 06	73	75
100.0	82	0.39E 06	0.46E 06	128	131
150.0	115	0.52E–06	0.64E–06	182	186
200.0	147	0.12E–05	0.15E–05	235	239
250.0	180	0.83E–06	0.11E–05	287	292
300.0	212	0.13E–05	0.17E–05	340	345
350.0	245	0.75E–06	0.10E–05	392	398
400.0	277	0.10E–05	0.14E–05	443	450
450.0	309	0.13E–05	0.18E–05	495	502
500.0	341	0.16E 05	0.22E 05	547	554
1000.0	662	0.16E 05	0.24E 05	1058	1068
1500.0	982	0.15E 05	0.25E 05	1566	1578
2000.0	1301	0.20E–05	0.35E–05	2072	2086

Table 4. Interpolation performance for varying precisions for $c = 25$.

		Maximum errors		N_{pol}	
ε	n	Roots	Refined	Cheb.	Leg.
0.10E 01	21	0.38E 01	0.43E 01	31	34
0.10E–02	23	0.37E–02	0.41E–02	34	36
0.10E–03	25	0.29E–03	0.31E–03	37	39
0.10E–04	26	0.74E–04	0.81E–04	39	41
0.10E–05	28	0.44E–05	0.47E–05	41	43
0.10E–06	30	0.22E–06	0.23E–06	43	45
0.10E–07	31	0.46E–07	0.49E–07	45	47
0.10E–08	32	0.95E–08	0.10E–07	47	49
0.10E–09	34	0.36E–09	0.38E–09	49	51
0.10E 10	35	0.67E 10	0.70E 10	51	52
0.10E 11	37	0.21E 11	0.22E 11	53	54
0.10E–12	38	0.36E–12	0.37E–12	54	56
0.10E–13	39	0.59E–13	0.63E–13	98	61

norm of the derivative of each normalized Legendre polynomial $\overline{P}_j(x)$ over the same range; and plotted below, on the same horizontal scale, are the absolute values of the eigenvalues λ_j. The graph shows that, for this value of c, computing the derivatives of a function given by a prolate series is a better-conditioned operation than computing the derivatives of a function given by a Legendre series of the same number of terms. (Obviously, if the number of terms can also be reduced, as in the situations of tables 1–4, there is a further improvement in the

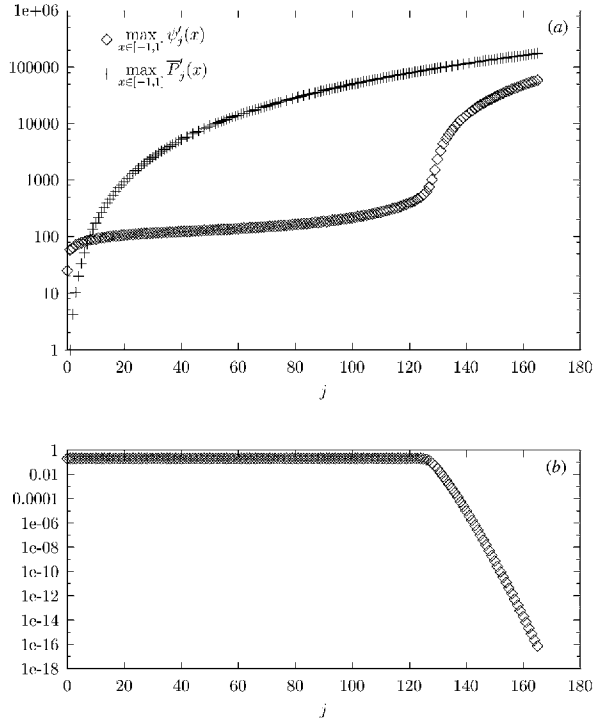

Figure 2. (*a*) Maximum norms of derivatives of PSWFs for $c = 200$, and of normalized Legendre polynomials. (*b*) Norms of eigenvalues λ_j for $c = 200$.

condition number.) The same general pattern of behaviour is exhibited for other values of c; as c approaches zero (and the prolate functions approach the Legendre polynomials), the value of j at which the maximum norm of the derivative rises sharply also approaches zero (as is to be expected, since for $c = 0$ the prolate functions reduce to Legendre polynomials). Finally, tables 5 and 6 contain samples of quadrature weights and nodes.

Remark 8.1. In this paper, detailed discussion of issues encountered in the implementation of numerical algorithms has been deliberately avoided, as well as any discussion of CPU time requirements, memory requirements, etc. Thus, we limit ourselves to observing that all algorithms have been implemented in FORTRAN, that with the exception of the procedure for the evaluation of PSWFs described in section 4 we have not designed or implemented any new or original numerical algorithms, and that the procedure of section 4 consists of applying standard tools of numerical analysis (diagonalization of a tridiagonal matrix) to the well-known recursion (61). The resulting algorithm for the evaluation of PSWFs has the CPU time requirements proportional to c^2, with a fairly large proportionality constant. The procedure

Table 5. Quadrature nodes for band-limited functions, with $c = 50$ and $\varepsilon = 10^{-7}$. This table contains only half of the nodes and weights, in particular those for which the node is less than or equal to zero; reflecting these nodes around zero yields the remaining nodes, the weight for the node at $-x$ being the same as the weight for the node at x.

Node	Weight
−0.990 452 245 996 0804E+00	0.241 306 423 492 2188E−01
−0.952 560 110 664 3832E+00	0.502 434 721 709 5568E−01
−0.892 796 086 145 9153E+00	0.680 178 767 783 0858E−01
−0.818 611 753 060 9125E+00	0.795 215 599 910 0788E−01
−0.735 062 413 196 5875E+00	0.870 668 070 837 6023E−01
−0.645 287 802 726 0844E+00	0.921 624 076 576 3570E−01
−0.551 255 469 869 5428E+00	0.956 925 401 548 6106E−01
−0.454 250 528 152 5226E+00	0.981 725 776 631 1556E−01
−0.355 156 845 812 7944E+00	0.999 091 451 610 2242E−01
−0.254 617 346 381 3596E+00	0.101 088 017 264 8715E+00
−0.153 128 778 186 0989E+00	0.101 821 430 893 1439E+00
−0.511 012 148 405 0418E−01	0.102 173 518 998 6602E+00

of [2], when applied to the system of functions $\psi_0, \psi_1, \ldots, \psi_{2n+1}$ requires order n^3 operations, also with a fairly large proportionality constant. On the other hand, the cost of finding all roots n of the function ψ_n lying on the interval $[-1, 1]$ is proportional to n, and the proportionality constant is not large. The largest c we have dealt with in our experiments was about 6000, with resulting quadratures having about 1900 nodes. In this regime, the construction of the quadrature (both nodes and weights) took several minutes on a 300 MHz Sun workstation; while there are fairly obvious ways to reduce the cost of the calculation (both in terms of asymptotic CPU time requirements and in terms of associated proportionality constants) we have made no effort to do so.

The following observations can be made from the examples presented in this section, and from the more extensive tests performed by the authors.

(1) When the nodes obtained via the algorithm of [2] are used for the integration of band-limited functions, the resulting quadrature rules are significantly more accurate than the quadratures obtained from the nodes of appropriately chosen prolate functions; however, the *difference* between the numbers of nodes required by the two approaches to obtain a *prescribed* precision is not large. When the nodes obtained via the two approaches are used for the interpolation (as opposed to the integration) of band-limited functions, the performances of the two are virtually identical.

(2) For large c, the number of nodes required by a quadrature rule for the integration of band-limited functions with the band limit c is close to $\frac{c}{\pi}$; the dependence on the required precision of integration is weak (as one would expect from theorem 2.5 and subsequent developments).

(3) The numbers of nodes required by our quadrature rules to integrate band-limited functions is roughly $\pi/2$ times less than the numbers of Gaussian nodes; the numbers of nodes required by our interpolation formulae in order to interpolate band-limited functions is roughly $\pi/2$ times less than the number of Chebyshev (or Gaussian) nodes. Again, the dependence of the required number of nodes on the accuracy requirements is weak.

(4) The norm of the differentiation operator based on our nodes is of the order $c^{3/2}$, as compared to the norm of the spectral differentiation operators obtained from classical polynomial expansions; this might be useful in the design of spectral (or pseudospectral) techniques.

Table 6. Quadrature nodes for band-limited functions, with $c = 150$ and $\varepsilon = 10^{-14}$ This table contains only half of the nodes and weights, in particular those for which the node is less than or equal to zero; reflecting these nodes around zero yields the remaining nodes, the weight for the node at $-x$ being the same as the weight for the node at x.

Node	Weight
−0.998 288 301 095 9975E+00	0.437 448 337 175 2129E−02
−0.991 135 469 159 6528E+00	0.984 261 923 614 9078E−02
−0.978 831 528 098 2487E+00	0.146 351 830 025 0369E−01
−0.962 134 893 790 1911E+00	0.186 239 611 128 7527E−01
−0.941 838 669 845 4396E+00	0.218 498 873 921 7138E−01
−0.918 650 957 680 2944E+00	0.244 285 867 093 2862E−01
−0.893 154 185 029 3142E+00	0.264 886 457 925 8096E−01
−0.865 808 389 404 1821E+00	0.281 437 594 041 3615E−01
−0.836 970 958 825 4746E+00	0.294 852 862 479 5690E−01
−0.806 918 710 818 5302E+00	0.305 835 616 043 5090E−01
−0.775 867 033 139 6409E+00	0.314 918 106 663 3766E−01
−0.743 984 950 115 2674E+00	0.322 501 550 620 3403E−01
−0.711 406 497 617 5457E+00	0.328 889 371 307 9314E−01
−0.678 239 168 691 0609E+00	0.334 312 642 162 0424E−01
−0.644 570 159 409 8660E+00	0.338 948 893 155 1181E−01
−0.610 471 001 338 4929E+00	0.342 935 820 687 7410E−01
−0.576 001 020 298 0960E+00	0.346 381 251 389 2117E−01
−0.541 209 941 325 7457E+00	0.349 370 403 387 9884E−01
−0.506 139 869 774 2787E+00	0.351 971 209 589 5683E−01
−0.470 826 813 447 3433E+00	0.354 238 249 991 7732E−01
−0.435 301 864 359 8344E+00	0.356 215 680 855 7525E−01
−0.399 592 125 924 2572E+00	0.357 939 435 277 6868E−01
−0.363 721 448 125 7228E+00	0.359 438 890 077 8062E−01
−0.327 711 016 711 4320E+00	0.360 738 138 124 7460E−01
−0.291 579 830 581 9667E+00	0.361 856 966 038 5742E−01
−0.255 345 093 038 8687E+00	0.362 811 609 573 7887E−01
−0.219 022 536 350 1577E+00	0.363 615 339 339 9723E−01
−0.182 626 694 572 1476E+00	0.364 278 915 436 4812E−01
−0.146 171 136 245 0572E+00	0.364 810 939 379 6617E−01
−0.109 668 666 134 7072E+00	0.365 218 124 225 7066E−01
−0.731 315 033 936 5902E−01	0.365 505 498 230 3338E−01
−0.365 714 422 012 2915E−01	0.365 676 553 168 5031E−01
0	0.365 733 345 155 6860E−01

9. Miscellaneous properties

PSWFs possess a rich set of properties, vaguely resembling the properties of Bessel functions. This section lists some of those properties. Some of the identities below can be found in [5, 18, 21]; others are easily derivable from the former.

The identity

$$e^{icxt} = \sum_{j=0}^{\infty} \lambda_j \, \psi_j(x) \, \psi_j(t) \tag{140}$$

(see section 5) has a number of consequences which, while fairly obvious, seem worth recording, since similar properties of other special functions have often been found useful.

Differentiating (140) m times with respect to x and n times with respect to t yields the formula

$$x^m t^n \mathrm{e}^{\mathrm{i}cxt} = \left(\frac{1}{\mathrm{i}c}\right)^{(m+n)} \sum_{j=0}^{\infty} \lambda_j \, \psi_j^{(m)}(x) \, \psi_j^{(n)}(t), \tag{141}$$

for all $x, t \in [-1, 1]$. Multiplying (140) by $\mathrm{e}^{-\mathrm{i}cut}$, and integrating with respect to t, converts it into

$$\frac{\sin(c \cdot (x-u))}{x-u} = \frac{c}{2} \sum_{j=0}^{\infty} \lambda_j^2 \, \psi_j(x) \, \psi_j(u). \tag{142}$$

Taking the squared norm of (140), and integrating with respect to x and t, yields the formula

$$\sum_{j=0}^{\infty} |\lambda_j|^2 = 4; \tag{143}$$

combining this with (21) yields

$$\sum_{j=0}^{\infty} \mu_j = \frac{2c}{\pi}. \tag{144}$$

Setting $x = t = 1$ converts (140) into

$$\mathrm{e}^{\mathrm{i}c} = \sum_{j=0}^{\infty} \lambda_j \, \psi_j^2(1). \tag{145}$$

The identity

$$\lambda_j \psi_j(x) = \int_{-1}^{1} \mathrm{e}^{\mathrm{i}cxt} \, \psi_j(t) \, \mathrm{d}t \tag{146}$$

(see section 2.5) also has a number of simple but potentially useful consequences. Differentiating it k times with respect to x, we get

$$\lambda_j \psi_j^{(k)}(x) = (\mathrm{i}c)^k \int_{1}^{1} \mathrm{e}^{\mathrm{i}cxt} \, t^k \, \psi_j(t) \, \mathrm{d}t. \tag{147}$$

We next consider the integral

$$f(x) = f(a, x) = \int_{1}^{1} \frac{\mathrm{e}^{\mathrm{i}cxt}}{t-a} \psi_j(t) \, \mathrm{d}t. \tag{148}$$

Differentiating (148) with respect to x, we have

$$\frac{\mathrm{d}}{\mathrm{d}x} f(a, x) = \mathrm{i}c \int_{-1}^{1} \frac{t \mathrm{e}^{\mathrm{i}cxt}}{t-a} \psi_j(t) \, \mathrm{d}t. \tag{149}$$

Multiplying (148) by $\mathrm{i}ca$, and subtracting it from (149), we obtain

$$\frac{\mathrm{d}}{\mathrm{d}x} f(a, x) - \mathrm{i}caf(a, x) = \mathrm{i}c \int_{-1}^{1} \mathrm{e}^{\mathrm{i}cxt} \, \psi_j(t) \, \mathrm{d}t = \mathrm{i}c\lambda_j \psi_j(x). \tag{150}$$

In other words, f satisfies the differential equation

$$f'(x) - \mathrm{i}caf(x) = \mathrm{i}c\lambda_j \psi_j(x). \tag{151}$$

The standard 'variation of parameter' calculation provides the solution to (151):

$$f(x) = \mathrm{i}c\lambda_j \int_{0}^{x} \mathrm{e}^{-\mathrm{i}ca(x-t)} \psi_j(t) \, \mathrm{d}t + f(0) \, \mathrm{e}^{\mathrm{i}cax}. \tag{152}$$

Introducing the notation

$$\mathcal{D} = \frac{1}{\mathrm{i}c} \circ \frac{\mathrm{d}}{\mathrm{d}x} \tag{153}$$

(i.e. $\mathcal{D}$ is the product of multiplication by $1/\mathrm{i}c$ and differentiation), we rewrite (147) as

$$\mathcal{D}^k(\psi_j)(x) = \frac{1}{\lambda_j}\int_{-1}^{1} t^k\, \mathrm{e}^{\mathrm{i}cxt}\, \psi_j(t)\,\mathrm{d}t; \tag{154}$$

for an arbitrary polynomial P (with real or complex coefficients),

$$P(\mathcal{D})(\psi_j)(x) = \frac{1}{\lambda_j}\int_{-1}^{1} P(t)\, \mathrm{e}^{\mathrm{i}cxt}\, \psi_j(t)\,\mathrm{d}t. \tag{155}$$

By the same token, the function ϕ defined by the formula

$$\phi(x) = \int_{-1}^{1} \frac{\mathrm{e}^{\mathrm{i}cxt}}{P(t)}\psi_j(t)\,\mathrm{d}t \tag{156}$$

satisfies the differential equation

$$P(\mathcal{D})(\phi)(x) = \lambda_m \psi_m(x). \tag{157}$$

The following lemma provides a recursion connecting the values of the kth derivative of the function ψ_m with its derivatives of orders $k-1$, $k-2$, $k-3$ and $k-4$.

Lemma 9.1. *For any positive real c, integer $m \geqslant 0$ and $x \in (-\infty, +\infty)$,*

$$\begin{aligned}(1-x^2)\,\psi_m^{(k+2)}(x) - 2\,(k+1)x\,\psi_m^{(k+1)}(x) + (\chi_m - k\,(k+1) - c^2\,x^2)\,\psi_m^{(k)}(x)\\ -2\,c^2\,k\,x\,\psi_m^{(k-1)}(x) - c^2\,k\,(k-1)\,\psi_m^{(k-2)}(x) = 0\end{aligned} \tag{158}$$

for all $k \geqslant 2$. Furthermore,

$$(1-x^2)\,\psi_m'''(x) - 4\,x\,\psi_m''(x) + (\chi_m - 2 - c^2\,x^2)\,\psi_m'(x) - 2\,c^2\,x\,\psi_m(x) = 0. \tag{159}$$

In particular,

$$\begin{aligned}-2\,(k+1)\,\psi_m^{(k+1)}(1) + (\chi_m - k\,(k+1) - c^2)\,\psi_m^{(k)}(1)\\ -2\,c^2\,k\,\psi_m^{(k\ \ 1)}(1) - c^2\,k\,(k-1)\,\psi_m^{(k\ \ 2)}(1) = 0\end{aligned} \tag{160}$$

for all $k \geqslant 2$, and

$$-2\,\psi_m'(1) + (\chi_m - c^2)\,\psi_m(1) = 0, \tag{161}$$

$$-4\,\psi_m''(1) + (\chi_m - 2 - c^2)\,\psi_m'(1) - 2\,c^2\,\psi_m(1) = 0. \tag{162}$$

Furthermore, for all integer $m \geqslant 0$ and $k \geqslant 2$,

$$\psi_m^{(k+2)}(0) + (\chi_m - k\,(k+1))\,\psi_m^{(k)}(0) - c^2\,k\,(k-1)\,\psi_m^{(k-2)}(0) = 0. \tag{163}$$

For all odd m,

$$\psi_m'''(0) + (\chi_m - 2)\,\psi_m'(0) = 0. \tag{164}$$

and for all even m,

$$\psi_m''(0) + \chi_m\,\psi_m(0) = 0. \tag{165}$$

Finally, for all integer $m \geqslant 0$ and $k \geqslant 0$,

$$\psi_m(1) \neq 0, \tag{166}$$

$$\psi_{2m+1}^{(2k)}(0) = 0, \tag{167}$$

$$\psi_{2m}^{(2k+1)}(0) = 0. \tag{168}$$

Proof. All of the identities (158)–(165), (167) and (168) are immediately obtained by repeated differentiation of (24). In order to prove (166), we assume that

$$\psi_m(1) = 0 \tag{169}$$

for some integer $m \geqslant 0$ and observe that the combination of (169) with (160)–(162) implies that

$$\psi_m^{(k)}(1) = 0 \tag{170}$$

for all $k = 0, 1, 2, \ldots$. Due to the analyticity of $\psi_m(x)$ in the complex plane, this would imply that

$$\psi_m(x) = 0 \tag{171}$$

for all $x \in \mathbb{R}^1$. □

The following is an immediate consequence of the identity (161) of lemma 9.1.

Corollary 9.2. *For all integer $m, n \geqslant 0$,*

$$\psi_m'(1) \cdot \psi_n(1) - \psi_n'(1) \cdot \psi_m(1) = (\chi_n - \chi_m) \cdot \psi_n(1) \cdot \psi_m(1), \tag{172}$$

where $\chi_m, \chi_n \in \mathbb{R}$ are as defined in theorem 2.6.

Theorem 3.1, in section 3.1, gives formulae for the entries of matrices for differentiation of prolate series and for multiplication of prolate series by x. Matrices for any combination of differentiation and multiplication by a polynomial can obviously be constructed from these two matrices; for instance, calling the differentiation matrix D, and the multiplication-by-x matrix X, the matrix for taking the second derivative of a prolate series, then multiplying it by $5 - x^2$, is equal to $(5I - X^2)D^2$.

In many cases, however, there are simpler formulae for the entries of such matrices, that is, for inner products of $\psi_j(x)$ with its derivatives and with polynomials. The following theorems establish several such formulae, as well as a few formulae for inner products which do not involve $\psi_j(x)$ itself but only its derivatives. Their proofs proceed along much the same lines as those of theorem 3.1 and are omitted.

Theorem 9.3. *Suppose that c is real and positive, and that the integers m and n are non-negative. If $m \neq n \pmod 2$, then*

$$\int_{-1}^{1} x\, \psi_n'(x)\, \psi_m(x)\, \mathrm{d}x = 0, \tag{173}$$

$$\int_{1}^{1} x^2\, \psi_n''(x)\, \psi_m(x)\, \mathrm{d}x = 0, \tag{174}$$

$$\int_{-1}^{1} x^2\, \psi_n'(x)\, \psi_m'(x)\, \mathrm{d}x = 0, \tag{175}$$

$$\int_{-1}^{1} \psi_n(x)\, \psi_m''(x)\, \mathrm{d}x = 0, \tag{176}$$

$$\int_{1}^{1} x^2\, \psi_n(x)\, \psi_m(x)\, \mathrm{d}x = 0. \tag{177}$$

If $m = n \pmod 2$, then

$$\int_{-1}^{1} x\, \psi_n'(x)\, \psi_m(x)\, \mathrm{d}x = \frac{\lambda_m}{\lambda_m + \lambda_n}(2\, \psi_m(1)\, \psi_n(1) - \delta_{mn}). \tag{178}$$

If $m = n \pmod 2$ and $m \neq n$, then

$$\int_{-1}^{1} x^2\, \psi_m''(x)\, \psi_n(x)\, \mathrm{d}x = \frac{2\lambda_n}{\lambda_m - \lambda_n}(\psi_n'(1)\, \psi_m(1) - \psi_m'(1)\, \psi_n(1)) - \frac{4\lambda_n}{\lambda_n + \lambda_m}\, \psi_n(1)\, \psi_m(1) \tag{179}$$

$$= \frac{\lambda_n}{\lambda_m - \lambda_n}\, (\chi_n - \chi_m)\, \psi_n(1)\, \psi_m(1) - \frac{4\lambda_n}{\lambda_n + \lambda_m}\, \psi_n(1)\, \psi_m(1), \tag{180}$$

$$\int_{1}^{1} x^2\, \psi_m'(x)\, \psi_n'(x)\, \mathrm{d}x = 2\, \psi_m'(1)\, \psi_n(1) + \frac{2\lambda_n}{\lambda_m - \lambda_n}\, (\psi_m'(1)\, \psi_n(1) - \psi_n'(1)\, \psi_m(1)) \tag{181}$$

$$= 2\, \psi_n'(1)\, \psi_m(1) + \frac{2\lambda_m}{\lambda_n - \lambda_m}\, (\psi_n'(1)\, \psi_m(1) - \psi_m'(1)\, \psi_n(1)) \tag{182}$$

$$= \psi_m(1)\, \psi_n(1) \left(\frac{\lambda_n \chi_m - \lambda_m \chi_n}{\lambda_m - \lambda_n} - c^2 \right), \tag{183}$$

$$\int_{1}^{1} \psi_n(x)\, \psi_m''(x)\, \mathrm{d}x = \frac{2\, \lambda_n^2}{\lambda_m^2 - \lambda_n^2}\, (\psi_n'(1)\, \psi_m(1) - \psi_n(1)\, \psi_m'(1)) \tag{184}$$

$$= \frac{\lambda_n^2}{\lambda_m^2 - \lambda_n^2}\, (\chi_n - \chi_m)\, \psi_m(1)\, \psi_n(1), \tag{185}$$

$$\int_{1}^{1} x^2\, \psi_n(x)\, \psi_m(x)\, \mathrm{d}x = -\frac{2}{c^2}\, \frac{\lambda_m \lambda_n}{\lambda_m^2 - \lambda_n^2}\, (\psi_n'(1)\, \psi_m(1) - \psi_n(1)\, \psi_m'(1)) \tag{186}$$

$$= -\frac{1}{c^2}\, \frac{\lambda_m \lambda_n}{\lambda_m^2 - \lambda_n^2}\, (\chi_n - \chi_m)\, \psi_m(1)\, \psi_n(1), \tag{187}$$

where χ_m, $\chi_n \in \mathbb{R}$ are as defined in theorem 2.6.

Theorem 9.4. *Suppose that c is real and positive, and that the integers m and n are non-negative. Let*

$$\Psi_n(y) = \int_0^y \psi_n(x)\, \mathrm{d}x. \tag{188}$$

If n is odd and m is even, then

$$\int_{1}^{1} \frac{1}{t}\, \psi_n(t)\, \psi_m(t)\, \mathrm{d}t = \mathrm{i}\, c\, \frac{2\, \lambda_m\, \lambda_n}{\lambda_n^2 + \lambda_m^2}\, \Psi_n(1)\, \Psi_m(1) + 2\, \frac{\lambda_m}{\lambda_n^2 + \lambda_m^2}\, \Psi_m(1) \int_{1}^{1} \frac{1}{t}\, \psi_n(t)\, \mathrm{d}t. \tag{189}$$

If $m = n \pmod 2$, then

$$\int_{1}^{1} \frac{1}{t}\, \psi_n(t)\, \psi_m(t)\, \mathrm{d}t = 0. \tag{190}$$

The above theorems do not use much of the detailed structure of the integral operators of which the functions $\{\psi_j\}$ are eigenfunctions. Thus many of them generalize easily to the case of an operator $L : L^2[0, 1] \to L^2[0, 1]$ defined via the formula

$$L(\psi)(x) = \int_0^1 K(xt)\, \psi(t)\, \mathrm{d}t, \tag{191}$$

for some function $K : [0, 1] \to \mathbb{C}$; the following theorem is an example of this.

Theorem 9.5. *Let λ_1, λ_2 be two eigenvalues of the operator L defined by (191), that is,*

$$\int_0^1 K(xt)\,\psi_1(t)\,\mathrm{d}t = \lambda_1\psi_1(x), \tag{192}$$

$$\int_0^1 K(xt)\,\psi_2(t)\,\mathrm{d}t = \lambda_2\psi_2(x). \tag{193}$$

Then

$$\frac{\lambda_2}{\lambda_1} = \frac{\int_0^1 x\,\psi_1'(x)\,\psi_2(x)\,\mathrm{d}x}{\int_0^1 x\,\psi_2'(x)\,\psi_1(x)\,\mathrm{d}x}, \tag{194}$$

provided that neither λ_1 nor the denominator of the right-hand side of (194) is zero.

The following theorem establishes the relation between the norm of each function ψ_j on $[-1, 1]$ (which in this paper is taken to be one) and its norm on $(-\infty, \infty)$.

Theorem 9.6. *Suppose that c is real and positive, and that the integer n is non-negative. Then*

$$\int_{\infty}^{\infty} \psi_n^2(x)\,\mathrm{d}x = \frac{1}{\mu_n}, \tag{195}$$

where μ_n is given by (21).

Proof.

$$\begin{aligned}\int_{\infty}^{\infty} \psi_n^2(x)\,\mathrm{d}x &= \int_{\infty}^{\infty}\left(\frac{1}{\pi\mu_n}\int_1^1 \psi_n(t)\,\frac{\sin(c\cdot(x-t))}{x-t}\,\mathrm{d}t\right)\psi_n(x)\,\mathrm{d}x\\ &= \frac{1}{\mu_n}\int_{-1}^{1}\psi_n(t)\cdot\left(\frac{1}{\pi}\int_{-\infty}^{\infty}\frac{\sin(c\cdot(x-t))}{x-t}\,\psi_n(x)\,\mathrm{d}x\right)\mathrm{d}t\\ &= \frac{1}{\mu_n}\int_{-1}^{1}\psi_n^2(t)\,\mathrm{d}t = \frac{1}{\mu_n}.\end{aligned}$$

□

The following theorem extends theorem (9.6) to any band-limited function with band limit c. Its proof proceeds along the same lines and is omitted.

Theorem 9.7. *Suppose that c is real and positive, that the integer n is non-negative, and that $f : \mathbb{R} \to \mathbb{C}$ is a band-limited function with band limit c. Then*

$$\int_{\infty}^{\infty} \psi_n(x)\,f(x)\,\mathrm{d}x = \frac{1}{\mu_n}\int_1^1 \psi_n(x)\,f(x)\,\mathrm{d}x. \tag{196}$$

Theorem 9.8. *Suppose that c is real and positive, and that the integer n is non-negative. Then*

$$\int_{\infty}^{\infty} \mathrm{e}^{\mathrm{i}cxt}\psi_m(t)\,\mathrm{d}t = \begin{cases}\dfrac{\lambda_m}{\mu_m}\psi_m(x), & \text{if} \quad -1 < x < 1,\\ 0, & \text{if} \quad x > 1 \quad \text{or} \quad x < -1.\end{cases} \tag{197}$$

Proof. Since ψ_m is an eigenfunction of the operator Q_c defined in (19), and μ_m is the corresponding eigenvalue,

$$\mu_m\psi_m(t) = \frac{1}{\pi}\int_{-1}^{1}\frac{\sin(c\cdot(x-u))}{x-u}\,\psi_m(u)\,\mathrm{d}u. \tag{198}$$

Thus

$$\int_{-\infty}^{\infty} e^{icxt}\,\psi_m(t)\,dt = \frac{1}{\mu_m}\int_{-\infty}^{\infty} e^{icxt}\left(\frac{1}{\pi}\int_{-1}^{1}\frac{\sin(c\cdot(x-u))}{x-u}\,\psi_m(u)\,du\right)dt \tag{199}$$

$$= \frac{1}{\mu_m}\int_{-1}^{1}\psi_m(u)\left(\frac{1}{\pi}\int_{-\infty}^{\infty}\frac{\sin(c\cdot(x-u))}{x-u}\,e^{icxt}\,dt\right)du. \tag{200}$$

Since the innermost integral is the orthogonal projection operator onto the space of functions of band limit c on $(-\infty,\infty)$, applied to the function e^{icxt}, it follows that

$$\int_{\infty}^{\infty} e^{icxt}\,\psi_m(t)\,dt$$

$$= \frac{1}{\mu_m}\int_{-1}^{1}\psi_m(u)\left(\begin{cases} e^{icxu}, & \text{if} \quad -1 < x < 1, \\ 0, & \text{if} \quad x > 1 \quad \text{or} \quad x < -1 \end{cases}\right)du \tag{201}$$

$$= \begin{cases} \dfrac{1}{\mu_m}\displaystyle\int_{1}^{1}\psi_m(u)\,e^{icxu}\,du, & \text{if} \quad -1 < x < 1, \\ 0, & \text{if} \quad x > 1 \quad \text{or} \quad x < -1, \end{cases} \tag{202}$$

from which (197) follows immediately. □

The following five theorems establish formulae for the derivatives of prolate functions and their associated eigenvalues with respect to c. Proofs of the first theorem can be found in [6, 25].

Theorem 9.9. *For all positive real c and non-negative integer m,*

$$\frac{\partial\lambda_m}{\partial c} = \lambda_m\,\frac{2\,\psi_m^2(1) - 1}{2\,c} \tag{203}$$

and

$$\frac{\partial\mu_m}{\partial c} = \frac{2}{c}\,\mu_m\,\psi_m^2(1). \tag{204}$$

The following theorem is an immediate consequence of the preceding one.

Theorem 9.10. *For all positive real c and non-negative integer m, n,*

$$\left(\frac{\lambda_m}{\lambda_n}\right)' = \frac{\lambda_m}{\lambda_n}\,\frac{1}{c}\,(\psi_m^2(1) - \psi_n^2(1)). \tag{205}$$

$$\left(\frac{\mu_m}{\mu_n}\right)' = \frac{\mu_m}{\mu_n}\,\frac{2}{c}\,(\psi_m^2(1) - \psi_n^2(1)). \tag{206}$$

Theorem 9.11. *Suppose that c is real and positive, and the integers m, n are non-negative. If $m \neq n$, then*

$$\int_{-1}^{1}\psi_m(t)\,\frac{\partial\psi_n}{\partial c}(t)\,dt = -\frac{2}{c}\,\frac{\lambda_n\,\lambda_m}{\lambda_m^2 - \lambda_n^2}\,\psi_m(1)\,\psi_n(1). \tag{207}$$

If $m = n$, then

$$\int_{-1}^{1}\psi_m(t)\,\frac{\partial\psi_n}{\partial c}(t)\,dt = 0. \tag{208}$$

Proof. Since the norm of ψ_n on $[-1, 1]$ remains constant as c varies, ψ_n must be orthogonal on $[-1, 1]$ to its own derivative with respect to c, which immediately yields (208). To establish (207), we start with the identity

$$\lambda_n \psi_n(x) = \int_{-1}^{1} e^{icxt}\, \psi_n(t)\, dt. \tag{209}$$

Differentiating (209) with respect to c, we get

$$\frac{\partial \lambda_n}{\partial c}\, \psi_n(x) + \lambda_n \frac{\partial \psi_n}{\partial c} = \int_{-1}^{1} \left(ixt e^{icxt}\, \psi_n(t) + e^{icxt} \frac{\partial \psi_n(t)}{\partial c} \right) dt. \tag{210}$$

Multiplying both sides of (210) by $\psi_m(x)$ and integrating with respect to x, we have

$$\lambda_n \int_{-1}^{1} \psi_m(x) \frac{\partial \psi_n(x)}{\partial c}\, dx = \frac{\lambda_n}{c} \int_{-1}^{1} x\, \psi_n'(x)\, \psi_m(x)\, dx + \lambda_m \int_{-1}^{1} \psi_m(t) \frac{\partial \psi_n(t)}{\partial c}\, dt, \tag{211}$$

which, using (178), we rewrite as

$$(\lambda_n - \lambda_m) \int_{-1}^{1} \psi_m(t) \frac{\partial \psi_n(t)}{\partial c}\, dt = \frac{\lambda_n}{c} \frac{\lambda_m}{\lambda_m + \lambda_n} (2\, \psi_m(1)\, \psi_n(1) - \delta_{mn}). \tag{212}$$

Assuming that $m \neq n$, and dividing by $\lambda_n - \lambda_m$, we then get (207). □

Theorem 9.12. *Suppose that c is real and positive, and the integer m is non-negative. Then*

$$\frac{\partial \chi_m}{\partial c} = 2c \int_{-1}^{1} x^2 \psi_m^2(x). \tag{213}$$

Proof. Due to theorem 2.6,

$$(1 - x^2)\psi_m''(x) - 2x\psi_m'(x) + (\chi_m - c^2x^2)\, \psi_m(x) = 0. \tag{214}$$

Making the infinitesimal changes $c = c + h$, $\chi_m = \chi_m + \varepsilon$ and $\psi_m(x) = \psi_m(x) + \delta(x)$, this becomes

$$\begin{aligned}(1 - x^2) \cdot (\psi_m''(x) + \delta''(x)) - 2x \cdot (\psi_m'(x) + \delta'(x)) \\ +(\chi_m + \varepsilon - (c + h)^2x^2) \cdot (\psi_m(x) + \delta(x)) = 0.\end{aligned} \tag{215}$$

Expanding each term, discarding infinitesimals of the second order or greater (that is, products of two or more of the quantities h, ε and $\delta(x)$), and subtracting (214), we get

$$(1 - x^2)\, \delta''(x) - 2x\delta'(x) + (\chi_m - c^2x^2)\, \delta(x) + (\varepsilon - 2chx^2)\psi_m(x) = 0. \tag{216}$$

Let the self-adjoint differential operator L be defined by the formula

$$L(f)(x) = (1 - x^2) f''(x) - 2xf'(x) + (\chi_m - c^2x^2) f(x). \tag{217}$$

Then, multiplying (216) by $\psi_m(x)/h$ and integrating on $[-1, 1]$, we get

$$\int_{-1}^{1} L\left(\frac{\partial \psi_m}{\partial c} \right)(x)\, \psi_m(x)\, dx + \frac{\varepsilon}{h} - \int_{-1}^{1} 2cx^2 \psi_m^2(x) = 0. \tag{218}$$

Now $\frac{\varepsilon}{h} = \frac{\partial \chi_m}{\partial c}$. In addition, since L is self-adjoint,

$$\int_{1}^{1} L\left(\frac{\partial \psi_m}{\partial c} \right)(x)\, \psi_m(x)\, dx = \int_{1}^{1} \frac{\partial \psi_m}{\partial c}(x)\, L(\psi_m)(x)\, dx. \tag{219}$$

But due to (214), $L(\psi_m)(x) = 0$ for all $x \in [-1, 1]$, so the integral (219) is zero. Thus (218) becomes

$$\frac{\partial \chi_m}{\partial c} = 2c \int_{-1}^{1} x^2 \psi_m^2(x). \tag{220}$$

□

10. Generalizations and conclusions

In this paper, we design quadrature rules for band-limited functions, based on the properties of PSWFs, and the connections of the latter with certain fundamental integral operators (see (17) and (19) in section 2.5). The quadratures are a surprisingly close analogue for band-limited functions of Gaussian quadratures for polynomials, in that they have positive weights, are optimal in the appropriately defined sense, and their nodes, when used for approximation (as opposed to integration), result in extremely efficient interpolation formulae. Thus, sections 5–7 of this paper can be viewed as reproducing for band-limited functions much of the standard polynomial-based approximation theory (for which see, e.g., [26]). Generally, there is a striking analogy between the band-limited functions and polynomials.

Obviously, there are certain differences between the resulting apparatus and the standard numerical analysis. To start with, where the classical techniques are optimal for polynomials, the approach of this paper is optimal for band-limited functions; whenever the functions to be dealt with are naturally represented by trigonometric expansions on finite intervals, our quadrature and interpolation formulae tend to be more efficient than those based on the polynomials. When the functions to be dealt with are naturally represented by polynomials, the classical approach is more efficient; however, many physical phenomena involve band-limited functions, and very few involve polynomials.

Qualitatively, the quadrature (and interpolation) nodes obtained in this paper behave like a compromise between the Gaussian nodes and the equispaced ones: near the middle of the interval, they are very nearly equispaced, and near the ends, they concentrate somewhat, but much less than the Gaussian (or Chebyshev) nodes do. For large c, the distance between nodes near the ends of the interval is of the order of $1/c^{3/2}$, with the total number of nodes close to c/π. In contrast, the distance between the Gaussian nodes near the ends of the interval is of the order of $1/n^2$, with n the total number of nodes. A closely related phenomenon is the reduced norm of the differentiation operator based on the prolate expansions: for an n-point differentiation formula, the norm is of the order $n^{3/2}$, as opposed to n^2 for polynomial-based spectral differentiation. Thus, PSWF's are likely to be a better tool for the design of spectral and pseudo-spectral techniques than the orthogonal polynomials and related functions.

Much of the analytical apparatus we use was developed more than 30 years ago (see [18,19,21,22]); the fundamental importance of these results in certain areas of electrical engineering and physics has also been understood for a long time. However, there appears to have been no prior attempt made to view band-limited functions as a source of *numerical* algorithms. Generally, there is a fairly limited amount of information in the literature about the PSWFs, especially when compared to the wealth of facts on many other special functions. Section 9 of this paper is an attempt to remedy this situation to a small degree.

The apparatus built in this paper is a strictly one-dimensional one. Obviously, one can construct discretizations of rectangles, cubes, etc, by using direct products of one-dimensional grids; the resulting numerical algorithms are satisfactory but not optimal. Furthermore, representation of band-limited functions on regions in higher dimensions is of both theoretical and engineering interest. Obvious applications include seismic data collection and processing, antenna theory, NMR imaging, and many others. When the region of interest is a disc, most of the necessary analytical apparatus can be found in [22]. At the present time, we have constructed and implemented somewhat rudimentary versions of the relevant numerical algorithms; we are conducting numerical experiments with these, and will report the results at a later date. A much more difficult set of questions is presented by the structure of band-limited functions on more general regions.

Acknowledgments

The authors were supported in part by DARPA/AFOSR under Contract F49620-97-1-0011, and in part by DARPA/DoD under Contract MDA972-00-1-0033.

References

[1] Bouwkamp C J 1947 On spheroidal wave functions of order zero *J. Math. Phys. Mass. Inst. Tech.* **26** 79–92
[2] Cheng H, Yarvin N and Rokhlin V 1999 Non-linear optimization, quadrature, and interpolation *SIAM J. Optim.* **9** 901–23
[3] Debnath L 1995 *Integral Transforms and Their Applications* (New York: CRC Press)
[4] Gripenberg G, Londen S O and Staffans O 1990 *Volterra Integral and Functional Equations, Encyclopedia of Mathematics and its Applications* (Cambridge: Cambridge University Press)
[5] Flammer C 1956 *Spheroidal Wave Functions* (Stanford, CA: Stanford University Press)
[6] Fuchs W H J 1964 On the eigenvalues of an integral equation arising in the theory of band-limited signals *J. Math. Anal. Appl.* **9** 317–30
[7] Gantmacher F and Krein M 1950 *Oscillation Matrices and Kernels and Small Oscillations of Mechanical Systems* 2nd edn (Moscow: Gosudarstv. Izdat. Tehn-Teor. Lit.) (in Russian)
[8] Grünbaum F A 1981 Toeplitz matrices commuting with tridiagonal matrices *J. Linear Algebra Appl.* **40** 25–36
[9] Grünbaum F A 1981 Eigenvectors of a Toeplitz matrix: discrete version of the prolate spheroidal wave functions *SIAM J. Algebra Discr. Methods* **2** 136–41
[10] Grünbaum F A, Longhi L and Perlstadt M 1982 Differential operators commuting with finite convolution integral operators: some non-Abelian examples *SIAM J. Appl. Math.* **42** 941–55
[11] Karlin S 1964 The existence of eigenvalues for integral operators *Trans. Am. Math. Soc.* **113** 1–17
[12] Karlin S and Studden W J 1966 *Tchebycheff Systems with Applications In Analysis And Statistics* (New York: Wiley-Interscience)
[13] Krein M G 1959 The ideas of P L Chebyshev and A A Markov in the theory of limiting values of integrals *Am. Math. Soc. Trans.* **12** 1–122
[14] Ma J, Rokhlin V and Wandzura S 1996 Generalized Gaussian quadratures for systems of arbitrary functions *SIAM J. Numer. Anal.* **33** 971 96
[15] Markov A A 1898 On the limiting values of integrals in connection with interpolation *Zap. Imp. Akad. Nauk Fiz.-Mat. Otd.* (8) 6, no 5 (in Russian) (pp 146–230 of [16])
[16] Markov A A 1948 *Selected Papers on Continued Fractions and the Theory of Functions Deviating Least From Zero* (OGIZ: Moscow) (in Russian)
[17] Morse P M and Feshbach H 1953 *Methods of Theoretical Physics* (New York: McGraw-Hill)
[18] Landau H J and Pollak H O 1961 Prolate spheroidal wave functions, Fourier analysis, and uncertainty—II *Bell Syst. Tech. J.* **January** 65–94
[19] Landau H J and Pollak H O 1962 Prolate spheroidal wave functions, Fourier analysis, and uncertainty III: the dimension of space of essentially time- and band-limited signals *Bell Syst. Tech. J.* **July** 1295–336
[20] Landau H J and Widom H 1980 Eigenvalue distribution of time and frequency limiting *J. Math. Anal. Appl.* **77** 469 81
[21] Slepian D and Pollak H O 1961 Prolate spheroidal wave functions, Fourier analysis, and uncertainty—I *Bell Syst. Tech. J.* **January** 43–63
[22] Slepian D 1964 Prolate spheroidal wave functions, Fourier analysis, and uncertainty—IV: extensions to many dimensions, generalized prolate spheroidal wave functions *Bell Syst. Tech. J.* **November** 3009–57
[23] Slepian D 1978 Prolate spheroidal wave functions, Fourier analysis, and uncertainty V: the discrete case *Bell Syst. Tech. J.* **57** 1371–430
[24] Slepian D 1983 Some comments on Fourier analysis, uncertainty, and modeling *SIAM Rev.* (3) 379–93
[25] Slepian D 1965 Some asymptotic expansions for prolate spheroidal wave functions *J. Math. Phys.* **44** 99 140
[26] Stoer J and Bulirsch R 1992 *Introduction To Numerical Analysis* 2nd edn (Berlin: Springer)
[27] Yarvin N and Rokhlin V 1998 Generalized Gaussian quadratures and singular value decompositions of integral operators *SIAM J. Sci. Comput.* **20** 699–718